ABSTRACT

Title of Document: NONLINEAR OPTICAL STUDIES OF MOLECULAR ADSORPTION AND SOLVATION AT SOLID/LIQUID AND LIQUID/LIQUID INTERFACES

Antonie Renee Siler, Doctor of Philosophy, 2011

Directed By: Dr. Robert A. Walker, Department of Chemistry and Biochemistry, University of Maryland; Department of Chemistry and Biochemistry, Montana State University

Interfacial solvation is responsible for promoting biological phenomena *in* vivo including protein folding, solute transfer across membranes and enzymatic activity. The specific solvation interactions responsible for these and other processes can be both cooperative and complex. Because many cellular processes rely on interfacial effects, understanding how forces at an interface influence a solute will give insight into how molecules behave within these cellular bodies. The studies presented here are focused on isolating how these solvation interactions vary systematically with the identity of the solute and solvent at an interface.

The interfaces probed in these experiments varied from weakly to strongly associating interfaces defined as such by the identity of the solvent used to form the silica/liquid interface. Findings from strongly associating interfaces gave rise to surprising results from both the silica/methanol and silica/ethanol interfaces. The

silica/ethanol interface forms a very polar interface as probed by the solute p-nitroanisole (pNAs). At the silica/methanol interface, a *very* nonpolar region was probed by several solutes sensitive to solvent polarity.

The findings from the silica/methanol interface, led us to the research completed in the final chapter of this thesis. Data obtained from these measurements described the interfacial solvation and adsorption behavior of two solutes, pNAs and p-nitrophenol (pNP). Several silica/liquid interfaces were used in this study including, water, dimethyl sulfoxide (DMSO), acetonitrile (ACN), n-hexane, decane, cyclohexane, and methyl-cyclohexane. The two solutes are sensitive to solvent polarity and show similar solvatochromic behavior in bulk solvents. The solutes sample different interfacial polarities at the *same* silica/liquid interfaces according to SHG spectra obtained. pNAs is shown to be more sensitive to solvent identity at an interface than pNP, but less surface active. The sensitivity of pNAs to solvent identity at a silica/liquid interface is attributed to the solute's higher solubility in the solvents than pNP's solubility in the same solvents. On average, pNP has ~10 kJ/mol more adsorption energy at the measured interfaces than pNAs, and this too can be attributed to the inability of pNP to sufficiently solvate in many of the alkane solvents, forcing the solute out of solution and into the interface.

NONLINEAR OPTICAL STUDIES OF MOLECULAR ADSORPTION AND SOLVATION AT SOLID/LIQUID AND LIQUID/LIQUID INTERFACES

By

Antonie Renee Siler

Dissertation submitted to the Faculty of the Graduate School of the
University of Maryland, College Park, in partial fulfillment
of the requirements for the degree of
Doctor of Philosophy
2011

Advisory Committee:
Professor Robert A. Walker, Chair
Professor Jeffery T. Davis
Professor John T. Fourkas
Professor Christopher Jarzynski
Professor Michael A. Coplan, Dean's Representative

Dedicated to the two people who taught me that there was always something to be learned – even in the most unlikely of places – Mom and Dad.

Acknowledgements

I would first and foremost like to express sincere and heartfelt gratitude to my advisor Dr. Robert A. Walker. There is no hyperbole in this expression. His tireless efforts and fearsome devotion to both the project and my progress in the program made these last five years of work an extraordinary experience. His words of encouragement and laughs while in the lab and teaching will always be fond memories for me. I am also thankful for his cultivation in the scientist that I am today.

I would like to thank the members of my committee, Dr. Christopher Jarzynski, Dr. Jeffery Davis, Dr. John Fourkas, and Dr. Coplan. I would particularly like to thank them for their patience while dealing with a student that was not only "off-site," but also in two different time zones.

Another word of thanks must go to the past and present members of the Walker Research Group. I am grateful to have worked with Dr. Michael Brindza, Dr. Michael Pomfret, Dr. Suleyman Can, Dr. Anthony Dylla, and Dr. Debjani Roy while in College Park. I'd also like to thank the current members of Walker Research Group West: Bryan Eigenbrodt, John Kirtley, Lauren Woods, and Eric Gobrogge. The group, both in Maryland and Montana, has provided me with stimulating and helpful discussions at all hours of the day. I'd like to thank Dr. Jane Klassen for giving me the opportunity to "give back" with community service projects. A special thank you to Dr. Wendy Heiserman for her endless faith in me, and making those first years of graduate school a lot of fun. I also have to thank Shelby Wilson for her encouragement, friendship and help with all things conceptual.

NOBCChE – UMD also deserves sincere thanks. The group has provided me with an opportunity to meet and discuss research with chemists from different divisions and make long lasting friendships with amazing scientists.

Finally, but most importantly, I'd like to thank my family. My aunts, uncles, and grandparents for always believing in me; and my sisters, Ashley, Harlynn and Fehryn for always loving and encouraging me. My greatest thanks are to my parents for providing me with the desire and drive to complete anything I begin.

Table of Contents

List of Tables

List of Figures

List of Abbreviations

7AC	7-aminocoumarin
ACN	acetonitrile
C151	coumarin 151
C152	coumarin 152
C440	coumarin 440
C461	coumarin 461
CRF	controlled release formula
CT	charge transfer
DFT	density functional theory
DMSO	dimethyl sulfoxide
ETOH	ethanol
H20	water
HBA	hydrogen bond accepting
HBD	hydrogen bond donating
LC	liquid chromatography
M	mixed light polarization
MEOH	methanol
NHB	non hydrogen bonding
NLO	nonlinear optical
NMMA	n-methyl-p-methoxyaniline
P	vertical light polarization
pNAs	*para*-nitroanisole
pNP	*para*-nitrophenol
S	horizontal light polarization
SF	sum frequency
SH	second harmonic
SHG	second harmonic generation
t-boc	di-tert-butyl dicarbonate
VSFG	vibrational sum frequency generation
λ_{bulk}	maximum absorption wavelength in bulk solution
λ_{max}	maximum absorption wavelength
λ_{SHG}	maximum second harmonic wavelength

Chapter 1: Introduction

1.1 Motivation

Innumerable questions in technology, biology and environmental sciences motivate the need to understand how molecules behave at interfaces.[1-5] For example, the properties of liquid interfaces are responsible for colloid stability,[5] and materials such as paints require that small particles be stabilized in solution through interactions across a solid/liquid interface.[6-8] In a biological context, molecular adsorption to solid/liquid interfaces will preferentially summon some species from solution leaving other solutes available for uptake by organisms.[9-12] The biological importance of interfaces is also readily apparent when studying the surfaces of lung alveoli where surfactant mixtures must be able to facilitate rapid expansion and compression to allow oxygen to move across the liquid/gas interface.[13] In each of these instances, interfacial properties will control the concentration, structure, and organization of adsorbed solutes.[14] More importantly, the properties of molecules adsorbed to surfaces are likely to be different from the properties of those same molecules in bulk solution.[15] How different interfaces change solute properties and how these changes impact the overall solution phase surface chemistry is largely unknown. Research described in this thesis explores the effects of interfaces on solute solvation.

An example of how surfaces affect solute properties can be seen when 1-octanol self-assembles at the water/vapor interface. In a saturated solution most 1-octanol solutes remain within the bulk solution, but some self-assemble at the

interface forming a tightly packed monolayer with each molecule occupying an area of 20Å^2/molecule.[16,17] Molecules in solution will have random conformations, but at the aqueous/vapor interface adsorbed 1-octanol species are highly ordered. The hydroxyl group hydrogen bonds to the water and the chains are oriented in extended all-*trans* conformations. This long-range organization allows both the hydrophilic and hydrophobic ends of the octanol molecule to individually minimize their energetic requirements.

Just as surfaces can alter solute structure from bulk solution limits, solutes are also solvated differently at interfaces because of intrinsic asymmetry found at the boundaries between two different media.[18] Here, the term solvation describes all noncovalent interactions between a solute and its surroundings. The ability to selectively probe this microscopically thin region is difficult. Three significant challenges exist:

1. **Small number of solutes at the surface** – The low population of molecules at a surface relative to bulk leads to small signals from those very species that one seeks to investigate. For example, the number of 1-octanol molecules in 1cm^2 of a tightly packed monolayer corresponds to the same number found in 1cm^3 of a 1μM solution.
2. **Optical transparency –** Probing solutes at buried liquid interfaces requires the ability to irradiate the interface with light having a particular wavelength and being able to detect a signal, without the bulk solution interfering or attenuating the incident or outgoing light. This requirement forces one or both phases to be optically transparent,

and any absorbance from species in the bulk restricts the ability to carry out experiments.[19]

3. **Defining the interface** – The interface is not necessarily a well defined boundary. In the case of a solid/liquid interface, the junction between the two phases is demarcated clearly, but how far surface effects extend into solution is less clear.[20] Furthermore, in the case of liquid/liquid interfaces, one often lacks direct, validated information about the extent of interphase mixing that can occur between two immiscible solvents

To overcome these challenges, experiments in this thesis employ surface specific, nonlinear optical methods to measure the electronic structure and orientation of solvatochromic molecules adsorbed to weakly and strongly associating liquid/liquid and silica/liquid interfaces. Weakly associating interfaces, including water/alkane interfaces (interfacial tensions of 50mN/m) and silica/alkane interfaces,[21] are characterized by dipole-induced dipole interactions. Strongly associating interfaces, such as water/alcohol and acetonitrile/silica interfaces, have strong interfacial interactions (with interfacial tensions approaching 0 mN/m or interfacial contact angles approaching 0˚.)

The electronic responses of the solutes at the interfaces mentioned above were measured using the surface specific technique of resonance enhanced second harmonic generation (SHG) spectroscopy. SHG is a nonlinear optical technique that is forbidden in centrosymmetric environments. Because of this restriction, SHG is ideally suited to investigate surfaces and interfaces. Unlike in isotropic, bulk

solutions, interfacial anisotropy ensures that signal will come from only those molecules sensitive to the two distinct phases. The effective electronic excitation spectra of solutes sensitive to both specific and nonspecific solvation interactions were measured at a wide range of silica/liquid interfaces using this technique.[22] The primary goal of this work was to identify and understand how interfacial identity alters solvation from bulk solution limits and how these changes can affect solution phase surface chemistry.

1.2 Solvation – Nonspecific and Specific

Understanding interfacial solvation requires understanding how both specific and nonspecific solvation forces can change in the anisotropic environment presented by boundaries between two phases. Nonspecific solvation describes averaged interactions between a solute dipole and a surrounding solvent continuum.[23,24] Solvent polarity is one type of nonspecific solvation.[25,26] The importance of solvent polarity in solvation is that the polarity of a solvent determines the types of solutes capable of going into solution, e.g. "like dissolves like," as well as the energetics of the solute once it is in solution. Numerous scales have been generated to characterize nonspecific solvation. π^*[10] and $E_T(30)$[11,12] scales empirically quantify solvent effects on chromophores. These empirical scales have a wide range of usage due to their ease of application. Defining the parameters of these scales involve measuring an observable quantity of a solute transition energy or fluorescence lifetime in a particular solvent and then comparing these results to standard, reference solvents.[10] These polarity scales often utilize a multiple parameter equation to relate

the observable (such as an excitation wavelength) to its unperturbed observable. This same observable can also be related to a number of solvent parameters including localized, directional solvation properties including hydrogen bond donating and accepting properties.

For example, Reichardt[11] attempted to develop an individual empirical parameter for each distinct solute-solvent interaction and combine them into a master equation:

$$XYZ = (XYZ)_O + aA + bB + cC + ... \quad (1.1)$$

In this expression, XYZ is the observable and the regression coefficients describe the sensitivity of the solute/solvent interactions. The utility of this expression depends upon the ability of investigators to find solvatochromic probes that interact with solvents through individual, easily isolated intermolecular solute/solvent mechanisms. This constraint initially forced parameters involving hydrogen bonds to be omitted and the equation shown above was reduced to:[9]

$$\nu = \nu_O + s\pi^* \quad (1.2)$$

The values of π^* were compiled for a multitude of solvents. These equations – known as "linear solvation free energy relationships"[13] (or LSERs) – empirically adjust a series of unrelated intermolecular parameters until calculated results begin to agree with experimental values. The $E_T(30)$ polarity scale follows a similar strategy. The π^*[14] polarity scale is based on the molecule p-nitroanisole (pNAs), and the $E_T(30)$ polarity scale is based on the molecule n-phenoxide betaine-30.[11] These two probes differ in size and sign of solvatochromic shift. pNAs has a large, positive change in dipole moment, μ, accompanying electronic excitation. N-phenoxide

betaine-30 undergoes a large negative change in dipole with excitation. Due to differential solvation forces present in the excited state vs. the ground state, shifts in excitation wavelength can be observed. Repeated studies have shown that empirical scales quantifying aspects of solvation work well at reproducing experimental results when specific solvation – namely, hydrogen bonding – is left out.

All of the work described in this thesis characterize solvents based on their Onsager polarity function:[25]

$$f(\varepsilon) = \frac{2(\varepsilon - 1)}{2\varepsilon + 1} \qquad (1.3)$$

where ε is a solvent's static dielectric constant. The Onsager function ranges from 0.4 to ~1.0 as solvents vary from nonpolar alkanes (ε~2.0) to water (ε~80*)*. Solutes sensitive to long-range, nonspecific solvation forces typically show a decrease in excitation energy that is monotonic with $f(\varepsilon)$, assuming that the excited state molecular dipole, μ_e, is greater than the ground state molecular dipole, μ_g.[2] f(ε) captures polarity differences, but it can not account for changes in solute electronic structure arising from hydrogen bonding properties of a solvent. Nevertheless, this property of solvents serves as a useful comparison to earlier studies examining polarity at interfaces.

Solvation – both specific and nonspecific – will affect solute electronic structure. In the case of nonspecific solvation, increasing polarity will lead to monotonic shifts in electronic excitation. If a solute's excited state dipole (μ_e) is larger than its ground state dipole (μ_g), then increasing solvent polarity will preferentially stabilize the excited state leading to a red shift in excitation wavelength. This effect is shown on the left side of Figure 1.1. For specific solvation, the solute's

ability to donate and accept hydrogen bonds leads to different shifts in electronic excitation. This effect is shown on the right side of Figure 1.1.[28]

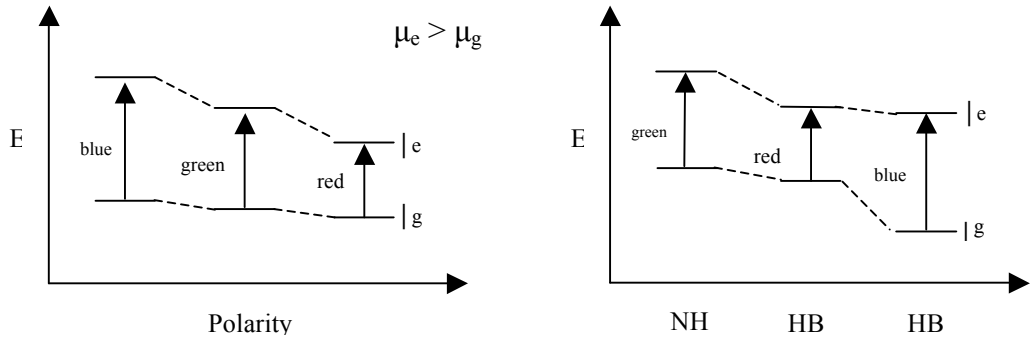

Figure 1.1: These figures describe the different effects of solvent polarity versus hydrogen bonding sensitive solvents on the electronic excitation of a hydrogen bonding sensitive molecule. (NHB, non-hydrogen bonding; HBA, hydrogen bond accepting; and HBD, hydrogen bond donating)

Specific solvation, in contrast to nonspecific solvation, describes the directional localized interactions between a solute and the surrounding solvent molecules. Hydrogen bonding is a type of specific solvation. Hydrogen bonding plays an important role stabilizing many biological systems[4] and is responsible, in part, for protein stabilization, solute transfer across membranes and promoting enzymatic reactions.[27] Hydrogen bonding has a key role in determining the structure and properties of water and biomolecules in solution.[15] Quantitatively determining the hydrogen bond donating and accepting opportunities that exist across an interface is essential for understanding solution phase surface chemistry.

Many studies have attempted to account for these shifts, leading researchers to conclude that the shifts are due to electron density redistribution. The studies provide insight into the processes responsible for weakening or strengthening the

hydrogen bond. For example, in systems where electron density in the excited state is delocalized, one often observes is a red shift for excitation wavelengths that can be explained by a change in electron density from the region between two atoms to the anti-bonding orbital.[29] Very little is understood about how a solute's ability to hydrogen bond affects the solvent. Utilizing the "new generation" of solvatochromic probes, we hoped to be able to better understand this interaction.

1.3 Experimental Methods – Overview

The primary method used in all of the experiments presented in this thesis is resonance enhanced second harmonic generation. To understand why resonance enhanced SHG is both molecule and surface specific, one must consider the interaction of light with molecules – both in bulk and at surfaces. Incident light induces an instantaneous, time dependent polarization in a molecule. This polarization depends upon an incident field strength and the properties of the molecule and can be expanded as a power series in field strength:[30]

$$P = P^{(0)} + P^{(1)} + P^{(2)} + ... = P^{(0)} + \chi^{(1)} \cdot E + \chi^{(2)} : E^2 ..... \qquad (1.4)$$

where $P^{(0)}$ is the static polarization and $P^{(1)}$ is the optical response that depends linearly on incident field strength. $P^{(2)}$ is the second-order polarization that is proportional to the square of the incident field strength and the system's second-order nonlinear susceptibility, $\chi^{(2)}$.

$\chi^{(2)}$ is a third rank tensor containing 27 different elements, each describing the system's susceptibility of generating a second order polarization for different incident

and outgoing field orientations. The tensor itself is anti-symmetric with respect to inversion:

$$\chi^{(2)}_{x,y,z} = -\chi^{(2)}_{-x,-y,-z} \tag{1.5}$$

In bulk, isotropic media, this requirement forces $\chi^{(2)}$ to vanish. At interfaces, however, $z \neq -z$ and thus, $\chi^{(2)}$ can assume non-zero values. $\chi^{(2)}$ contains both resonant (R) and nonresonant (NR) terms:

$$\chi^{(2)} = \chi^{(2)}_{NR} + \chi^{(2)}_{R} = \chi^{(2)}_{NR} + \Sigma_{k,e} \frac{\mu_{gk}\mu_{ke}\mu_{eg}}{\left(\omega_{gk} - \omega - i\Gamma\right)\left(\omega_{eg} - 2\omega + i\Gamma\right)} \tag{1.6}$$

In Equation 1.6, the μ_{ij} correspond to transition matrix elements and the summation runs over all real and virtual excitation energies. Tuning the frequency of the incident light and measuring I(2ω) leads to effective excitation spectra of those molecules subject to interfacial anisotropy.

To relate this quantity, $\chi^{(2)}$, to the molecules at the interface, the nonlinear susceptibility can be expressed in terms of the orientationally averaged molecular hyperpolarizability and the total number of molecules present at the surface:[31]

$$\chi_R^{(2)} = N_s \left\langle \alpha^{(2)} \right\rangle \tag{1.7}$$

The brackets represent the orientational average over the interfacial molecules.[31] N_s is the number of molecules at the interface, and the alpha term is the molecular hyperpolarizability. The molecular hyperpolarizability is defined as:[32]

$$\alpha = \sum \frac{\left\langle g\left|\frac{\partial \mu}{\partial Q}\right|k\right\rangle\left\langle k\left|\frac{\partial N}{\partial Q}\right|e\right\rangle}{2\omega - \omega_o - i\Gamma} \tag{1.8}$$

where the numerator is the transition matrix element between the ground and excited states of a given molecule, 2ω is the frequency of the second harmonic light, ω_o is the

resonant frequency of an allowed electronic transition, and Γ is the spectral line width. Whenever 2ω approaches ω_o, α gets large making SHG molecularly specific, as well as surface specific.

The intensity of the generated second harmonic polarization can be written as a function of the susceptibility term such that:[32]

$$I(2\omega) = \left|P^{(2)}\right|^2 = \left|\chi^{(2)}\right|^2 * I(\omega)^2 = (\chi_R{}^2 + 2\chi_R\chi_{NR} + \chi_{NR}^2) * I(\omega)^2 \qquad (1.9)$$

where $I(\omega)^2$ is the square of the intensity of the incoming light. Thus, we see that the intensity of the second harmonic signal depends quadratically both on the incident field intensity and the number of molecules present (N^2).

Data acquired from the second harmonic experiments were fit using a procedure written for Igor Pro. The basis of the fit is derived from the square of the nonlinear susceptibility shown above including the explicit form of the molecular hyperpolarizability. When squared, the equation for the molecular hyperpolarizability gives rise to a Lorentzian line shape. This resonance enhancement can be skewed to either longer or shorter wavelength by the nonresonant contribution of $\chi^{(2)}$ that is present as both first and second powers in Equation 1.9. In most instances, the resonant contribution to the total nonlinear susceptibility is 10-100 times larger than the nonresonant piece, although one needs to note that the nonresonant piece can vary from system to system depending on the exact influence a surface has on the adjacent solvent and solute. In this thesis, data were fit using adjustable parameters for ω_1 (excitation wavelength), ω_2 (amplitude), ω_3 (width) and ω_4 (nonresonance). The "initial guess" for the excitation wavelength was the corresponding wavelength value for the highest

normalized signal for the spectrum being analyzed. The initial values for amplitude, width and nonresonance were more standardized and spectra analyzed began with values of 0.001, 0.01, and 0, respectively. Typical spectra have relative errors of 1, 5, 10 and 8 % for the excitation wavelength, amplitude, width and nonresonance, respectively.

Additionally, I(2ω) depends upon average orientation, and different polarization combinations of ω and 2ω can be used to determine the average orientation of solute electronic transitions. This dependence is of great importance in Chapter 4 of this work where adsorption characteristics of both pNAs and pNP are measured at different silica/liquid interfaces. The relationship between the inverse of the s-polarized contribution of the SH-intensity generated at the sample induced by a mixed (m)-polarized fundamental beam can be used to determine the surface activity and adsorption free energies. By measuring the dependence of the second harmonic response (or, technically, the square root of the SH signals) one can readily identify whether or not an analyte in solution is strongly driven to associate with the surface. The two-step Langmuir model was used to fit the data and showed that pNP is more surface active than pNAs uniformly across the solvents measured in the study.

1.4 Thesis Organization

This thesis describes a series of experiments designed to probe interfacial solvation at a variety of silica/liquid interfaces. We used solute solvatochromic sensitivity to our advantage in order to differentiate the types of environments created at a given interface, and the ability of the solute used to sample this environment.

Many unpredicted results occurred throughout the experiments completed in this work, and our hope is that these findings may one day aid in the construction of models that can be used in the prediction of interfacial solvation for any given solute.

Previous studies using polarity-sensitive surfactants showed that nonspecific solvation across solid/liquid and liquid/liquid interfaces depended sensitively on solvent structure and inter-phase forces.[14,15,17,33,34] Specifically, polarity across water/alkane interfaces varied systematically between two bulk limits. Water/alcohol interfaces, however, created regions where polarity could not be described as a weighted average from the adjacent bulk phases. Rather, the interfacial polarity passed through a distinct alkane-like minimum between the very polar aqueous phase and the moderately polar alcohol.[33] What these previous findings could not clarify is how hydrogen bonding changes across these same weakly and strongly associating interfaces.

Chapter 2 of this thesis investigates how specific solvation forces change across weakly associating interfaces using a new generation of hydrogen bonding solvatochromic probes, or molecular rulers. The synthetic method for making these surfactants is presented, along with the schematic for an analogue to the specific solvation sensitive probes. Material presented in Chapter 3 begins to address how properties change across interfaces created by both silica/methanol and silica/ethanol.

The solutes used in these measurements are pNAs and p-nitrophenol (pNP). These two solutes share similar electronic structures, but they are markedly different in their affinity for different solvents. pNAs is ~20 times more soluble in alkanes than in aqueous solution; whereas pNP is ~100 times more soluble in water than in

alkanes. Surprisingly, the silica/methanol interface appears to be a much more nonpolar region than expected. An explanation of this observed behavior is rationalized in terms of surface effects on anisotropic solvent organization.

Chapter 4 develops these ideas further by examining adsorption of both pNP and pNAs to different silica/liquid interfaces *and* by characterizing the local polarity sampled by the adsorbed solutes. Results from Chapter 4 are surprising in that pNP consistently has higher adsorption energy to the interface than pNAs and is insensitive to solvent identity. pNAs, however, is very sensitive to solvent identity and varies in both adsorption energies and interfacial excitation based on the solvent.

1.5 References

(1) Hayes, P. L.; Malin, J. N.; Korek, C. T.; Geiger, F. M. *J. Phys. Chem. A* **2008**, *112*, 660.

(2) Hiemenz, P. C.; Rajagopalan, R. *Principles of Colloid and Surface Chemistry*; Marcel Decker: New York, 1997.

(3) Israelachvili, J. *Intermolecular and Surface Forces*; Academic Press: California, 1992.

(4) McClelland, A.; Fomenko, V.; Borguet, E. *J. Phys. Chem. B* **2006**, *110*, 19784.

(5) Rosen, M. J. *Surfactants and Interfacial Phenomena*; Wiley-Interscience: New Jersey, 2004.

(6) Durbing, D. P.; El-Aasser, M. S.; Vanderhoff, J. W. *Ind. Eng. Chem. Prod. Res. Dev.* **1984**, *23*, 569.

(7) Liddell, P. V.; Boger, D. V. *Ind. Eng. Chem. Res.* **1994**, *33*, 2437.

(8) Williamson, R. V. *J. Phys. Chem.* **1931**, *35*, 354.

(9) Connell, D. B.; Sander, J. G.; Riedel, G. F.; Abbe, G. R. *Environ. Sci. Technol.* **1991**, *25*, 921.

(10) Dodge, E. E.; Theis, T. L. *Environ. Sci. Technol.* **1979**, *13*, 1287.

(11) Montgomery, J. R.; Price, M. T. *Environ. Sci. Technol.* **1979**, *13*, 546.

(12) Thomann, R. V. *Environ. Sci. Technol.* **1989**, *23*, 699.

(13) Hills, B. A.; Barrow, R. E. *Phys. Med. Biol.* **1984**, *29*, 1399.

(14) Wang, H. F.; Borguet, E.; Eisenthal, K. B. *J. Phys. Chem. A* **1997**, *101*, 713.

(15) Beildeck, C. L.; Steel, W. H.; Walker, R. A. *Langmuir* **2003**, *19*, 4933.

(16) Lin, S.; Wang, W.; Hsu, C. *Langmuir* **1997**, *13*, 6211.

(17) Steel, W. H.; Walker, R. A. *Nature* **2003**, *424*, 296.

(18) Steel, W. H.; Damkaci, F.; Nolan, R.; Walker, R. A. *J. Am. Chem. Soc.* **2002**, *124*, 4824.

(19) Yang, Y. J.; Pizzolatto, R. L.; Messmer, M. C. *J. Opt. Soc. B* **2000**, *17*, 638.

(20) Curtis, A. D.; Reynolds, S. B.; Calchera, A. R.; Patterson, J. E. *J. Phys. Chem. Lett.* **2010**, *1*, 2435.

(21) Horng, P.; Brindza, M. R.; Walker, R. A.; Fourkas, J. T. *J. Phys. Chem. C* **2010**, *114*, 394.

(22) Siler, A. R.; Brindza, M. R.; Walker, R. A. *Anal. Bioanal. Chem.* **2008**, *395*, 1063.

(22) Eisenthal, K. B. *Chem. Rev.* **1996**, *96*, 1343.

(23) Mellein, B. R.; Ladewski, R. L.; Brennecke, J. F. *J. Phys. Chem. B* **2007**, *111*, 131.

(24) Onsager, L. *J. Am. Chem. Soc.* **1936**, *58*, 1486.

(25) Wu, Y. G.; Tabata, M.; Takamuku, T. *J. Soln. Chem.* **2007**, *31*, 381.

(26) Boyer, R. F. *Concepts in Biochemistry*; John Wiley and Sons: New York, 2002.

(27) Suppan, P.; Ghoneim, N. *Solvatochromism*, 1st ed.; The Royal Society of Chemistry: London, 1997.

(28) Esenturk, O.; Walker, R. A. *Phys. Chem. Chem. Phys.* **1999**, *1*, 1957.

(29) Boyd, R. W. *Nonlinear Optics*; Academic Press: New York, 2003.

(30) Eisenthal, K. B. *Chem. Rev.* **2006**, *106*, 1462.

(31) Zhang, X. Y.; Cunningham, M. M.; Walker, R. A. *J. Phys. Chem. B* **2003**, *107*, 3183.

(32) Steel, W. H.; Beildeck, C. L.; Walker, R. A. *J. Phys. Chem. B* **2004**, *108*, 13370.

(33) Steel, W. H.; Beildeck, C. L.; Walker, R. A. *J. Phys. Chem. B* **2004**, *108*, 16170.

Chapter 2: Hydrogen Bonding Molecular Ruler Surfactants as Probes of Specific Solvation at Liquid/Liquid Interfaces

2.1 Introduction

In the most general sense, solvation describes the interactions between a solute and its solvent environment. These interactions may be nonspecific and averaged over an entire solute cavity or specific and therefore unique to individual solute/solvent combinations.[1-4] Most models of solvation begin by assuming that a solute is solvated by an isotropic solvent medium and specific interactions are included by introducing explicit solvent molecules to the solute cavity.[4-7] These models cannot apply to solvation at surfaces, where the asymmetry intrinsic to any boundary necessarily forces solvents to organize in ways not observed in bulk. Many experimental techniques and theoretical methods have been used to refine our understanding of solvent structure at surfaces.[8-16] Less clear is how this altered solvent structure changes interfacial solvation from bulk solution limits. This situation is especially true at buried interfaces – boundaries between two condensed phases – where few experimental tools have the necessary surface *and* molecular specificity to probe quantitatively the relatively small numbers of solutes subject to interfacial solvation forces. Given that solvation at surfaces controls interfacial solute concentration, structure and reactivity, identifying how interfacial solvation differs from solvation in bulk solution is essential for formulating predictive models of solution phase surface chemistry. Experiments described in this work begin to probe

the hydrogen bonding properties experienced by solutes adsorbed to liquid/liquid interfaces.

Recent reports have begun to answer questions about how *nonspecific* interfacial solvation depends on the molecular structure of liquids and how far into solution surface effects extend.[17-28] Answering these questions has required coupling sophisticated, nonlinear optical measurements with strategies carefully crafted to vary solute distributions across the interfacial region.[29,30] Data from these studies have begun to clarify how and why solvent polarity at liquid surfaces differs from bulk solution limits. In this context, solvent polarity describes the nonspecific interactions between a solute dipole and the surrounding dielectric continuum. Studies found that weakly associating interfaces formed between aqueous solutions and alkanes were characterized by polarity that converged monotonically from aqueous to alkane limits, although the distance required to reach alkane-like polarity depended sensitively on solvent structure.[20] In contrast, polarity across strongly associating liquid/liquid interfaces – such as those formed between aqueous solutions and long chain (liquid) alcohols – were dominated by a nonpolar region that could not be described by weighted properties of the two bulk solvents.[19,21] This nonpolar region was thought to originate from interfacial ordering of alcohol alkyl chains in a Langmuir-film type assembly. Recent X-ray scattering studies and classical molecular dynamics simulations support this picture.[31-35]

Despite the insight into how interfacial polarity depends on inter-phase forces, solvent structure and ionic strength, findings from these studies have yet to address how hydrogen bonding, a specific interaction, changes across liquid/liquid and

liquid/solid interfaces. Resolving this issue requires decoupling dipolar (or nonspecific) solvation interactions from directional, localized solvation forces. Work presented below describes our successful efforts to create variable length surfactants capable of probing specific solvation interactions across liquid/liquid interfaces. These surfactants consist of a charged, cationic headgroup and a hydrophobic solute. The solute itself, n-methyl-p-methoxyaniline (NMMA) is ~4 times more soluble in alkanes than in water, and this solute's electronic structure depends solely on hydrogen bond donating and accepting opportunities, not on local dielectric effects.

This chapter describes the synthetic methods used to create these surfactants as well as surfactant characterization. Of particular interest are results from both surface tension and bulk UV-Vis absorbance studies that show the surfactants a) to be much more surface active at aqueous/alkane interfaces compared to aqueous/vapor interfaces, and b) to be much more likely to associate at low concentrations in lower polarity, mixed solvent systems than in polar solvents. Resonance enhanced second harmonic generation (SHG) data show that NMMA adsorbed to alkane/silica liquid/solid interfaces experiences relatively strong hydrogen bond donation from surface silanol groups. Similarly, at a CCl_4/aqueous interface, NMMA also reports the presence of hydrogen bond donating opportunities even stronger than those in bulk aqueous solution. This result is consistent with recent reports from vibrational studies of intermolecular hydrogen bonding of water at silica and immiscible organic interfaces. SHG spectra from the newly synthesized C_5 molecular ruler surfactant adsorbed to aqueous/alkane interfaces suggest that as NMMA begins to move across

a liquid/liquid interface and into a nonpolar organic solvent, the solute carries with it strongly associated water molecules that serve as hydrogen bond acceptors.

2.1.1 Experimental Considerations and Characterization

In order to probe specific solvation across liquid interfaces, molecular ruler surfactants must be sensitive to directional, localized solvent-solute interactions. Furthermore, the solute itself must be hydrophobic so that when the surfactant adsorbs to the interface, the solute attempts to minimize its solvation energy solely in the organic phase. Finally, the surfactant rulers must be modular with simple synthetic methods that allow simple variation of the length between the charged headgroup and hydrophobic model solute.

2.1.2 Solute Sensitivity to Specific Solvation

The solvatochromic behavior of a given solute serves as a marker of local solvation environment. Solvatochromism describes the solvent sensitive shifts of a chromophore's transition energy and arises from the differential solvation of a solute's ground and excited states. Typically, solvatochromic behavior is used to describe a solute's sensitivity to local dielectric environment, and numerous molecules have been used to measure the polarity of different environments.[36-38] More sophisticated treatments of solute solvatochromism take into account solute properties such as hydrogen bond accepting and donating behavior. This dependence is captured with empirical solvation scales such as π^* and E_T30.[38-40]

Table 2.1. Solvents used to characterize NMMA's specific solvation in bulk solution. f(e) is a solvent's Onsager polarity function as defined in text. All absorbance data were acquired on a Beckman UV-Vis 5500 spectrophotometer with a resolution of 2 nm.

Solvent	f(ε)	NMMA (nm)	C_3^+	C_5^+
n-octane	0.387	314	-	-
decane	0.396	317	-	-
cyclohexane	0.406	314	-	-
CCl_4	0.452	316	-	-
diethyl ether	0.685	315	-	-
tetrahydrofuran (THF)	0.813	317	318	316
dichloromethane	0.841	316	-	-
1-butanol	0.918	309	-	-
1-propanol	0.930	312	315	314
ethanol	0.942	318	313	316
methanol	0.955	311	306	310
acetonitrile (ACN)	0.960	315	316	316
dimethylsulfoxide (DMSO)	0.969	320	320	320
water (H_2O)	0.981	300	300	300

In order to probe specific solvation at liquid interfaces, solutes should be sensitive only to localized, directional solvent-solute interactions. Several solutes stand out including a series of substituted aromatic amines. N-methyl-p-methoxyaniline (NMMA) is a solute that is sensitive to specific solvation forces but not to nonspecific, averaged dielectric interactions. Solvatochromic data for NMMA in different solvents are shown in Figure 2.1 and listed in Table 2.1. In non-hydrogen bonding solvents, NMMA's excitation wavelength remains approximately constant at 315 nm. In hydrogen bond accepting solvents (such as DMSO or DMF) the excitation wavelength shifts to 320 nm, while in water, the excitation shifts to shorter wavelengths (300 nm). The hydrogen-bond accepting ability of DMSO leaves the

NMMA nitrogen's lone pair isolated and inductively promotes lone pair delocalization into the aromatic ring following excitation. The resulting larger change in permanent dipole leads to a shift in excitation to lower energies (and longer wavelength). In contrast, the hydrogen bond donating property of water stabilizes NMMA in its ground state thereby increasing the energetic gap between ground and excited electronic states leading to the experimentally observed blue shift in excitation wavelength.[36]

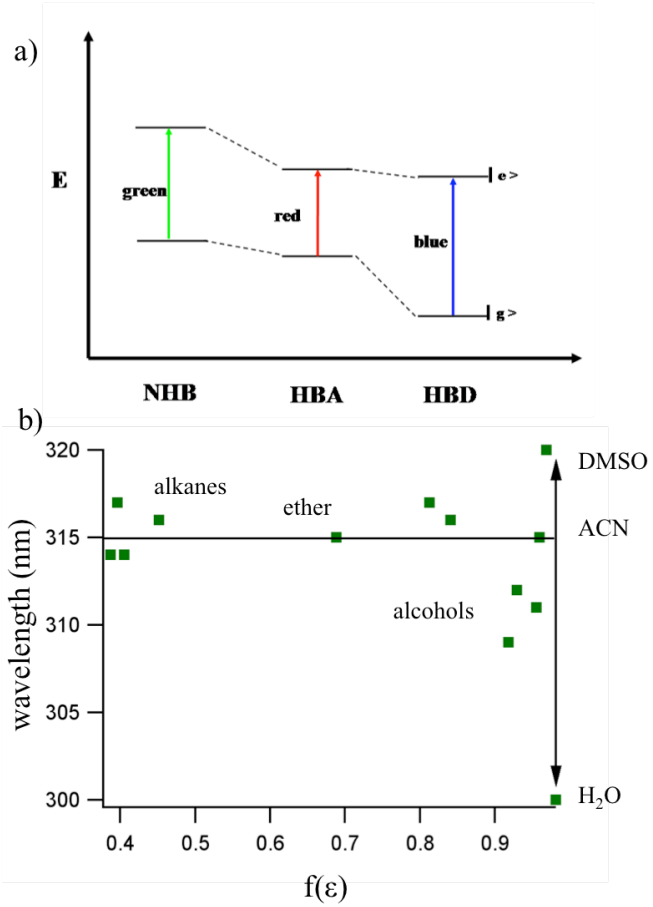

Figure 2.1: (a) The top figure represents the solvatochromic response of a molecule sensitive to specific solvation solvated in non-hydrogen bonding, hydrogen bond accepting, and hydrogen bond donating solvents. (b) The UV-Vis absorption maxima of NMMA in different solvents with varying Onsager polarity functions. f(e) varies from 0.4 for alkanes to ~1.0 for water and DMSO.

The NMMA chromophore is ideal for use in molecular rulers because of its photochemical stability and its sensitivity to hydrogen bonding opportunities. Furthermore, the small size of NMMA imparts finer spatial resolution to molecular rulers than would be afforded with large chromophores having extensive, delocalized electronic structures. Partitioning experiments show NMMA to be ~4 times more soluble in nonpolar, alkane solvents than in aqueous environments, meaning that NMMA will preferentially lower its solvation energy by migrating from an aqueous to an alkane phase. This preferential solvation in the nonpolar phase is highlighted in differences in surface tension measurements between the aqueous/air and aqueous/cyclohexane interfaces. Molecular rulers described in this work incorporate a derivative of NMMA into cationic alkyl surfactants having variable lengths. Experiments profiling interfacial width exploit these properties by using 2nd order nonlinear optical spectroscopy to measure effective excitation spectra of NMMA based molecular rulers adsorbed to different liquid/liquid interfaces.

2.1.3 Surface Activity

The pairing of a hydrophobic probe and ionic headgroup leads molecular ruler surfactants to be surface active. Surface activity is monitored by measuring the interfacial tension at liquid/liquid interfaces. The Gibbs isotherm for soluble monolayers provides a relationship between the surface excess concentration (Γ) and the interfacial pressure (Π):[41,42]

$$\Pi A = (\gamma_o - \gamma)A = \Gamma k_B T \ln(c) \qquad (2.1)$$

Here, Π, is the interfacial pressure (the difference in surface tensions between the neat system (γ_o) and the system under study (γ)), A is the interfacial area, Γ is the

surface excess concentration, k_B is the Boltzmann constant, T is the temperature of the system in Kelvin, and *ln*(c) is the natural log of the concentration of the solution. At low bulk concentrations, the activity is assumed to be equivalent to concentration. Differentiating surface pressure with respect to *ln*(c) leads to the expression:

$$\frac{\delta \Pi}{\delta \ln(c)} = \frac{\Gamma}{A} kT. \qquad (2.2)$$

By plotting Π vs. *ln*(c) and determining the slope of steepest ascent, the limiting surface concentration of the molecular ruler monolayers can be determined.

2.2 Experimental

Figure 2.2 shows the synthetic scheme used to create this family of surfactants, starting with 4-methylaminophenol sulfate. The amino group is first protected with di-tert-butyl dicarbonate (t-Boc). The newly protected starting material is converted to the desired product by adding the dibromoalkane of desired length in a ratio to maximize the yield of the monomer. After purification, the bromine terminated headgroup is converted to a cationic, quaternized amine upon reaction with trimethylamine according to published procedures.[29] The molecular ruler is then deprotected using trifluoroacetic acid. Alcohol terminated molecular ruler surfactants can be prepared by reacting the ruler with sodium acetate and crown ether after the creation of the purified alkyl-bromo product. The acetate head is then reacted with sodium ethoxide and purified. The ruler is then deprotected as above.

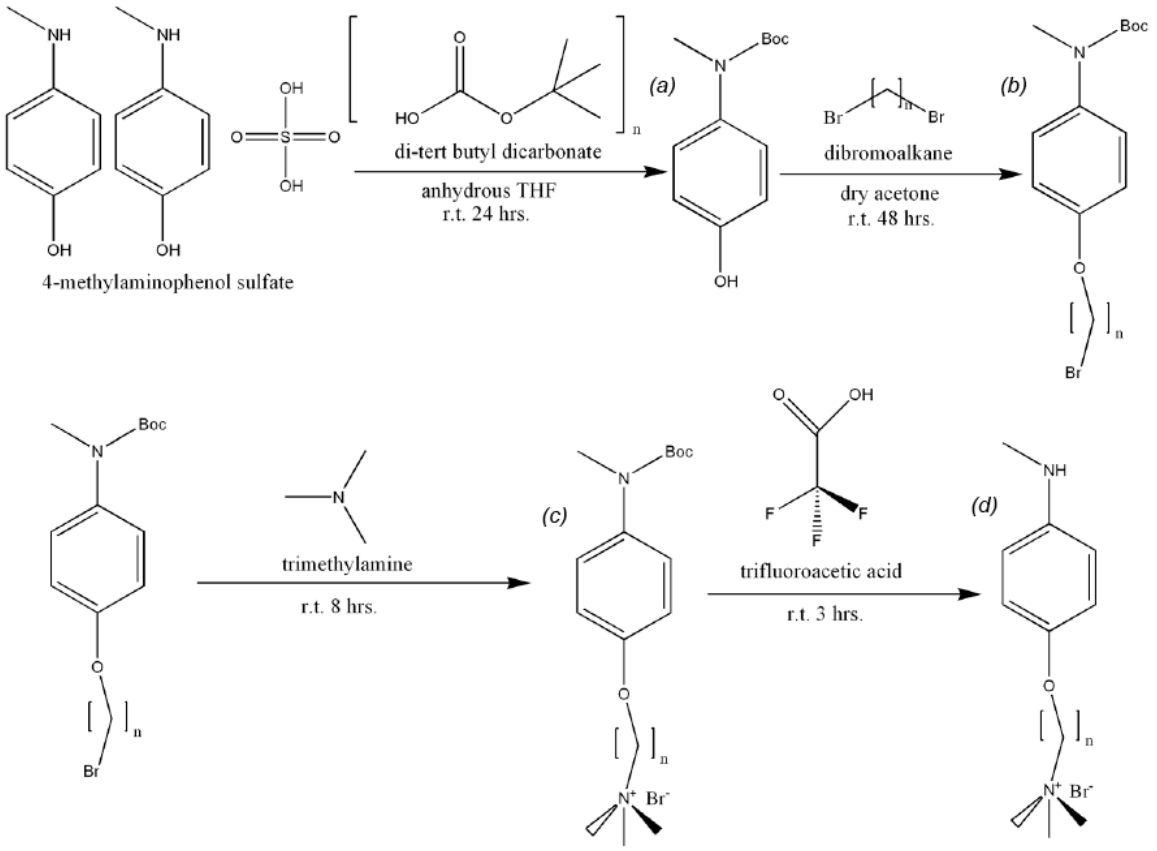

Figure 2.2: Synthetic scheme for making hydrogen-bond sensitive molecular ruler surfactants.

Representative surfactants having alkyl lengths of 3, 5 and 6 methylene groups in the spacer have been synthesized and purified. Assuming an all-*trans* conformation, each methylene group increases the separation between the hydrophilic headgroup and hydrophobic chromophore by approximately 1.25 Å, although this assumption is certain to break down with surfactants having longer chains. Previous work using polarity sensitive anionic molecular ruler surfactants implied that alkyl spacers having up to five CH_2 groups show little evidence of systematic enhanced conformational disorder with increasing chain length.[29] The issue of alkyl chain conformation is discussed below in greater detail.

All reagents used were purchased from Aldrich and used without further purification. All reactions were run under an atmosphere of nitrogen. All compounds were >95% pure as determined by ^{1}H NMR spectroscopy and mass spectrometry. Nuclear magnetic resonance spectra were recorded on a 400 MHz spectrometer. Chemical shifts are reported in parts per million (ppm) relative to the deuterated solvent peak. Coupling constant (J values) are reported in hertz (Hz), and spin multiplicities are indicated by the following symbols: s (singlet), d (doublet), t (triplet), q (quartet), m (multiplet), br s (broad singlet). Band positions are given in reciprocal centimeters (cm^{-1}) and relative intensities are listed as br (broad), s (strong), m (medium), or w (weak). Thin-layer chromatography (TLC) was performed with the compounds being identified in one or more of the following manners: UV (254 nm) and iodine.

2.2.1 Synthesis

General Procedure for the Synthesis of (steps 1-3). 4-methylaminophenol sulfate was protected using di-tert-butyl dicarbonate (t-boc) according to published procedures. The dibromoalkane was syringed into the reaction vessel and the mixture was allowed to stir in dry acetone at RT for 48 hours. The reaction mixture was poured into a sodium bicarbonate solution and extracted with ethyl acetate. In addition to the desired product, residual starting material was also extracted into the acetate. Purification of the reaction mixture residue by flash chromatography (hexanes: EtOAc, 4:1) gave the desired starting material. The spectral data of the individual compounds are reported below.

Alkylation. Compound (b) was prepared by following the general procedure employing bocprotected 4-methylaminophenol sulfate (1.400 g, 6.67 mmol) and dibromopentane (9.13 mL, 66.7 mmol). Purification of the reaction mixture gave 1.611 g (71%) of the bocprotected ruler as a brown oil: $R_f = 0.3$ (hexanes: EtOAc, 4:1); ^{1}H NMR ($CDCl_3$) 1.44 (s, 1H), 1.65 (mm, 1H), 1.92 (mm, 1H), 3.21 (d, 1H), 3.44 (q, 1H), 3.95 (t, 1H), 6.84 (d, 1H), 7.12 (d, 1H).

Ionic Salt and Deprotection. Trimethylamine was added to the solution of the corresponding bromine terminated ruler in methanol at RT and stirred for ten hours. The remaining amine was removed by rotary evaporation. The product is then deprotected in TFA by stirring at RT for three hours.

Quartenization. Compound (c) was prepared by following the general procedure employing the bromine terminated ruler (1.611 g, 4.74 mmol) with trimethylamine (3.028 mL, 50 mmol) in methanol. Purification of the reaction mixture gave 1.607 g (88%) of (c) as a yellow oil. $R_f = 0.25$ (hexanes: EtOAc, 4:1); ^{1}H NMR (D_2O) 1.27 (s, 1H), 1.36 (m, 1H), 1.69 (m, 1H), 2.95 (d, 1H), 3.03 (s, 1H), 3.19 (d, 1H), 3.96 (t, 1H), 6.85 (d, 1H), 7.07 (d, 1H).

Deprotection. ^{1}H NMR (D_2O) 1.0 (t, 1H), 1.36 (m, 1H), 1.67 (q, 1H), 2.93 (d, 1H), 3.17 (t, 1H), 3.95 (t, 1H), 6.94 (d, 1H), 7.24 (d, 1H).

Alcohol Terminated Ruler Synthesis. This version of the molecular rulers was not used further in this work, but these rulers can be used to study solid/liquid interfaces. Similar versions, see Zhang, et al.,[26] were synthesized for polarity sensitive rulers. The alternative alcohol terminated ruler was prepared following the general procedure employing the bromine terminated ruler (2.149 g, 5.8 mmol) with sodium acetate

(0.309 g, 0.58 mmol) and dibenzo-18-crown-6 ether (0.213 g, 2.6 mmol) in dimethyl sulfoxide. The reaction was allowed to stir at 60^{o}C for 24 hours. The product was extracted using pentanes. The starting material was then reacted with a fresh solution of sodium ethoxide at RT for five hours. The product was purified using flash chromatography (hexanes: EtOAc, 1:1). Product was then deprotected using the above procedure.

Acetate. ^{1}H NMR ($CDCl_3$) 1.44 (s, 1H), 1.65 (mm, 1H), 1.92 (mm, 1H), 3.21 (d, 1H), 3.44 (q, 1H), 3.95 (t, 1H), 6.84 (d, 1H), 7.12 (d, 1H).

Alcohol Terminated Ruler. ^{1}H NMR ($CDCl_3$) 1.44 (s, 1H), 1.65 (mm, 1H), 1.92 (mm, 1H), 3.21 (d, 1H), 3.44 (q, 1H), 3.95 (t, 1H), 6.84 (d, 1H), 7.12 (d, 1H).

2.2.2 Surface Second Harmonic Generation

SHG experiments in these studies were conducted with a variety of solutions consisting of NMMA dissolved in organic or aqueous solvents that were then brought into contact with a hydrophilic silica prism or the adjacent liquid phase. NMMA was purchased from Aldrich and used without further purification. (Reported purity was 98%.) The SHG cell and detection assembly has been described previously.[19,20] For experiments requiring a hydrophilic silica surface the prism was cleaned in a 50/50 mixture (by volume) of sulfuric and nitric acids for several hours, thoroughly rinsed with deionized water (Millipore) and allowed to dry under N_2. Given that all experiments were carried out with solvents that contained varying amounts of dissolved H_2O, no additional efforts were made to remove any H_2O film that likely remained adsorbed to the hydrophilic silica surface. Solution concentrations ranged from 1-10 mM. Smaller concentrations led to anticipated reductions in signal

intensity but not to qualitative changes in electronic resonance wavelengths or band shapes.

The SHG apparatus uses the 1 kHz output of a Ti:sapphire regeneratively amplified, femtosecond laser (Clark-MXR CPA 2001, 130 fs pulse duration, 700 μJ). The output of the Ti:sapphire laser pumps a commercially available visible optical parametric amplifier (OPA, Clark-MXR). The visible output of the OPA is tunable from 550 – 675 nm with a bandwidth of 2.5 ± 0.5 nm. The polarization of the incident beam is controlled using a Glan-Taylor polarizer and a half wave plate. The fundamental 775 nm and any SH light generated from preceding optics are blocked with a series of filters prior to the detector. The incident light impinges on the interface at an angle of 68˚ relative to the surface normal and the second harmonic response is detected in reflection using photon counting electronics. A second polarizer selects the SH polarization, and a short pass filter and monochromator serve to separate the signal from background radiation due to scattering or fluorescence.

All reported spectra were collected using p-polarized incident light, and passing p-polarized second harmonic signal. SH signals were normalized for incident power, and care was taken to confirm quadratic behavior of $I(2\omega)$ on $I(\omega)$ at all wavelengths. Spectra shown in this work represent the average of 2-4 separate experiments acquired on separate days with new solutions and freshly cleaned cells. Each data point in a spectrum represents the average of at least three, ten-second integrations of detected SHG signal.

2.3 Results and Discussion

Solvatochromic behavior of selected molecular ruler surfactants and NMMA, the parent solute appear in Figure 2.3. The f(e) scale used in Figure 2.3 extends only from 0.81 – 1.00 due to the surfactants' lack of solubility in nonpolar solvents. Data in Figure 2.3 are encouraging because they show the electronic structure of the NMMA-containing surfactant to be relatively insensitive to the functionalization that occurs at the 4-position *para* to the amine group. For the range of solvents tested, the excitation maxima of solutes at the end of the different length surfactants still reflect the 20 nm difference between strong hydrogen bond donating solvents and strong hydrogen bond accepting solvents. Furthermore, both the shorter (C_3) and longer (C_5) surfactants show no sign of *intra*molecular interactions that appeared in similar short chain, *polarity* sensitive, molecular ruler surfactants.[29] From the perspective of using these surfactants as probes of hydrogen bonding across liquid/liquid interfaces, these results indicate that experiments should measure the same observable – electronic

excitation wavelengths – regardless of surfactant alkyl chain length.

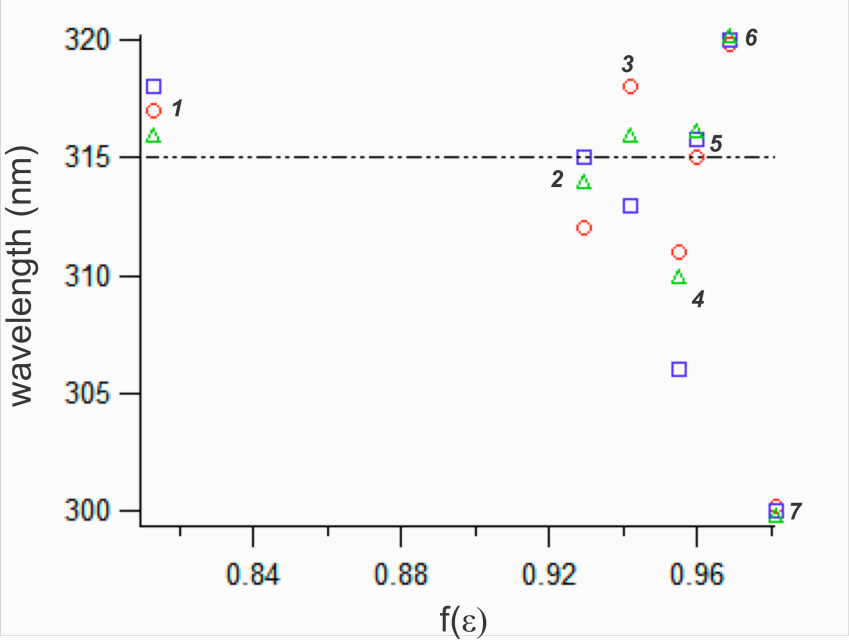

Figure 2.3: Comparison of the UV-Vis peak maximum wavelength responses of NMMA and molecular rulers of five and three chain lengths versus the Onsager polarity function. The x-scale only spans 0.81 – 0.98 due to the molecular rulers insolubility in alkanes. The solvents used: (1) tetrahydrofuran (2) propanol (3) ethanol (4) methanol (5) acetonitrile (6) dimethyl sulfoxide (7) water.

The second criterion that the molecular rulers must meet is that they must be surface active. Surface activity was determined by measuring surface pressure vs. concentration isotherms of surfactant rulers having different chain lengths. Figure 2.4 shows isotherms acquired for C_3 and C_5 surfactant rulers adsorbed to the aqueous/vapor and aqueous/cyclohexane interfaces. The first observation that stands out is that neither surfactant shows an affinity for the aqueous/vapor interface. Surface pressure rises almost linearly with concentration, and the effects of the molecular ruler surfactants on surface pressure are identical regardless of chain

length. If fit to a Gibbs isotherm, these data yield equivalent surface coverages of less than 2 x 10^{13} molecules/cm^2. At the aqueous/cyclohexane interface, however, these surfactants show activity more typical to that of common surfactants.[41,42] At this liquid/liquid boundary, surface pressure rises to asymptotic limits of ~12 mN/m for the C_3 surfactant and ~20 mN/m for the C_5 surfactant. Again, analyzing these data with a Gibbs isotherm yields surface excess concentrations of 1.1 ± 0.2 x 10^{14} and 1.4 ± 0.2 x 10^{14} molecules/cm^2 for the C_3 and C_5 surfactants, respectively.

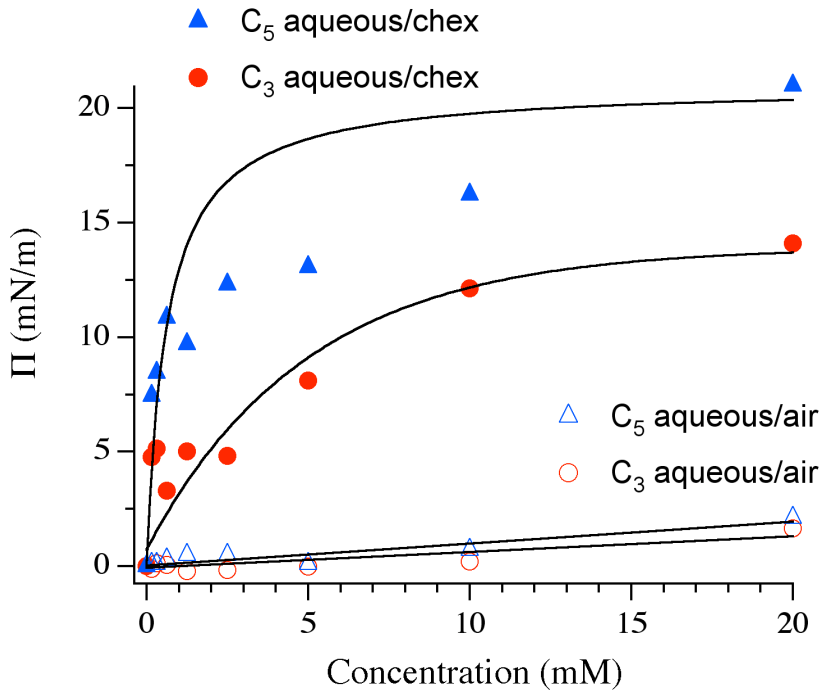

Figure 2.4: The surface pressure isotherms of the C_3 and C_5 molecular rulers at the aqueous/air and aqueous/cyclohexane interfaces. The solid lines are intended as guides for the eye.

The contrasting behavior of these surfactants at the aqueous/vapor and aqueous/cyclohexane interface is, at first glance, surprising. In general, most surfactants that adsorb to aqueous/organic interfaces show similar affinity for

aqueous/vapor interfaces.[43,44] However, given that the "hydrophobic" end of the surfactant consists of a secondary amine capable of both accepting and donating hydrogen bonds, one might reasonably anticipate that any surfactants adsorbed to the aqueous/vapor interface would adopt an orientation parallel to the surface. Such a geometry would allow the charged head-group to remain solvated in the aqueous phase while also allowing the aromatic amine group to form hydrogen bonds with the interfacial water molecules. This orientation would account for the very large terminal monolayer surface concentrations corresponding to 2×10^{13} molecules/cm^2 reported by the surface pressure measurements at the aqueous/vapor interface.

At the aqueous/cyclohexane interface, solubility considerations begin to override hydrogen bonding with the aqueous phase. As noted in the experimental section, simple partitioning measurements using a Beer's Law analysis to evaluate neutral solute concentrations in adjacent solvent phases, show the parent solute, NMMA, to be 4-fold more soluble in alkanes than in water. We propose that the energetic penalty paid by a molecular ruler when it adsorbs to the aqueous/vapor interface is lessened at the aqueous/alkane interface due to favorable solvation of the NMMA-containing tail in the organic phase. Allowing the solute to move away from the interface and become solvated more in the alkane would allow for more adsorption and the corresponding rise in surface excess concentration observed in these experiments. We note that the surface excess for the C_3 and C_5 surfactants compare favorably to the $\sim 8 \times 10^{13}$ molecules/cm^2 surface concentrations measured for polarity-sensitive cationic surfactants.[29] As was the case with the *p*-nitroanisole based, polarity sensitive surfactants, the longer chain surfactants form monolayers

having slightly higher surface coverage than the shorter surfactants. We attribute this difference to the greater hydrophobic character of the surfactant having the longer alkyl chain.

Table 2.2. Bulk solution and interfacial absorbance data of NMMA and the C_5^+ surfactant. Interfacial data are shown in Figure 5 and were acquired using resonance enhanced second harmonic generation. [a]NMMA adsorbed to the aqueous/CCl_4 liquid/liquid interface; [b]NMMA adsorbed to the cyclohexane/silica interface; [c]Short wavelength absorption of NMMA in a C_5^+ surfactant ruler adsorbed to the aqueous/methylcyclohexane interface and [d]Anticipated long wavelength excitation of NMMA in a C_5^+ surfactant ruler adsorbed to the aqueous/methylcyclohexane interface.

	HBD_{bulk} (nm)	NHB_{bulk} (nm)	HBA_{bulk} (nm)	Interface (nm)
NMMA	300	315	320	298[a]
				307[b]
C_5^+	300	316	320	306[c]
				328[d]

To evaluate the ability of NMMA and the newly synthesized surfactants to serve as probes of specific solvation across different interfaces, we carried out several resonance-enhanced SHG measurements. First, we examined the electronic structure of NMMA adsorbed both to silica/cyclohexane and aqueous/CCl_4 interfaces. We then measured the SHG spectrum of the C_5 surfactant adsorbed to the aqueous/methyl-cyclohexane interface. Results are shown in Figure 2.5 and Table 2.2.

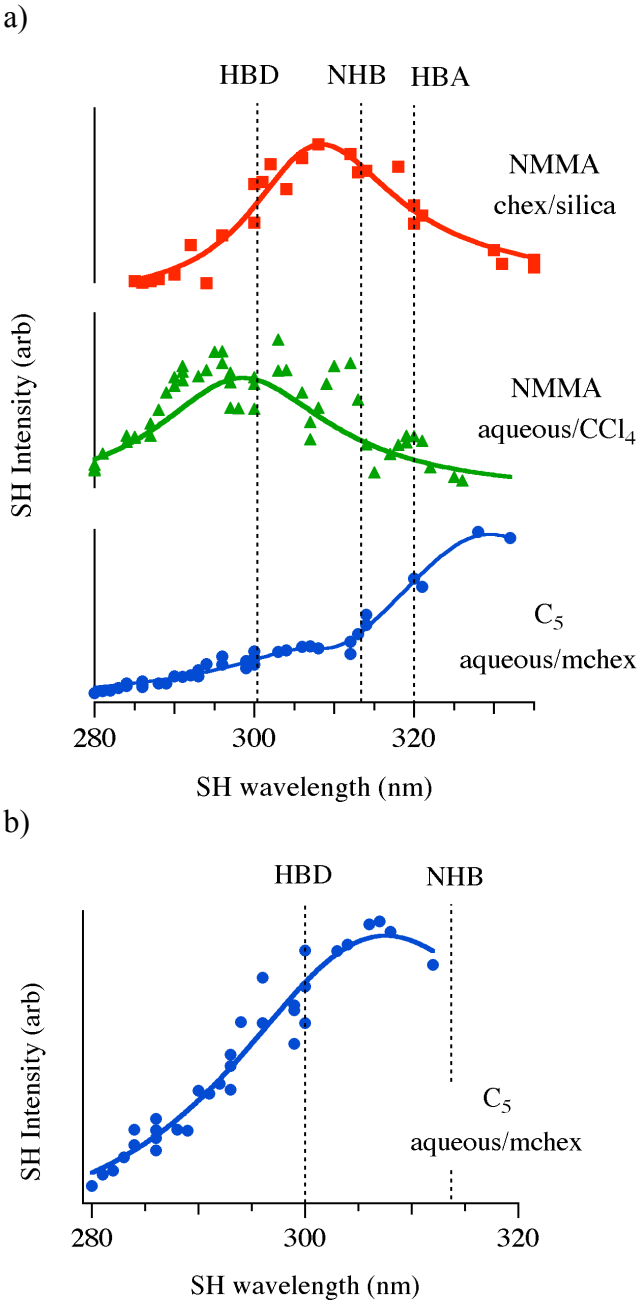

Figure 2.5: (a) Spectra show resonance enhanced SHG spectra of NMMA adsorbed to the cyclohexane/silica interface (top); the aqueous/CCl_4 interface (middle) and the C_5 surfactant adsorbed to the aqueous/methylcyclohexane interface. (b) An expanded view of the short wavelength data from the C_5 surfactant absorbed to the aqueous/methylcyclohexane interface, illustrating the small population of solute molecules that accept hydrogen bonds from nearby solvent donors.

The first experiment – NMMA adsorbed to the cyclohexane/silica liquid/solid interface – served both as a control as well as a test of photochemical stability. Earlier work has shown that indoline, a secondary amine resembling NMMA in several respects, is also a sensitive probe of specific solvation interactions. Furthermore, studies of indoline adsorbed to polar solid surfaces have shown that specific solvation interactions at these liquid/solid interfaces are dominated primarily by the hydrogen bond donating properties of the substrate, regardless of solvent identity.[45] Consistent with these findings, NMMA adsorbed to the cyclohexane/silica interface has an excitation wavelength of 307 ± 2 nm indicating that it interacts with the silica primarily by accepting hydrogen bonds donated by surface silanol groups. The relatively good signal/noise and clear resonance enhancement provide encouragement that NMMA and NMMA-based surfactants are capable of probing specific solvation interactions at liquid surfaces.

We next sought to test specific solvation at liquid/liquid interfaces. Due to experimental limitations that require both the incident and outgoing optical fields to pass through the top liquid phase, the aqueous/carbon tetrachloride interface was chosen to be representative of boundaries formed between water and nonpolar, immiscible organic solvents. For NMMA in equilibrium between two adjacent liquid phases, solute partitioning will lead to higher organic phase concentrations. Given that the outgoing SHG signal produced at the liquid/liquid interface must pass through one of the two liquids, NMMA solvated in bulk will necessarily absorb some of the SHG light. This consideration led us to use a nonpolar, immiscible organic solvent that was more dense than water. Like alkanes, CCl_4 is nonpolar (e = 2.2,

f(e) = 0.44) and forms an interface with water having a relatively high interfacial tension (44 mN/m compared to ~50 mN/m for alkane/water boundaries). The data shown in Figure 2.5 (middle panel) have been corrected for SH absorbance by the thin (~1.8 mm) path traveled by the surface produced SHG signal through the aqueous phase using the 1:4 partitioning coefficient between water and CCl_4.

Like NMMA adsorbed to the cyclohexane/silica interface, NMMA adsorbed to the aqueous/CCl_4 interface shows clear resonance enhancement and can be fit to a single feature centered at 298 ± 2 nm. While slightly outside of the solvatochromic window covered by strong hydrogen bond donating and accepting solvents, this result is consistent with interfacial NMMA molecules accepting strong hydrogen bonds from H_2O solvent molecules at the surface. This result is also consistent with recent studies that used surface specific vibrational spectroscopy to study hydrogen bonding and adsorption to aqueous/vapor interfaces. These vibrational experiments found the vibrational band frequencies and linewidths assigned to surface water molecules indicated stronger than expected intermolecular hydrogen bonding and less inhomogeneous broadening than in bulk solution. Additional evidence of stronger than expected hydrogen bonding at liquid/liquid interfaces comes from fluorescence studies of complexation at these boundaries. A thermodynamic analysis of enthalpy of hydrogen bond formation between modified riboflavin and triazine-triamine species at a water/CCl_4 interface demonstrated conclusively that hydrogen bonds formed at the interface were much stronger than those formed in bulk solution.[46-48]

The final SHG result presented in this work is the spectrum of the C_5 ruler surfactants adsorbed from 10 mM solutions to the aqueous/methyl-cyclohexane

interface. (Figure 2.5, bottom panel) These data are more difficult to interpret. At wavelengths above ~315 nm, the detected SH signal starts to rise dramatically and shows no sign of returning to baseline. Instrument limitations do not allow data acquisition beyond 335 nm. This unexpected response from NMMA-based, cationic surfactants was consistent, reproducible and invariant to 2-fold changes in surfactant bulk concentration. Furthermore, the observed behavior contrasts with that of the NMMA solute adsorbed to both liquid/solid and liquid/liquid interfaces. UV-VIS absorption data for both the neutral solute (in all solvents) and the cationic surfactants (in polar solvents) show a single electronic absorbance centered between 300 nm and 320 nm depending on the solvent-solute hydrogen bonding. Looking at the C_5 data more closely, one sees evidence of a second, weak resonance feature centered near ~310 nm before the signal levels begin to rise abruptly. Fitting just the short wavelength data (<315 nm) leads to a calculated excitation wavelength of 306 ± 2 nm. (Figure 2.5b) This result indicates that some solutes at the ends of cationic surfactants remain associated with water molecules and that the water molecules are donating hydrogen bonds to the amine lone-pair. The strength of this hydrogen bonding is comparable to the hydrogen bonding NMMA experiences at the silica/alkane interface.

We are uncertain about how to interpret the growth in signal intensity at longer wavelengths. The reproducibility of this effect demonstrates that the presence of the C_5^+ cationic surfactants is changing the nonlinear susceptibility of the liquid/liquid interface. Whether or not this effect reflects resonance enhancement would require tuning the incident light to longer wavelengths and observing if the SH

signal returns to baseline. If the full data set is fit to two features (with one held at 306 nm), then the second feature is predicted to have a resonance wavelength of 328 nm. This result lies well outside of NMMA's solvatochromic window in bulk solution, but would be consistent with a strong hydrogen bond accepting partner associated closely with the proton of the NMMA secondary amine.

2.4 Conclusion

Experiments described in this work used nonlinear optical spectroscopy to characterize specific solvation interactions at interfaces and differentiate how specific solvation at liquid/liquid and liquid/solid interfaces is different from bulk solution limits. In this context, specific solvation refers to localized, directional interactions between a solute and its surroundings. N-methyl-*p*-methoxyaniline (NMMA) is a solute whose electronic structure changes very little in non-hydrogen bonding solvents regardless of solvent polarity. In hydrogen bond accepting solvents, however, the lowest energy, allowed electronic transition shifts 5 nm to longer wavelengths (315 to 320 nm), while in strong hydrogen bond donating solvents such as water or methanol, excitation corresponding to the same electronic transition blue-shifts substantially (from 315 nm to 300 nm).

To take advantage of NMMA's sensitivity to hydrogen bonding opportunities and examine how specific solvation changes across liquid/liquid interfaces, NMMA was integrated into a surfactant structure to form variable length, surface active species dubbed hydrogen bonding molecular rulers. The synthetic strategy couples NMMA to cationic, quaternary ammonium headgroups with variable length alkyl chains. NMMA itself is 4 times more soluble in alkanes than in water, meaning that

at aqueous/organic interfaces, the NMMA solute should solvate itself in the nonpolar phase while the charged headgroup remains solvated in the aqueous phase. At aqueous/alkane interfaces, the NMMA-based molecular ruler surfactants show similar surface activity as other quaternary ammonium alkyl surfactants.

Resonance enhanced second harmonic generation (SHG) was used to exploit NMMA's sensitivity to hydrogen bonding opportunities by measuring effective excitation spectra of NMMA and surfactants containing NMMA adsorbed to liquid/solid and liquid/liquid interfaces. NMMA adsorbed to an alkane/polar silica surface as well as to an aqueous/CCl_4 surface showed evidence of strong hydrogen bonding with the solvent (or surface silanol groups of silica) functioning as strong hydrogen bond donating species. In contrast, at an aqueous/alkane liquid/liquid interface, NMMA attached to a 5 carbon C_5^+ molecular ruler surfactant appears to sample two distinct types of specific solvation. A minority population has an excitation wavelength of ~307 nm, consistent with being in a moderately strong hydrogen bond donating environment. A second, majority population appears to sample an environment capable of *accepting* very strong hydrogen bonds as evidenced by an excitation wavelength much longer than what is predicted based on NMMA's solvatochromic window. If, in fact, this second assignment is correct, then the result implies that solutes migrating across the aqueous/alkane liquid/liquid interface can carry with them solvent species that accept hydrogen bonds from the solutes themselves.

2.5 References

(1) Suppan, P.; Ghoneim, N. *Solvatochromism*, 1st ed.; The Royal Society of Chemistry: London, 1997.

(2) Wu, Y. G.; Tabata, M.; Takamuku, T. *J. Soln. Chem.* **2007**, *31*, 381.

(3) Quantitative treatments of solute/solvent interactions; Politzer, P.; Murray, J. S., Eds.; Elsevier: Amsterdam, 1994.

(4) Onsager, L. *J. Am. Chem. Soc.* **1936**, *58*, 1486.

(5) Mellein, B. R.; Aki, S. N. V. K.; Ladewski, R. L.; Brennecke, J. F. *J. Phys. Chem. B* **2007**, *111*, 131.

(6) Tomasi, J.; Mennucci, B.; Cammi, R. *Chem. Rev.* **2005**, *105*, 2999.

(7) Matyushov, D. V.; Schmid, R.; Ladanyi, B. M. J. *Phys. Chem. B* **1997**, *101*, 1035.

(8) Benjamin, I. *Ann. Rev. Phys. Chem.* **1997**, 48, 407.

(9) Benjamin, I. *Chem. Rev.* **2006**, *106*, 1212.

(10) Chowdhary, J.; Ladanyi, B. M. *J. Phys. Chem. B* **2006**, *110*, 15442.

(11) Eisenthal, K. B. *Chem. Rev.* **1996**, *96*, 1343.

(12) Hayes, P. L.; Malin, J. N.; Konek, C. T.; Geiger, F. M. *J. Phys. Chem. A* **2008**, *112*, 660.

(13) Israelachvili Intermolecular and Surface Forces; 2nd ed.; Academic Press: New York, 1992.

(14) McFearin, C. L.; Beaman, D. K.; Moore, F. G.; Richmond, G. L. *J. Phys. Chem. C* **2009**, *113*, 1171.

(15) Mitrinovic, D. M.; Tikhonov, A. M.; Li, M.; Huang, Z. Q.; Schlossman, M. L. *Phys. Rev. Lett*. **2000**, *85*, 582.

(16) Shen, Y. R. *Ann. Rev. Phys. Chem.* **1989**, *40*, 327.

(17) Ishizaka, S.; Kinoshita, S.; Nishijima, Y.; Kitamura, N. *Anal. Chem.* **2003**, *75*, 6035.

(18) Ishizaka, S.; Kitamura, N. *Anal. Sciences* **2004**, *20*, 1587.

(19) Steel, W. H.; Beildeck, C. L.; Walker, R. A. *J. Phys. Chem. B* **2004**, *108*, 16107.

(20) Steel, W. H.; Lau, Y. Y.; Beildeck, C. L.; Walker, R. A. *J. Phys. Chem. B* **2004**, *108*, 13370.

(21) Steel, W. H.; Walker, R. A. *Nature* **2003**, *424*, 296.

(22) Steinhurst, D. A.; Owrutsky, J. C. *J. Phys. Chem. B* **2001**, *105*, 3062.

(23) TamburelloLuca, A. A.; Hebert, P.; Antoine, R.; Brevet, P. F.; Girault, H. H. *Langmuir* **1997**, *13*, 4428.

(24) Wang, H. F.; Borguet, E.; Eisenthal, K. B. *J. Phys. Chem. A* **1997**, *101*, 713.

(25) Wang, H. F.; Borguet, E.; Eisenthal, K. B. *J. Phys. Chem. B* **1998**, *102*, 4927.

(26) Zhang, X. Y.; Cunningham, M. M.; Walker, R. A. *J. Phys. Chem. B* **2003**, *107*, 3183.

(27) Zhuang, X.; Miranda, P. B.; Kim, D.; Shen, Y. R. *Phys. Rev. B* **1999**, *59*, 12632.

(28) Tsukahara, S.; Watarai, H. *Chemistry Letters* **1999**, 89.

(29) Beildeck, C. L.; Steel, W. H.; Walker, R. A. *Langmuir* **2003**, *19*, 4933.

(30) Steel, W. H.; Damkaci, F.; Nolan, R.; Walker, R. A. *J. Am. Chem. Soc.* **2002**, *124*, 4824.

(31) Benjamin, I. *Chem. Phys. Lett* **2004**, *393*, 453.

(32) Napoleon, R. L.; Moore, P. B. *J. Phys. Chem. B* **2006**, *110*, 3666.

(33) Pingali, S. V.; Takiue, T.; Luo, G.; Tikhonov, A. M.; Ikeda, N.; Aratono, M.; Schlossman, M. L. *J. Disp. Sci. Tech.* **2006**, *27*, 715.

(34) Schlossman, M. L.; Tikhonov, A. M. *Ann. Rev. Phys. Chem.* **2008**, *59*, 153.

(35) Sloutskin, E.; Bain, C. D.; Ocko, B. M.; Deutsch, M. *Faraday Disc.* **2005**, *129*, 339.

(36) Esenturk, O.; Walker, R. A. *Phys. Chem. Chem. Phys.* **2003**, *5*, 2020.

(37) Novaki, L. P.; El Seoud, O. A. *Phys. Chem. Chem. Phys.* **1999**, *1*, 1957.

(38) Reichardt, C. *Chem. Rev.* **1994**, *94*, 2319.

(39) Catalan, J. *J. Org. Chem.* **1997**, *62*, 8231.

(40) Laurence, C.; Nicolet, P.; Dalati, M. T.; Abboud, J. L. M.; Notario, R. *J. Phys. Chem.* **1994**, *98*, 5807.

(41) Rosen, M. J. Surfactants and Interfacial Phenomena, 3rd Edition, 2004.

(42) Hiemenz, P. C.; Rajagopalan, R.; Editors Principles of Colloid and Surface Chemistry; 3rd ed., 1997.

(43) Carnali, J. O.; Shah, P. *J. Phys. Chem. B* **2008**, *112*, 7171.

(44) Yaseen, M.; Lu, J. R.; Webster, J. R. P.; Penfold, J. *Langmuir* **2006**, *22*, 5825.

(45) Brindza, M. R.; Walker, R. A. *J. Am. Chem. Soc.* **2009**, *131*, 6207.

(46) Benjamin, I. *J. Phys. Chem. B* **2005**, *109*, 13711.

(47) Ishizaka, S.; Nishijima, Y.; Kitamura, N. *Anal. Bioanal. Chem.* **2006**, *386*, 749.

(48) Sovago, M.; Kramer-Campen, R.; Bakker, H. J.; Bonn, M. *Chem. Phys. Lett.* **2009**, *470*, 7.

Chapter 3: The Effects of Solvent Structure on Interfacial Polarity at Strongly Associating Silica/Alcohol Interfaces

3.1 Introduction

Interfacial solvation will depend sensitively on a subtle balance of solute-substrate, solute-solvent, *and* substrate-solvent interactions. Here, the term solvation is used to describe the local environment experienced by a solute. Interfacial solvation has often been described in terms of averaged contributions from the two adjacent phases.[1-6] Such models have proven successful at describing solvation across weakly associating interfaces characterized by large excess free energies. When experimental findings differ from predictions of this "averaged" model of interfacial solvation, results can usually be rationalized in terms of complex solvent structure that reorganizes under the constraint of reduced mobility and strong, directional forces imposed by the surface.[1,5,7-13] These interphase substrate-solvent interactions form local domains having properties that do not arise in bulk solution. Only recently have researchers begun to report how more subtle effects such as solute orientation and solute solubility in bulk solution can influence interfacial solvation.[9,14-19]

Strongly associating solid/liquid interfaces are characterized by low interfacial energies and strong, directional interactions between the substrate and the solvent. These forces impose long-range structure on the adjacent solvent that can extend several solvent diameters into bulk solution.[17,20-24] The effects of solid surfaces on solvent structure remain an area of active investigation. Fundamental studies attempt

to isolate and quantify asymmetric, intermolecular interactions, while empirical investigations parameterize inter-phase forces between solid substrates and different solvent mixtures to improve chromatographic separations and to tune surface reactivity.[25-33]

The affinity of a solute for a surface strongly influences adsorption energetics and the resulting environment that a solute samples. In the case of strong solute-substrate associations, *solvent* identity may not play a significant role in interfacial solvation. However, if *solvent*-substrate interactions are significantly stronger than those between the *solute* and substrate, then solute molecules might not accumulate at an interface at all. An example of how these competing energetics affect interfacial phenomena comes from detailed studies of adsorption and retention in chromatographic systems.

Wirth and co-workers reported tailing and line-broadening in model liquid chromatography measurements and assigned this effect to strong associations between solutes and the silica substrates.[29] They noted that this behavior occurs at both low and neutral pH values with neutral pH values leading to longer retention times and more broadening. Rendering the mobile phase acidic reduces retention time, but still results in eluent tailing due to strong adsorption sites on the silica composed of acidic silanols. Broadening that occurs at neutral pH values is assumed to be driven by Coulomb interactions between the negatively charged substrate and solute. Taken together, these studies illustrate how bulk solvent properties can affect interfacial solvation and retention of solute molecules at solid/liquid interfaces.

Another aspect of interfacial solvation that has motivated interest is the role of solvent structure on solute organization. For example, the self-assembly of alkythiols from the gas phase onto metals such as gold is well characterized, but self-assembly of thiols from solution onto metal surfaces is less well understood.[34-36] Calvente and Andreu[16] have recently reported that alkylthiols adsorbed to electrified aqueous/mercury interfaces will adopt a prostrate position on the mercury surface. The authors monitored the change in orientation of thiols to an upright position on the mercury electrode after the introduction of different solvent mixtures. The change in orientation was inferred from a narrowing of the voltammetric line width when the solute was in the presence of high concentrations of either ethanol or acetonitrile. Based on their surface specific vibrational studies, Buchbinder and Geiger have observed similar solute reorientation in binary solvent mixtures at alumina/*n*-hexanol-cyclohexane solid/liquid interfaces.[15] Both the electrochemical and spectroscopic studies provide empirical benchmarks that can be used to evaluate qualitatively the role that solvent composition plays in controlling solute solvation and organization at surfaces. Understanding the effects of solvent structure on interfacial solvation is essential to the development of models describing solution phase surface chemistry.

The role of interfacial solvation – particularly solvation of solutes at silica/alcohol interfaces – is important in many industrial applications.[26,37-40] For example, a scarcity of commercially produced acetonitrile in 2008-2009 motivated many laboratories to search for suitable alternatives to use in liquid chromatography (LC) applications.[26,38,41,42] Acetonitrile is often the preferred solvent in LC experiments because of its elution strength and low backpressure and also because it

is polar, aprotic and water-miscible. These characteristics are important for both reversed phase chromatography and ion-pair reversed phase chromatography. Methanol, ethanol and n-propanol were tested as substitutes despite their protic properties.[38] Brettschneider et al. determined that ethanol as a carrier solvent showed comparable and at times better performance than acetonitrile in separating polyphosphates and proteins. The protic nature of ethanol did not negatively impact the ability of the mobile phase to separate large molecules, and ethanol is considered a "green" solvent due to its low toxicity, renewability, and ease of disposal.[41,42]

Experiments described in this chapter use resonance-enhanced second harmonic generation (SHG) spectroscopy to examine adsorption and polarity at hydrophilic silica/methanol and silica/ethanol solid/liquid interfaces. Both solvents are polar and capable of forming strong hydrogen bonds, and both solvents wet hydrophilic silica completely. The solute used in these studies is *p*-nitroanisole (pNAs, Figure 3.1).

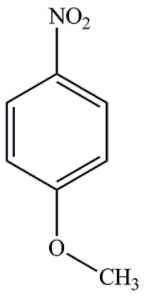

pNAs

Figure 3.1: The structure of *p*-nitroanisole (pNAs) the solute used in these experiments. This solute is sensitive solely to solvent polarity.

pNAs has been used to formulate semi-empirical scales describing solvent polarity.[43] The solute has a larger excited state molecular dipole relative to its

respective ground state meaning that the excitation energy shifts to lower energy with increasing solvent polarity.[44] The solvatochromic window of pNAs stretches from 294 nm in alkanes to 318 nm in very polar solvents. Similar excitation wavelengths in both H_2O (317 nm) and DMSO (318 nm) illustrate this solute's insensitivity to specific solvation interactions such as hydrogen bonding. By measuring the excitation wavelength of pNAs at the silica/air, silica/methanol, and silica/ethanol interfaces, we explore the role of solvent structure on interfacial solvation at strongly associating solid/liquid interfaces.

3.2 Experimental Methods

3.2.1 SHG Measurements

In Equation 1.6, the μ_{ij} correspond to transition matrix elements and the summation runs over all real and virtual excitation energies. Tuning the frequency of the incident light and measuring I(2ω) leads to effective excitation spectra of those molecules subject to interfacial anisotropy. This approach has been used in previous studies to characterize the dielectric and time-dependent properties of solutes at surfaces.[2-5,14,45-53] An important point to note is that the nonresonant contribution to the second order susceptibility is intrinsic to all interfacial systems and can lead to asymmetry in resonance enhanced line shapes. Depending on its magnitude and sign, $\chi^{(2)}_{NR}$ can result in calculated excitation wavelengths that differ noticeably from the experimentally measured λ_{max}. For spectra presented in this work this difference

between λ_{max} as measured in the spectrum and λ_{exc} as calculated from Eq. 1.6 can be as large as 4 nm.

The SHG spectrometer uses the output of a 1kHz regeneratively amplified, femtosecond laser (Coherent, Libra-HE, 85 fs pulse duration, 3.6W) to pump a visible optical parametric amplifier (Coherent, OPerA Solo). The second harmonic output of the OPA is tunable from 467 to 810 nm with a bandwidth of 10 nm. The polarization of the incident beam is controlled with a Glan-Taylor polarizer and a half wave plate fitted with a filter to remove inherent second harmonic signal generated in the crystal. The fundamental light impinges on the sample surface at an angle of 67° (relative to the surface normal), and the second harmonic signal is collected in a reflected geometry after passing through a series of polarizing optics and filters to remove remaining incident light.

Spectra are acquired by tuning a monochromator/photomultiplier tube assembly to the second harmonic wavelength being generated at the sample. Data are represented by the average of 3 – 4 10-second acquisitions with photon counting electronics. Typical uncertainties for SH-λ_{max} values are ± 2 – 3 nm. We note that linewidths in SH spectra are generally more narrow than in linear absorption or emission spectra due to the quadratic dependence of the signal on incident power,[5] but surface heterogenity can, in some instances, lead to broader linewidths if the interface is sufficiently heterogeneous.[54] The average molecular orientation of pNAs at the different interfaces was determined from the polarization dependent SH response.[55-58] The polarization dependent intensity was fit using previously reported elements of the pNAs hyperpolarizability.[14]

3.2.2 Sample Preparation

The solute and solvents used in these experiments were purchased and used without further purification. To measure the response of pNAs at the silica/vapor interface, a film was formed on a silica slide that had been cleaned in a 50:50 (v:v) mixture of sulfuric and nitric acids and rinsed with 18 MΩ H2O. The slides dried and were then allowed to equilibrate with a 50 mM solution of pNAs in cyclohexane. This concentration was chosen based on signal intensity considerations. SH spectra of films formed from lower bulk concentration solutions were weak with larger uncertainties in the fitting parameters. Films were allowed to air dry and SH spectra were acquired within 60 min of slides being removed from solution. Based on isotherm data that show pNAs adsorption approaching an asymptotic limit with increasing bulk concentration and the absence of any noticeable interference effects that could arise from adjacent layers, we assume that the pNAs film at the silica/vapor interface is no thicker than the thickness of a single monolayer. Resonance enhanced SHG spectra of pNAs adsorbed to the silica/methanol and silica/ethanol interfaces were taken with 200 mM solutions of pNAs. The silica slides and Teflon sample cells were similarly prepared by cleaning all pieces in the 50:50 mixture of sulfuric and nitric acids. SH spectra from the solid/liquid interfaces were taken within 120 min of samples being prepared, although waiting additional time led to no change in linewidths or peak wavelengths.

Table 3.1. Data below report the bulk and interfacial λ_{max} values for pNAs in different solvents. The calculated Onsager polarity function values are also listed for each of the solvents, as well as the effective constants of the interfacial regions based on λ_{max} measured by SHG. The average molecular orientations of pNAs at the different interfaces and the calculated Gibbs free energy of adsorption values are also listed for the alcohol interfaces.

solvent	f(ε)	pNAs λ_{max} (nm)	Orientation (θ)	ΔG_{ads} (kJ/mol)
water	0.98	317		
dmso	0.97	317		
methanol	0.95	313		
ethanol	0.94	311		
methyl-cyclohexane	0.41	294		
gas-phase[69]	0	277		
silica/vapor	"0.94"	314 ± 2	35° ± 6.0°	
silica/methanol	"0.75"	307 ± 3	31° ± 1.3°	-23.1 ± 1.0
silica/ethanol	">1"	323 ± 3	31° ± 8.8°	-25.6 ± 1.3

To quantify the surface activity of pNAs for the silica/methanol and silica/ethanol systems, adsorption isotherms were acquired using 9 different solutions of pNAs having concentrations ranging from 8 to 200 mM. After allowing the system to equilibrate, single wavelength intensity measurements were made from several different locations at the silica/liquid interface. Results were averaged for each concentration and the square roots of the intensities were plotted as a function of bulk solution concentration. In the limit that average adsorbate orientation does not depend on surface coverage, the square root of the signal intensity is directly proportional to the number of adsorbed species. Data were fit to a Langmuir isotherm[59] and results for the silica/methanol and silica/ethanol interfaces are reported in Figure 3.2 & Table 3.1.

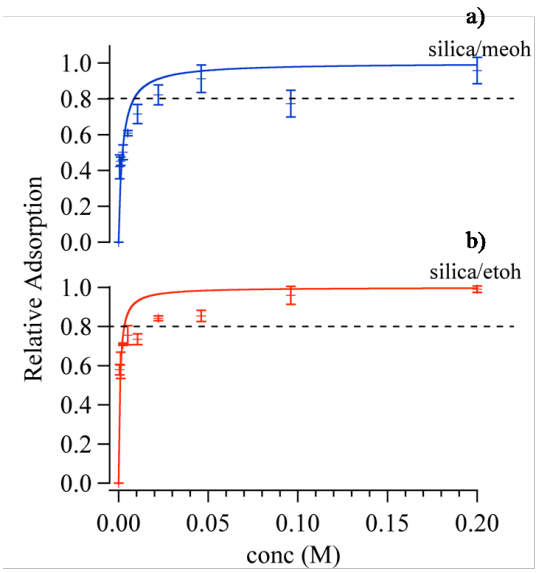

Figure 3.2: The isotherm data for pNAs at the silica/methanol (a) and silica/ethanol (b) interfaces. The silica/methanol interface gives rise to a Gibbs free energy of adsorption value of -23.1 ± 1.0 kJ/mol and the silica/ethanol interface has a Gibbs free energy of adsorption of -25.6 ± 1.3 kJ/mol. A dashed line for each isotherm marks the 80% relative surface coverage for each system where the data begin to deviate from Langmuir expected trend lines.

3.3 Results and Discussion

3.3.1 Adsorption Behavior

Adsorption isotherms were acquired for pNAs at both solid/liquid interfaces. If the average orientation does not change significantly with surface coverage, then we can equate N with $(I(2\omega))^{1/2}$ provided that $I(2\omega)$ depends only on a single element of the nonlinear susceptibility. Figure 3.2 shows normalized $(I(2\omega))^{1/2}$ data acquired at peak wavelengths (*vide infra)* using the $S_{out}M_{in}$ polarization combination. Data were fit with the Langmuir adsorption isotherm:[59]

$$\theta = \frac{\alpha C}{1 + \alpha C} \tag{3.1}$$

where θ is the relative surface coverage, α is a constant (=(θ/(1-θ)C_1), and C is the concentration of the bulk solution. At the silica/liquid interface one can describe the equilibrium between solutes in solution and potential binding sites on the silica surface with the following equilibrium expression:

$$M + ES \xleftrightarrow{k_{ads},k_{des}} FS \tag{3.2}$$

where M are bulk molecules, ES are empty sites on the silica surface, k_{ads} and k_{des} are the rates of adsorption and desorption, respectively, and FS are filled sites on the silica surface. At equilibrium for the sample the adsorption of the solute to the interface can be defined as:

$$\frac{dN}{dt} = 0 = k_1 \frac{C_1}{C_2}(N_{max} - N) - k_2 N \tag{3.3}$$

where N_{max} is the maximum number of adsorbed molecules at monolayer coverage, N is the number of adsorbed molecules at the interface, C_1 is the bulk concentration of the solution and C_2 is the solvent concentration. The equation can then be rearranged so that:

$$\frac{1}{N} = \frac{a}{N_{max} C_1} + \frac{1}{N_{max}} \tag{3.4}$$

where a is the Langmuir constant (=$C_2 \exp(\Delta G_{ads}/RT)$ where C_2 is the solvent concentration.) Given that I_{SHG} is proportional to N_{ads}, the inverse of the square root of the relative signal versus the inverse of concentration (in molarity) can be plotted and the slope is proportional to the fitting parameter a. Analyzing our adsorption data with Equation 3.4 we determine a and can then calculate the Gibbs free energy of solute adsorption to the solid/liquid interface.

The isotherms obtained for pNAs at the silica/methanol and silica/ethanol interfaces are also plotted in Figure 3.2. The fits lead to very similar pNAs adsorption energies for the two interfaces. ΔG_{ads} of pNAs to the silica/methanol interface is -23.1 ± 1.0 kJ/mol and to the silica/ethanol interface is -25.6 ± 1.3 kJ/mol. These values are slightly larger than the strength of a single hydrogen bond (~15 – 20 kJ/mol) and are consistent with a model where the solute is accepting strong hydrogen bonds from surface silanol groups.[14,29,31] The small deviations from Langmuir-film behavior observed at relatively high surface coverages (q ~ 0.75) may reflect the silica surface's known heterogeneity.[30,60,61]

3.3.2 Solvatochromic Behavior

The solvatochromic behavior of pNAs is well documented and this popular solute is one of several solutes used to define the empirical π* solvent polarity scale.[43,62] Upon excitation to the S_1 excited state, pNAs undergoes a large enhancement of its molecular dipole relative to the ground state meaning that the excitation energy of pNAs shifts to lower energy with increasing solvent polarity.[44] To quantify solvent polarity, we use the Onsager polarity function:[63]

$$f(\varepsilon) = \frac{2(\varepsilon - 1)}{2\varepsilon + 1} \tag{3.5}$$

where ε is the static dielectric constant of the solvent. f(ε) ranges from 0.4 in low dielectric solvents (such as alkanes, ε ~ 2.0) to ~1.0 in high dielectric media such as water (ε ~ 80). The solvatochromic behavior of pNAs is illustrated in Table 3.1 where the solute's excitation wavelengths in a range of solvents are reported.

3.3.3 Interfacial Solvatochromism

Effective excitation spectra of pNAs adsorbed to the silica/vapor and silica/alcohol interfaces were measured by SHG spectroscopy and compared to bulk solution results. Figure 3.3 shows the resonance enhanced SHG spectra of pNAs adsorbed to the silica/vapor, silica/methanol and silica/ethanol interfaces. Excitation maxima of pNAs at these three boundaries are 314 nm (silica/vapor), 307 nm (silica/methanol) and 323 nm (silica/ethanol). Superimposed on the spectra are the bulk excitation maxima for pNAs in bulk alkanes and water, as well as the interfacial excitation wavelengths resulting from fitting the SHG data to Equation 1.6. At the silica/vapor interface, assuming air to be an extremely nonpolar "solvent," an averaged model would predict that the interface should be moderately polar due to substrate-adsorbate interactions. Here, an averaged model describes an interface whose properties are simply weighted averages of properties of both bulk phases. While the 314 nm excitation wavelength of pNAs at the silica/vapor interface falls between polar and nonpolar solvatochromic limits of 317 nm and 294 nm, respectively, the result lies much closer to the polar edge. This result implies a very strong association between pNAs and the surface silanol groups; consistent with previous studies of solvent polarity at silica/alkane interfaces.[5,14]

a)

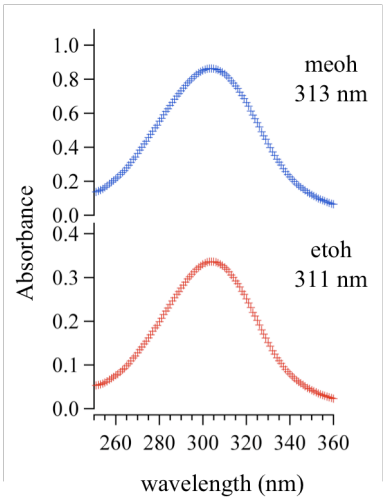

b)

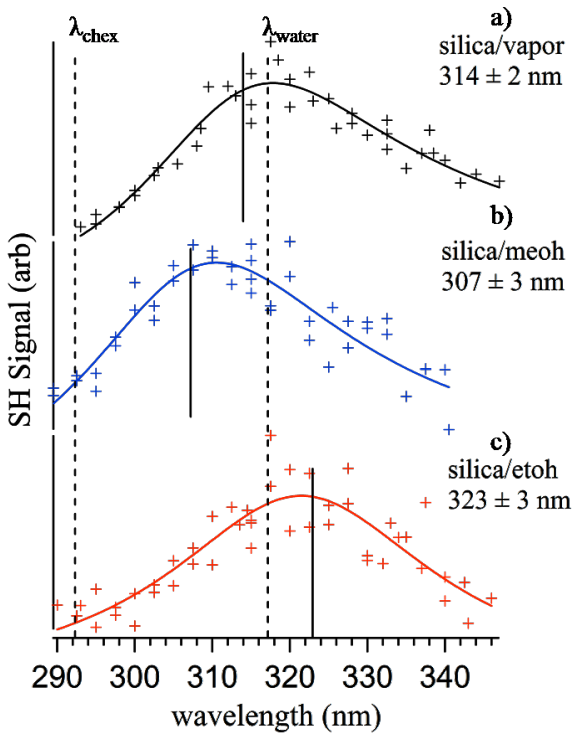

Figure 3.3: (a) The bulk excitation maxima of pNAs in methanol (top, 313 nm) and ethanol (bottom, 311 nm). The width of the absorbance spectra (~53 nm) are more than twice as wide as the SH spectra (~ 20 nm) shown in Figure 3.3(b). (b) The SH spectra of pNAs at the silica/vapor (black), silica/methanol (blue), and silica/ethanol (red) interfaces. The dashed lines represent bulk excitation maxima for pNAs in alkanes and water. The solid lines are the calculated interfacial maxima for pNAs at the corresponding interface.

Data from the silica/methanol and silica/ethanol interfaces present a curious dilemma. The excitation wavelength of pNAs in bulk methanol is 313 nm. If one assumes an average polarity description of the silica/methanol interface, and knowing that the silica/vapor interface is sufficiently polar to induce a 314 nm excitation wavelength in adsorbed pNAs, one would expect the excitation wavelength of pNAs adsorbed to this boundary to also be approximately 314 nm. Instead the data show the silica/methanol interface to be decidedly less polar than either bulk methanol or the silica/vapor interface with adsorbed pNAs having an excitation wavelength of 307 nm at this solid/liquid boundary. In bulk solution this excitation wavelength would correspond to being solvated in a lower dielectric solvent such as acetone or 1-propanol.

Nonpolar environments have been observed previously at interfaces between silica and longer chain *n*-alcohols ($n \geq 3$).[53] These results were interpreted in terms of surface induced structuring of interfacial solvent species creating alkane like regions. Methanol is small and unable to form such a Langmuir-like structure. However, because of its size, methanol *can* hydrogen bond effectively to the surface silanol groups, thereby reducing the unscreened interfacial dipole density and, apparently, interfacial polarity. Methanol's heat of adsorption to silica (from the gas phase) has been reported to be -60 ± 4 kJ/mole at high coverages.[64] This strong affinity of methanol for the silica surface will limit the surface activity of pNAs.

A similar argument can help explain why the silica/ethanol interface appears remarkably polar to adsorbed pNAs solutes. Ethanol will associate with a silica substrate through the same mechanism as methanol (accepting and donating hydrogen

bonds with the surface silanol groups). In fact, the heat of adsorption of ethanol to silica is -54 ± 4 kJ/mole,[64] comparable to the methanol result and implying similar substrate-solvent interactions. Assuming equivalent hydrogen bonding between the ethanol and silica as between methanol and silica, ethanol's will occupy an area that is ~50% larger than that of methanol based simply on geometric considerations. This difference in solvent size can leave the silica surface with free silanol groups not hydrogen bonded to the adjacent solvent. Furthermore, adsorbed ethanol will not have alkyl chains that are long enough to exploit cohesive, van der Waals interactions that lead to the formation of nonpolar regions observed at interfaces formed between silica and longer, *n*-alcohol solvents.[24,39,53,65]

Support for the notion that interfacial polarity depends sensitively on solvent structure can be found in surface specific vibrational studies of methanol adsorbed to a silica substrate.[66,67] Shen and co-workers reported that adsorbed methanol adopts well defined structure with the methyl group directed ~35° away from the surface normal.[66] At the silica/bulk methanol solid/liquid interface, the vibrational signal virtually disappears implying that the second solvent layer directs its methyl group towards the surface creating a hydrophobic bilayer structure with approximate inversion symmetry.[66] If this picture is correct, then the interfacial methanol species can effectively screen the surface silanol groups of the substrate from the adsorbed solutes. Furthermore, noncovalent association between adjacent methanol layers must be sufficiently strong to inhibit methanol from solvating adsorbed solutes. If interfacial pNAs sampled methanol-like polarity we would expect an SH excitation wavelength closer to the bulk 314 nm limit and not the observed 307 nm.

As noted above, the ethyl groups are sufficiently large enough to prevent ethanol molecules from occupying all surface silanol sites. Harrison et al. have studied the behavior of odd and even numbered alkyl chains self-assembled to a substrate.[68] They determined that odd numbered alkyl chains have terminal methyl groups at an angle of 27° from the surface normal, a result that is relatively close to the 35˚ calculated by Shen and coworkers from the surface spectra of methanol. Even numbered alkyl chains have their terminal methyl groups angled 58° away from the surface normal. These geometric conditions result in adsorbed ethanol molecules occupying approximately twice the area of a methanol molecule at the silica surface (Figure 3.4.)

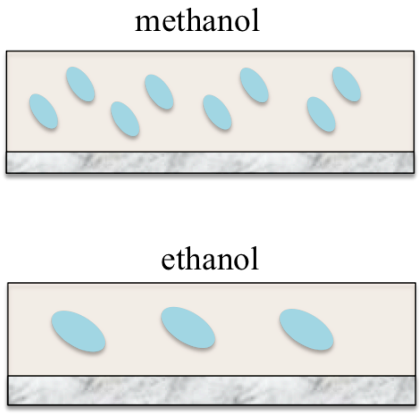

Figure 3.4: The ethanol molecules occupy approximately 1.5 times more area than methanol molecules at the silica surface. Based on molecular dynamics simulations and geometric considerations, we assume that interfacial ethanol hydrogen bound to the silica surface is oriented with the terminal methyl group ~30 degrees closer to the interfacial plane than the methanol molecules.

Given these considerations we expect the silica/ethanol interface to have more unscreened surface silanol groups that are free to associate strongly with adsorbed pNAs solutes. A consequence of this scenario would be a silica/ethanol interface that appears decidedly more polar than the silica/methanol interface. The fact that

interfacial solvation presents pNAs with a polarity that is even greater than the silica/vapor interface (where all surface silanol groups are unscreened) can be rationalized by considering the cooperative effect that the substrate and solvent can have on a solute's local dielectric environment. Solvent polarity is a nonspecific solvation property meaning that the interactions between a solute and its surroundings are averaged over the entire solute cavity.[14,63] When adsorbed to the silica/ethanol interface, pNAs can associate with unscreened surface silanol groups *and* sample favorable long range interactions with the surrounding ethanol solvent. To explain the data shown in Figure 3.3, we propose that the immediate, short range interactions (between pNAs and the surface silanol groups) and the averaged, longer range interaction (between pNAs and the ethanol solvent) conspire to create a local dieletric environment for pNAs at the silica/ethanol interface that is even more polar than what pNAs experiences in bulk aqueous and DMSO solutions. Despite not having the means to test this hypothesis directly, we note that our observations provide data that can be used to benchmark newly developed models of solvation at solid/liquid and liquid/liquid interfaces.

3.3.4 Average Orientation Measurements

The average molecular orientations of pNAs at the three interfacial regions were calculated to determine if differences in apparent interfacial polarity correlate with differences in solute organization at the surface. By monitoring the P-polarized SHG response of the molecule at varying incident polarization and the S-polarized SHG response at a mixed (or 45°) incident polarization and assuming a δ-function

distribution, the individual components of the surface nonlinear susceptibility tensor can be calculated:[14,56-58]

$$I_p = (a\cos^2\alpha + b\sin^2\beta)^2 \tag{3.6}$$

$$I_s = (c\cos\alpha\sin\alpha)^2 \tag{3.7}$$

where

$$a = L_{zz}^3\chi_{zzz}\sin^2\theta_i + L_{zz}L_{xx}^2(\chi_{zxx} - 2\chi_{xzx})\cos^2\theta_i \tag{3.8}$$

$$b = L_{zz}L_{yy}^2\chi_{zxx} \tag{3.9}$$

$$c = L_{zz}L_{yy}^2\chi_{xzx} \tag{3.10}$$

The L_{ii} are the nonlinear Fresnel factors for the second harmonic and incident light and θ corresponds to the averaged molecular orientation of the solutes at the interface where 90° is the angle normal to the surface. Figure 3.5 shows the orientation dependent data (acquired at the appropriate excitation wavelength maxima) as well as the fits to Equations 3.6 and 3.7. Small changes in pNAs orientation are observed between the silica/vapor and silica/alcohol interfaces, although all calculated orientations are comparable given experimental uncertainties. This result implies that pNAs solvation at the silica surface is dominated by substrate/solute affinity and suggests that differences in observed interfacial polarity result from differences in longer ranged, averaged interactions.

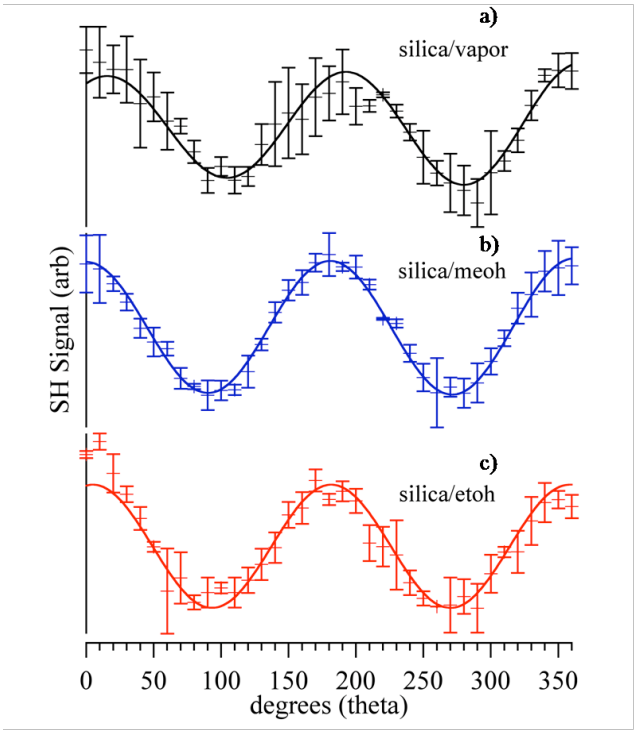

Figure 3.5: Orientation data for pNAs at the silica/vapor (black), silica/methanol (blue) and silica/ethanol (red) interfaces. The orientation data give rise to average molecular orientations of 35° ± 6.0° for the silica/vapor interface, 31° ± 1.3° for the silica/methanol interface and 31° ± 8.8° for the silica/ethanol interface.

3.3.5 Coumarins at the Silica/Methanol Interface

To test whether or not findings from the silica/methanol interface were general or specific to the pNAs solutes described above, we measured the resonance enhanced SHG spectra of four different coumarin dyes adsorbed to the silica/methanol solid/liquid interface. The four coumarins used in these follow-up experiments were Coumarin 151, Coumarin 152, Coumarin 440, and Coumarin 461; these coumarins will be referred to as C###, from this point forward. C151 and C152 have fluoro-groups where C440 and C461 have methyl groups. The two similar coumarins differ by the functional group at the nitro position: either terminating as $–NH_2$, or $–N(CH_3)_2$. The coumarins can be seen at the top of Figure 3.6. Table 3.2

contains bulk methanol excitation maxima for the coumarins, as well as calculated interfacial maxima. An important point to note about these different solutes is that the primary amine coumarins (C151 and C440) are capable of both accepting and donating hydrogen bonds while the tertiary amines (C461 and C152) can only serve as hydrogen bond acceptors.

Table 3.2: Bulk excitation maxima for C151, C152, C440 and C461 in methanol. The interfacial excitation maxima (λ_{SH}) are also recorded.

Solute	bulk alkane λ_{max} (nm)	bulk methanol λ_{max} (nm)	silica/methanol λ_{SH} (nm)
C151	348	377	364 ± 0.5
C152	367	371	364 ± 0.6
C440	332	365	356 ± 0.8
C461	348	369	354 ± 1.8

7-amino-coumarin (7AC) solutes can form several different resonance structures upon photoexcitation, including a charge transfer (CT) state with the nitrogen adopting a planar (sp^2 hybridized) geometry and a positive charge provided that the amine is not conformationally restricted. The resonance structure of the CT state also places a formal negative charge on the carbonyl oxygen at the 2-position. This excited state structure leads to a large change in molecular dipole (~6-8 D)[69] resulting in significant, well-studied solvatochromic behavior.[70] The difference between excitation wavelength maxima of these coumarin solutes in alkanes and in methanol is, on average, ~20-25 nm (with the excitation wavelength in methanol red-shifted from the alkane excitation wavelength). These results are reported in Table 3.2

The sample cells were prepared as previously discussed and coumarin solutions were made at ~100 μM in methanol. This bulk solution concentration was identified as sufficient for forming monolayers without extensive multi-layer formation.[71] The solutions were allowed to equilibrate for up to one hour, and then at least three 10-second acquisitions from our photon detection system were collected at each wavelength recorded. Data for all four coumarins show a shift towards the blue at the silica/methanol interface. These spectra confirm the findings at the pNAs silica/methanol interface to not be unique to solute identity. The shifts measured at the coumarin silica/methanol interface are even more nonpolar than the shift measured for pNAs (Figure 3.6.)

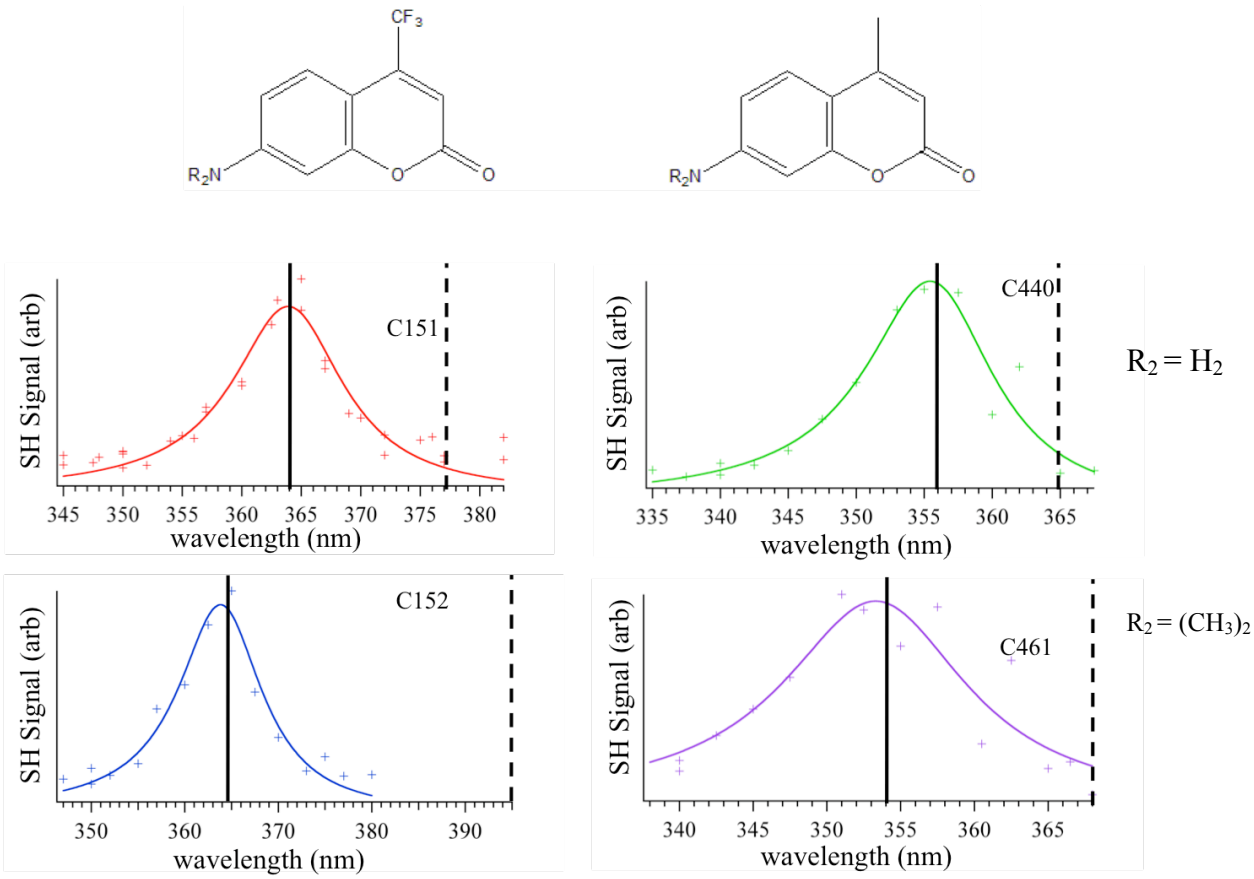

Figure 3.6: SHG Spectra of C151, C152, C440 and C461 at the silica/methanol interface. Bulk excitation maxima are denoted with the dashed lines, and SH excitation maxima are marked with the solid lines. A marked shift occurs towards the blue for all four solutes at the silica/methanol interface.

3.4 Conclusions

The adsorption, spectroscopic, and orientation measurements taken at the silica/vapor and silica/alcohol interfaces all emphasize the difficulties of predicting interfacial properties based solely on bulk solution considerations. If interfacial solvation could be described as weighted contributions from bulk phases, one would expect the silica/vapor interface to be the least polar, the silica/ethanol interface should show intermediate polarity and the silica/methanol interface should be the most polar. This prediction is not borne out by experimental results. The silica/vapor

interface is surprisingly polar, a result that is attributed to silica's high surface dipole density. The silica/methanol and silica/ethanol interfaces have significant qualitative differences. These results can only be interpreted in terms of surface mediated solvent structure and organization, and these effects have important consequences for models that attempt to predict mechanisms responsible for adsorption to surfaces commonly encountered in chromatographic and environmental applications. Through the combination of previous VSFG *and* current SHG measurements, the characterization of both solvent and solute effects at an interface can help predict interfacial environments for both solutes and solvents.

3.5 References

(1) Benjamin, I. *Annu. Rev. Phys. Chem.* **1997**, *48*, 407.

(2) TamburelloLuca, A. A.; Hebert, P.; Brevet, P. F.; Girault, H. H. *J. Chem. Soc., Faraday Trans.* **1996**, *92*, 3079.

(3) Wang, H. F.; Borguet, E.; Eisenthal, K. B. *J. Phys. Chem. A* **1997**, *101*, 713.

(4) Wang, H. F.; Borguet, E.; Eisenthal, K. B. *J. Phys. Chem. B* **1998**, *102*, 4927.

(5) Zhang, X. Y.; Cunningham, M. M.; Walker, R. A. *J. Phys. Chem. B* **2003**, *107*, 3183.

(6) Steel, W. H.; Lau, Y. Y.; Beildeck, C. L.; Walker, R. A. *J. Phys. Chem. B* **2004**, *108*, 13370.

(7) Huang, D. M.; Cottin-Bizonne, C.; Ybert, C.; Bocquet, L. *Langmuir* **2008**, *24*, 1442.

(8) Sanchez, V. M.; Sued, M.; Scherlis, D. A. *J. Chem. Phys.* **2009**, *131*, art. no.

(9) Sen, S.; Yamaguchi, S.; Tahara, T. *Ang. Chem.-Int. Ed.* **2009**, *48*, 6439.

(10) Somasundaran, P.; Huang, L. *Adv. Colloid Interface Sci.* **2000**, *88*, 179.

(11) Somasundaran, P.; Shrotri, S.; Huang, L. *Pure Appl. Chem.* **1998**, *70*, 621.

(12) Steel, W. H.; Beildeck, C. L.; Walker, R. A. *J. Phys. Chem. B* **2004**, *108*, 16107.

(13) Steel, W. H.; Walker, R. A. *Nature* **2003**, *424*, 296.

(14) Brindza, M. R.; Walker, R. A. *J. Am. Chem. Soc.* **2009**, *131*, 6207.

(15) Buchbinder, A. M.; Weitz, E.; Geiger, F. M. *J. Am. Chem. Soc.* **2010**, *132*, 14661.

(16) Calvente, J. J.; Andreu, R. *Phys. Chem. Chem. Phys.* **2010**, *12*, 13519.

(17) Ding, F.; Hu, Z. H.; Zhong, Q.; Manfred, K.; Gattass, R. R.; Brindza, M. R.; Fourkas, J. T.; Walker, R. A.; Weeks, J. D. *J. Phys. Chem. C* **2010**, *114*, 17651.

(18) Siler, A. R.; Brindza, M. R.; Walker, R. A. *Anal. Bioanal. Chem.* **2009**, *395*, 1063.

(19) Steel, W. H.; Walker, R. A. *J. Am. Chem. Soc.* **2003**, *125*, 1132.

(20) Mistry, M. K.; Choudhury, N. R.; Dutta, N. K.; Knott, R. *Langmuir* **2010**, *26*, 19073.

(21) Ocko, B. M.; Wu, X. Z.; Sirota, E. B.; Sinha, S. K.; Gang, O.; Deutsch, M. *Phys. Rev. E* **1997**, *55*, 3164.

(22) Sefler, G. A.; Du, Q.; Miranda, P. B.; Shen, Y. R. *Chem. Phys. Lett.* **1995**, *235*, 347.

(23) Tao, F.; Cai, Y. G.; Bernasek, S. L. *Langmuir* **2005**, *21*, 1269.

(24) Yam, C. M.; Tong, S. S. Y.; Kakkar, A. K. *Langmuir* **1998**, *14*, 6941.

(25) Chirica, G. S.; Remcho, V. T. *Anal. Chem.* **2000**, *72*, 3605.

(26) Tran, B. N.; Okoniewski, R.; Storm, R.; Jansing, R.; Aldous, K. M. *J. Agric. Food. Chem.* **2010**, *58*, 101.

(27) Zapala, W.; Waksmundzka-Hajnos, M. *J. Sep. Sci.* **2005**, *28*, 566.

(28) Zdziennicka, A.; Janczuk, B. *J. Colloid Interface Sci.* **2010**, *343*, 594.

(29) Smith, E. A.; Wirth, M. J. *J. Chromatogr. A* **2004**, *1060*, 127.

(30) Wirth, M. J.; Ludes, M. D.; Swinton, D. J. *Anal. Chem.* **1999**, *71*, 3911.

(31) Wirth, M. J.; Swinton, D. J.; Ludes, M. D. *J. Phys. Chem. B* **2003**, *107*, 6258.

(32) Rivera, D.; Harris, J. M. *Anal. Chem.* **2001**, *73*, 411.

(33) McCain, K. S.; Schluesche, P.; Harris, J. M. *Anal. Chem.* **2004**, *76*, 930.

(34) Battaglini, N.; Repain, V.; Lang, P.; Horowitz, G.; Rousset, S. *Langmuir* **2008**, *24*, 2042.

(35) Ederth, T.; Liedberg, B. *Langmuir* **2000**, *16*, 2177.

(36) Ron, H.; Rubinstein, I. *J. Am. Chem. Soc.* **1998**, *120*, 13444.

(37) Andanson, J. M.; Baiker, A. *Chem. Soc. Rev.* **2010**, *39*, 4571.

(38) Brettschneider, F.; Jankowski, V.; Gunthner, T.; Salem, S.; Nierhaus, M.; Schulz, A.; Zidek, W.; Jankowski, J. *J. Chromatogr. B* **2010**, *878*, 763.

(39) Dion, M.; Rapp, M.; Rorrer, N.; Shin, D. H.; Martin, S. M.; Ducker, W. A. *Colloids Surf., A* **2010**, *362*, 65.

(40) Maas, M.; Ooi, C. C.; Fuller, G. G. *Langmuir* **2010**, *26*, 17867.

(41) Chen, K.; Lynen, F.; De Beer, M.; Hitzel, L.; Ferguson, P.; Hanna-Brown, M.; Sandra, P. *J. Chromatogr. A* **2010**, *1217*, 7222.

(42) Ruiz-Angel, M. J.; Torres-Lapasio, J. R.; Carda-Broch, S.; Garcia-Alvarez-Coque, M. C. *J. Chromatogr. A* **2010**, *1217*, 7090.

(43) Reichardt, C. *Chem. Rev.* **1994**, *94*, 2319.

(44) Suppan, P.; Ghoneim, N. *Solvatochromism*, 1st ed.; The Royal Society of Chemistry: London, 1997.

(45) Beildeck, C. L.; Liu, M. J.; Brindza, M. R.; Walker, R. A. *J. Phys. Chem. B* **2005**, *109*, 14604.

(46) Gielis, J. J. H.; van den Oever, P. J.; Hoex, B.; van de Sanden, M. C. M.; Kessels, W. M. M. *Phys. Rev. B* **2008**, *77*, art. no.

(47) Liu, J.; Subir, M.; Nguyen, K.; Eisenthal, K. B. *J. Phys. Chem. B* **2008**, *112*, 15263.

(48) Mao, M. Y.; Miranda, P. B.; Kim, D. S.; Shen, Y. R. *Phys. Rev. B* **2001**, *64*, art. no.

(49) Onorato, R. M.; Otten, D. E.; Saykally, R. J. *J. Phys. Chem. C* **2010**, *114*, 13746.

(50) Petersen, P. B.; Saykally, R. J. *J. Phys. Chem. B* **2006**, *110*, 14060.

(51) Salafsky, J. S.; Eisenthal, K. B. *J. Phys. Chem. B* **2000**, *104*, 7752.

(52) Watanabe, H.; Yamaguchi, S.; Sen, S.; Morita, A.; Tahara, T. *J. Chem. Phys.* **2010**, *132*, art. no.

(53) Zhang, X. Y.; Steel, W. H.; Walker, R. A. *J. Phys. Chem. B* **2003**, *107*, 3829.

(54) Mondal, S. K., Yamaguchi, S., Tahara, T. *J. Phys. Chem. C* **2011**, *115*, 3083.

(55) Bell, A. J.; Frey, J. G.; Vandernoot, T. J. *J. Chem. Soc., Faraday Trans.* **1992**, *88*, 2027.

(56) Higgins, D. A.; Abrams, M. B.; Byerly, S. K.; Corn, R. M. *Langmuir* **1992**, *8*, 1994.

(57) Moad, A. J.; Simpson, G. J. *J. Phys. Chem. B* **2004**, *108*, 3548.

(58) Zhuang, X.; Miranda, P. B.; Kim, D.; Shen, Y. R. *Phys. Rev. B* **1999**, *59*, 12632.

(59) Hiemenz, P. *Principles of Colloid and Surface Chemistry*, 2nd ed.; Marcel Dekker, Inc.: New York, 1986; Vol. 9.

(60) Ong, S. W.; Zhao, X. L.; Eisenthal, K. B. *Chem. Phys. Lett.* **1992**, *191*, 327.

(61) Iler, R. K. *The Chemistry of Silica: Solubility, Polymerization, Colloid and Surface Properties, and Biochemistry*; John Wiley and Sons: New York, 1979.

(62) Laurence, C.; Nicolet, P.; Dalati, M. T.; Abboud, J. L. M.; Notario, R. *J. Phys. Chem.* **1994**, *98*, 5807.

(63) Onsager, L. *J. Am. Chem. Soc.* **1936**, *58*, 1486.

(64) Natal-Santiago, M. A.; Dumesic, J. A. *J. Catal.* **1998**, *175*, 252.

(65) Barnette, A. L.; Asay, D. B.; Janik, M. J.; Kim, S. H. *J. Phys. Chem. C* **2009**, *113*, 10632.

(66) Liu, W. T.; Zhang, L. N.; Shen, Y. R. *Chem. Phys. Lett.* **2005**, *412*, 206.

(67) Zhang, L. N.; Liu, W. T.; Shen, Y. R.; Cahill, D. G. *J. Phys. Chem. C* **2007**, *111*, 2069.

(68) Mikulski, P. T.; Herman, L. A.; Harrison, J. A. *Langmuir* **2005**, *21*, 12197.

(69) Rechthaler, K.; Kohler, G. *Chem. Phys.* **1994**, *189*, 99.

(70) Horng, M. L.; Gardecki, J. A.; Papazyan, A.; Maroncelli, M. *J. Phys. Chem.* **1995**, *99*, 17311.

(71) Roy, D. *Interfacial Solvation and Excited State Photophysical Properties of 7-Aminocoumarins at Silica/Liquid Interfaces*. Doctoral Thesis, University of Maryland, 2010.

(72) Buemi, G.; Millefiori, S.; Zuccarello, F.; Millefiori, A. *Can. J. Chem.* **1979**, *57*, 2167.

Chapter 4: Solute Adsorption and Solvation at Silica Interfaces

4.1 Introduction

Understanding solution-phase surface chemistry can be distilled into answering two simple questions: 1) do molecules adsorb to liquid surfaces? and 2) If so, what sort of environment do the adsorbates sample? While these questions may be simple to formulate, answers to these questions require detailed knowledge about the subtle, many-body interactions that occur between a solute and substrate, solvent and substrate, and solute and solvent. Furthermore, quantitative, predictive models describing adsorption to solid/liquid interfaces are important for a host of processes, including self-assembly of molecules and pollution control in both the atmosphere and in soil.[1-4] In order for a molecule to adsorb to a solid/liquid or liquid/liquid interface, it must diffuse to the surface, displace solvent molecules already present (requiring sufficiently weak solvent-substrate interaction), and orient to minimize its free energy.[5-7] Quantifying the energetics of these steps *a priori* is not easy. In the studies described below, we use nonlinear optical spectroscopy (NLO) to explore systematically the molecular origins of adsorption to weakly and strongly associating hydrophilic silica/liquid interfaces. Here, weakly associating describes silica/alkane interfaces where interfacial interactions are dominated by dipole-induced dipole forces.[8,9] Strongly associating systems describe those where the solvent can enjoy hydrogen bonding or more general dipolar interactions with the silanol terminated surface.[9-12] Experiments use resonance enhanced second harmonic generation (SHG)

to measure adsorption isotherms for *p*-nitrophenol (pNP) and *p*-nitroanisole (pNAs) at four different silica/alkane solid/liquid interfaces as well as boundaries formed between silica and acetonitrile, dimethyl sulfoxide (DMSO) and unbuffered water (pH = 7). Results show that across silica/liquid interfaces, pNP has stronger adsorption energies than pNAs and pNP solvation at the interface is insensitive to solvent identity. In contrast, pNAs with its lower affinity for the silica/liquid interface is more sensitive to solvent structure and organization.

One example of where adsorption figures prominently is the self-assembly of functionalized substituents onto metal nanoparticles that already support chemisorbed alkanethiol monolayers. These systems are attractive candidates for use in photovoltaic applications,[13-16] but the ability of devices to operate reliably and durably depends sensitively on the adsorbed film's structural homogeneity.[17] For example, Mukherjee et al. recently reported the effects of gravity driven self-assembly vs. electric field assisted assembly on films formed from Photosystem I (PS I), a target for use in hybrid bioelectronic/photovoltaic devices.[18] Gravity driven depositions were prepared by simply immersing alkanethiol/gold nanoparticles in 200 mM sodium phosphate buffer solutions. Electric field assisted assembly depositions of PS I were promoted by using a parallel plate electrode assembly. Films formed by the electric field assisted method produced uniform monolayer coverages along the surface of the nanoparticles. In contrast, gravity driven deposition in the absence of an electric field led to substantial aggregation on the surface, thereby limiting the functionality of PS I.

A second example of why predicatively quantifying adsorption is important comes from the field of environmental remediation. The leaching of herbicides from agricultural sites poses risks to public health, and new herbicides must undergo rigorous testing and characterization before they can be used in commercial applications. Migration and leeching in soil and water are common fates for most popular herbicides due to their functionalized structures consisting of aromatic rings and tail groups of alcohols, amines, and/or carbonyl groups.[19-21] These functionalized organic molecules can associate strongly with mineral surfaces through a variety of mechanisms. A strategy to reduce the surface migration of weed control treatments is to use a controlled-release formulation (CRF) so that the steady-state concentration of herbicides remains relatively low.[22] Goldreich, et al. recently reported a new CRF that reduces the effect of soil wetting and drying cycles on herbicide leaching by solvating the herbicide in cationic micelles. The micelles reduce interactions between the herbicide with both water and soil. Encapsulation of the herbicide metolachlor in the micelle reduced the adsorption of this particular herbicide to both sandy and heavy soils, although the mechanisms responsible for this effect remain speculative. Understanding how and why molecules adsorb to a given surface can help drive regulatory policy that is based on exposure estimates and environmental persistence.[23]

To isolate specific molecular driving forces responsible for adsorption to surfaces, our studies employed two closely related solutes. The molecules pNP and pNAs share a nitrobenzene framework, but differ in the functional group *para* to the nitro group: pNAs has a methoxy group in the 4-position while pNP's substituent is an alcohol. pNP is capable of both accepting and donating hydrogen bonds, whereas

pNAs can only accept hydrogen bonds or associate with its surroundings through general, dipole-dipole interactions. Both molecules have been used extensively to measure interfacial solvation and their surface activity has been well documented.[11,24-29] These molecules have very similar electronic structures and are sensitive primarily to solvent polarity. Both solutes undergo large, positive changes in their molecular dipoles upon excitation to their first allowed excited electronic states, meaning that excitation wavelengths shift monotonically to longer wavelengths in more polar environments. (Figure 4.1). Experiments described below were motivated by a need to correlate solute functional group composition with surface activity as well as a need to identify the sensitivity of adsorbed solutes to surrounding solvent structure.

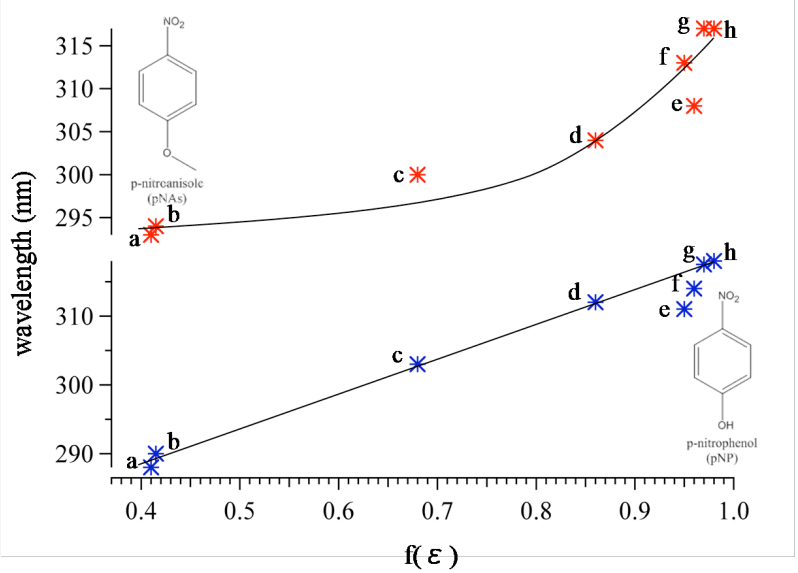

Figure 4.1: The solvatochromic response of pNP (top) and pNAs (bottom) versus solvent polarity where solvent polarity is defined as the Onsager polarity function:

$$f(\varepsilon) = \frac{2(\varepsilon - 1)}{(2\varepsilon + 1)}$$

where e is the solvent's static dielectric constant and f(ε) ranges from 0.4 for low dielectric constants (ε = 2) and 1.0 for polar solvents (such as water, ε = 80).[60,61] Solvents correspond to (a) cyclohexane, (b) methyl-cyclohexane, (c) ethyl ether, (d) 1-octanol, (e) methanol, (f) acetonitrile, (g) DMSO, (h) water. As the solvent changes from cyclohexane to DMSO there is an increase in the peak absorption wavelength.

4.2 Experimental

4.2.1 Adsorption Measurements

To measure the surface activity of pNP and pNAs, solutions of varying concentrations were prepared in different solvents. pNP solutions in alkanes were serially diluted from 1 mM concentrations, and solutions of pNAs were diluted from 100 mM solutions in alkanes. (pNAs is ~2000 times more soluble than pNP in alkane solvents.)[27,32] In acetonitrile, both solutes were diluted from solutions of 200 mM. Preparation of the sample cells has been discussed previously:[10,27,28] both the sample

cell and the silica slide were prepared by soaking in a 50:50(v:v) mixture of concentrated sulfuric and nitric acids. The slides and cells were then rinsed with ultrapure (18 MΩ) water.

Visible light tuned to produce SH signal at the peak SH-λ_{max} resulted from pumping an OPerA-Solo (Coherent) with the 1kHz regeneratively amplified Ti:sapphire laser (800 nm, 3.5W, 85fs Libra-HE (Coherent)). The fundamental beam was passed through a polarizer/half-wave plate combination to produce incident light linearly polarized at 45˚ (M_{in}). The light was then focused at the sample and the SH output from the sample was passed through a polarizer set to pass S-polarized light. This combination of polarizations was used to exploit the relationship of the S-polarized SH intensity generated at an interface to the SH electric field:[25,33]

$$N \propto E_{2\omega}^{s} \tag{4.1}$$

and

$$\left|E_{2\omega}^{s}\right|^2 = I_{2\omega}^{s} \tag{4.2}$$

where N is the number of molecules at an interface, $E_{2\omega}^{s}$ is the s-polarized SH electric field, and $I_{2\omega}^{s}$ is the intensity of the s-polarized SH generated at the interface. The SH signal was wavelength selected with a 12.5 cm monochrometer and detected with a photomultiplier and photon counting electronics. Each solution-interfacial system was allowed to equilibrate for at least 30 minutes before SHG measurements were made. Waiting additional time led to no systematic change in measured signal intensities. For each concentration, data were acquired in ≥ 3 ten second intervals at each wavelength and scaled for incident power.

4.2.2 SHG Spectroscopy

SHG spectra were acquired for both pNP and pNAs adsorbed to different silica/liquid interfaces using the laser system described above. Measurements were made at the highest concentrations used in the adsorption measurements. Visible light produced by the OPerA-Solo was passed through a Glan-Taylor polarizer set to pass P-polarized light and the half-wave plate set to pass P-polarized light, as well. The resulting SH generated at the sample was not passed through an additional polarizer. The data were fit to Equation 1.6 where the nonlinear susceptibility contains both resonant and nonresonant contributions.[30,34]

In Equation 1.6, the μ_{ij} correspond to transition matrix elements and the summation runs over all real and virtual excitation energies. Tuning the frequency of the incident light and measuring I(2ω) leads to effective excitation spectra of those molecules subject to interfacial anisotropy. This approach has been used in previous studies to characterize the dielectric and time-dependent properties of solutes at surfaces.[11,12,26,28,35-44] An important point to note is that the nonresonant contribution to the second order susceptibility is intrinsic to all interfacial systems and can lead to asymmetry in resonance enhanced line shapes. Depending on its magnitude and sign, $\chi^{(2)}_{NR}$ can result in calculated excitation wavelengths that differ noticeably from the experimentally measured λ_{max}.

4.3 Results and Discussion

4.3.1 Adsorption Measurements at Silica/Alkane Interfaces

We examined the surface activity of both pNP and pNAs at different silica/solvent interfaces. These experiments required measuring the intensity of the resonantly enhanced SHG signal at the calculated maximum wavelength and then plotting the inverse of the square root of the SHG signal vs. the inverse of the bulk solution concentration. This approach has been used to determine free energies of adsorption for a wide variety of solutes adsorbed to liquid/vapor, liquid/liquid, and solid/liquid interfaces.[25,31,33,45-48] Despite these many studies, a systematic, *a priori* description of solute and solvent behavior at buried interfaces remains elusive. Often, reported results will examine the behavior of a single solute and/or a single solvent. Comparisons between different reports must account for differences in experimental procedures, geometries, and methods. Our studies of adsorption presented below are unique because they compare systematically the behavior of two solutes having similar solvatochromic behavior but different functional composition at silica/liquid interfaces where the solvents themselves have similer bulk solvating behavior.

Representative adsorption data for pNP and pNAs are shown in Figure 4.2. All systems show qualitatively similar behavior, namely SH intensity generally rises steeply with increasing bulk concentration before reaching an asymptotic limit. The fact that SH intensity levels off implies that adsorption ceases with monolayer formation and higher bulk concentrations do not lead to multi-layer formation. Initial efforts to fit the data to a Langmuir adsorption model were unsuccessful. Deviation of the data from the Langmuir model is evident for both solutes at the silica/methyl-

cyclohexane interface as shown in Figure 4.2.

A Langmuir description of adsorption assumes that the substrate is homogeneous, the solute and solvent have equal molar surface areas, the surface and bulk phases exhibit ideal behavior, and that adsorption terminates with monolayer coverage.[49] If these four constraints are not met, adsorption can sometimes be modeled with a two-site Langmuir mechanism to account for surface heterogeneity.[50] Silica is known to have a heterogeneous surface with (at least) two types of surface silanol groups. Approximately 20% of the surface silanol groups are acidic with a pKa of ~4.5 while the remaining 80% are more basic with a pKa of 8.5.[51,52] Single molecule studies exploring surface diffusion have also isolated rare instances of strong binding sites where molecular adsorption happens irreversibly without any exchange of adsorbates between the surface and solution.[53]

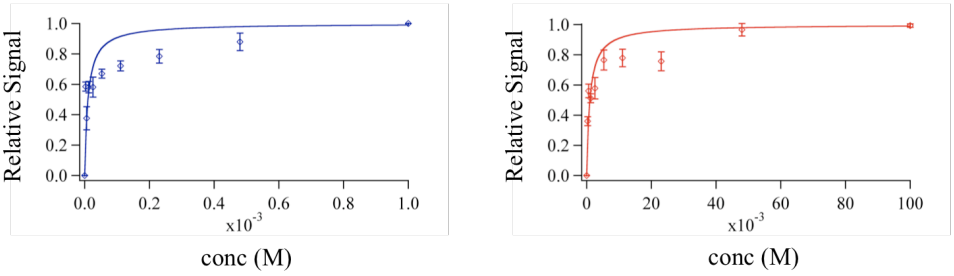

Figure 4.2: The attempt to fit pNP (left) and pNAs (right) to the silica/methyl-cyclohexane interface using the Langmuir adsorption model. Data deviations at higher concentrations are evident for both solutes.

The two-step Langmuir isotherm model has been proposed by Johnson to describe adsorption to heterogeneous surfaces having two distinct types of sites.[50,54]

The square root of the averaged results were plotted as a function of the inverse of the bulk solution concentration and the data were fit to a linear combination of adsorption mechanisms:

$$\frac{1}{N} = \frac{a_1}{N_{\max,1}} * \frac{1}{C_1} + \frac{1}{N_{\max,1}} \tag{4.3}$$

$$\frac{1}{N} = \frac{a_2}{N_{\max,2}} * \frac{1}{C_1} + \frac{1}{N_{\max,2}} \tag{4.4}$$

where N is the number of adsorbed molecules/cm^2, $N_{max,\#}$ is the maximum number of adsorbed molecules needed to occupy all available surface sites of a given type, C_1 is the bulk concentration of the solution, and a is the Langmuir adsorption constant (=$C_2\exp(\Delta G_{1,2}°/RT)$, where C_2 is the concentration of the solvent). This model was chosen because our measured adsorption data often could not be fit with sufficient precision using a single-step adsorption mechanism. The single step adsorption description fit the data qualitatively but not quantitatively. Given the silica surface's known heterogeneity *and* the precision of the data, the two-step Langmuir model stood out as a reasonable choice.

Table 4.1. The data below show the corresponding ΔG_{ads} values for pNP and pNAs at the silica/liquid interfaces explored in this study; each interface is fit with a two-step Langmuir adsorption isotherm to describe adsorption behavior at both low (top) and high (bottom) concentrations.

System	pNP (kJ/mol)	pNAs (kJ/mol)
silica/n-hexane	-31.3 ± 0.4	-20.5 ± 0.5
	-27.0 ± 0.9	-15.4 ± 1.1
silica/decane	-30.0 ± 0.1	-21.6 ± 0.4
	-26.8 ± 0.3	-16.9 ± 0.5
silica/methyl-cyclohexane	-33.1 ± 0.4	-23.5 ± 0.5
	-28.2 ± 0.5	-16.6 ± 0.6
silica/cyclohexane	-30.1 ± 0.5	-24.4 ± 0.9
	N/A	-21.1 ± 9.7
silica/acetonitrile	-27.2 ± 4.9	-20.3 ± 0.4
	-16.7 ± 0.1	-15.6 ± 0.2
silica/aqueous (pH = 7)	-30.4 ± 0.6	---
	-24.1 ± 1.5	---

The results from fitting the pNP and pNAs adsorption data to Equations 4.3 and 4.4 are reported in Table 4.1 and shown in Figure 4.3. For all of the interfaces examined, pNP exhibited consistently higher adsorption energies than pNAs, supporting the premise that pNP affinity at the silica/liquid interface is dominated by strong solute/substrate hydrogen bonding. Looking more closely at the adsorption free energies reported in Table 4.1, one notices several subtle but consistent patterns.

The pNP adsorption data for each silica/liquid interface are similar in magnitude and largely independent of solvent identity.

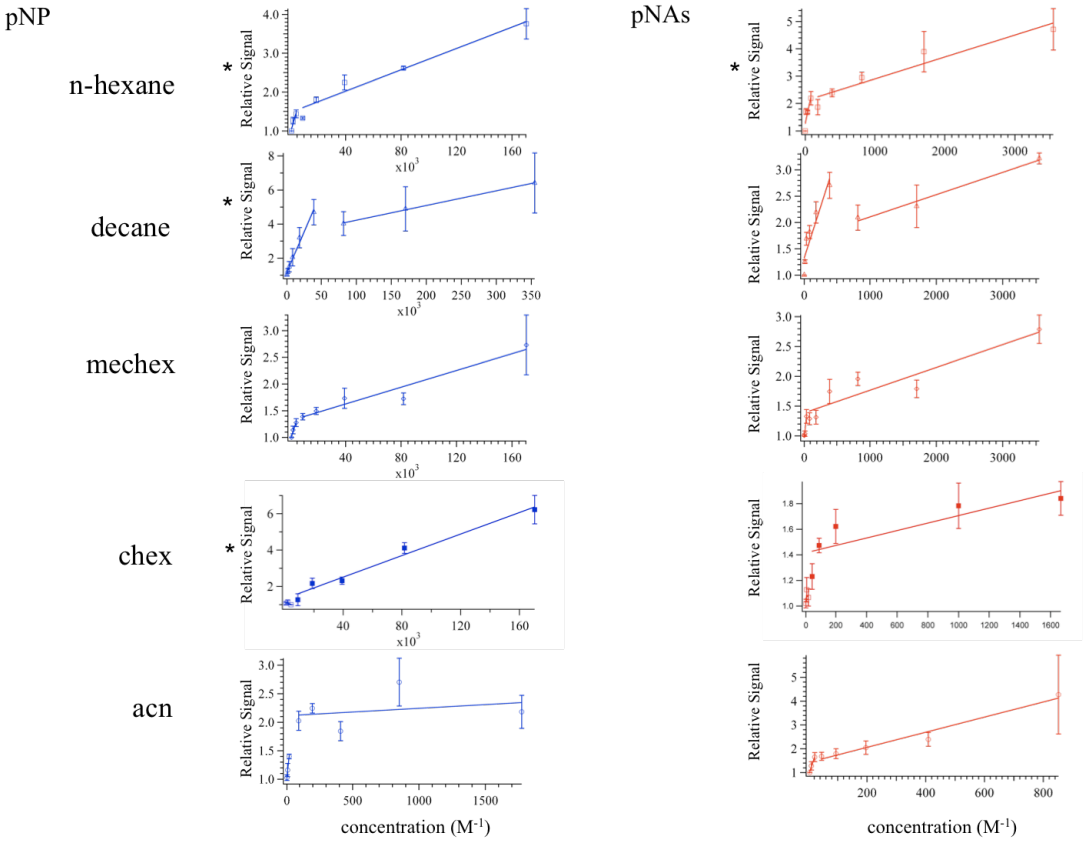

Figure 4.3: The interfacial adsorption isotherms of pNP (left) and pNAs (right) at various silica/polar and silica/non-polar interfaces. The adsorption isotherms are fit with a two-step Langmuir isotherm representing high and low concentration adsorption behavior. Isotherms denoted with an * could have been fit with a single Langmuir adsorption model.

Comparing pNAs adsorption to different silica/alkane interfaces, one notices that pNAs shows the strongest affinity for the silica/cyclohexane interface with adsorption energies of -24.4 ± 0.9 kJ/mol (low concentration) and -21.1 ± 9.7 kJ/mol (high concentration). Given the uncertainty of the adsorption energy at high concentrations, one could reasonably use a single site Langmuir model to describe adsorption in this system. Adsorption energies are smallest for pNAs at the

silica/hexane interface (with ΔG_{ads} values of -20.5 (low) and -15.4 kJ/mole (high)). For the *n*-hexane and all other alkane solvents *except* cyclohexane, the data show clearly the two-site mechanism responsible for adsorption. This observation highlights that silica/alkane interfaces are not equivalent from the perspective of pNAs and that solvent choice impacts chemical behavior of this boundary. Common denominators in the pNAs-silica-alkane systems include the solute and the solid substrate. Consequently, differences in the adsorption energies need to be interpreted in terms of solvent/substrate interactions *and* the effects that the silica surface has on the adjacent solvent's ability to solvate adsorbed solutes.

The stronger association of pNAs to the silica/cyclohexane interface correlates, in part, with interfacial solvent density differences noted by Doerr et al.[55] In these X-ray scattering experiments, the authors showed that a silicon oxide interface induced long-range order and enhanced solvent density in an adjacent cyclohexane solvent. In contrast, this same study reported that solvent density was depleted at a silicon oxide/*n*-hexane interface. These results were interpreted in terms of liquids with low bulk packing densities creating regions of "gas-like" layers near the substrate.[55] From the perspective of an adsorbed solute, increased interfacial solvent density would lead to stronger solvation forces and promote enhanced solute accumulation at the silica/cyclohexane interface. Similarly, reduced solvent density would favor interfacial solvation less and result in weaker adsorption energies.

An interesting point to note is that the adsorption energies of pNP to silica surfaces do not show the same systematic variation with solvent identity seen with pNAs. Spectroscopic data presented below further confirm the adsorbed pNP's lack

of sensitivity to solvent identity. We attribute this behavior to the poor solvation of pNP in alkane solvents and the ability of the solute to readily form hydrogen bonds with the silica substrate.

4.3.2 Adsorption at Silica/Polar Solvent Interfaces

The least favorable adsorption energies for both pNP and pNAs occur at the silica/acetonitrile interface. At this interface, pNP and pNAs compete for surface sites with a polar solvent capable of accepting weak hydrogen bonds with the substrate. If the first step in adsorption requires that the solute displace a solvent already at the interface, then one might assume that polar solvents would be harder to displace from the silica surface than nonpolar alkanes. Supporting this premise are the adsorption energies of pNP (-27.2 ± 4.9 kJ/mol (high); -16.7 ± 0.1 kJ/mol (low)) and pNAs (-20.3 ± 0.4 kJ/mol (low); -15.6 ± 0.2 kJ/mol kJ/mol (high)) to the silica/ACN interface. These values are measurably smaller (in magnitude) than those measured for silica/alkane interfaces and, in the limit that the solute-subrate association remains the same, the difference in adsorption energies between the silica/alkane and silica/ACN systems will reflect differences in affinity between the alkanes and ACN for the silica surface.

Consistent with these data were adsorption measurements carried out at the silica/DMSO and silica/aqueous (pH = 7) interfaces. Interestingly, DMSO effectively suppressed SH signal from the solid/liquid interface completely. This result is attributed to the strong hydrogen bonds donated from the silica surface to adjacent solvent DMSO. The solutes are also quite soluble in this solvent making solute

accumulation at the interface energetically unfavorable. Like DMSO, water can also accept hydrogen bonds but functions much more effectively as a hydrogen bond donating solvent.[27] Efforts to measure pNP adsorption to the silica/aqueous interface were unsuccessful for solutions with pH ≤ 6. At higher pH, pNP showed weak but measurable adsorption. (pNAs, being sparingly soluble in water, showed no evidence of adsorption to the silica/aqueous interface regardless of pH.) Representative data acquired at the silica/aqueous (pH = 7) interface for pNP show similar adsorption behavior as that seen at the other silica/liquid interfaces at low concentrations with an adsorption energy of -30.4 ± 0.6 kJ/mol (Figure 4.4). As the concentration increases, adsorption to the substrate becomes less favorable and the second adsorption energy data lie between the alkane and acetonitrile limits (-24.1 ± 1.5 kJ/mol).

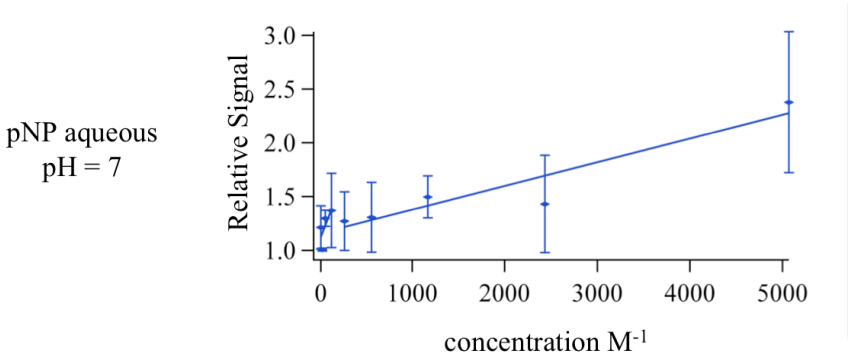

Figure 4.4: The interfacial adsorption isotherm of pNP at the silica/aqueous (pH = 7) interface. The isotherm is fit with a two-step Langmuir isotherm representing high and low concentration adsorption behavior.

4.4 Interfacial Polarity as Inferred from SHG Measurements

4.4.1 Solvent Polarity at Silica/Alkane Solvent Interfaces

SH-spectra of pNP adsorbed to weakly associating silica/alkane interfaces are all very similar. (Figure 4.5, left) At the silica/n-hexane, silica/decane, silica/methyl-cyclohexane and silica/cyclohexane interfaces, resonance enhanced SH spectra of pNP all report excitation wavelengths between 303 nm and 306 nm. (Table 4.2) Given experimental resolution and uncertainties, these results are virtually equivalent and imply that pNP at these silica/alkane boundaries samples an effective polarity similar to that of bulk ether solvents (with effective static dielectric constants of ~8). These results stand in contrast to the SH spectrum of pNP acquired from the silica/vapor interface where pNP's effective excitation wavelength is 316 nm, a result comparable to pNP in very polar environments such as bulk water or bulk DMSO. The silica/vapor data imply such strong association between the adsorbed pNP and the surface silanol groups that the solute is insensitive to the absence of solvent. With this picture in mind, we surmise that an alkane solvent mitigates in a nonspecific manner solute/substrate interactions (as evidenced by a shift in λ_{exc} to shorter wavelengths) leading to a lower effective polarity sampled by pNP at the solid/alkane interface compared to the silica/vapor interface.

Table 4.2. The data contained below corresponds to the SH-λ_{max} values obtained for pNAs and pNP at the corresponding silica/alkane interfaces.

System	pNP (nm)	pNAs (nm)
silica/vapor	317± 2	315± 2
silica/n-hexane	303 ± 1	300 ± 1
silica/decane	305 ± 2	305 ± 2
silica/methyl-cyclohexane	306 ± 1	312 ± 3
silica/cyclohexane	307 ± 2	318 ± 3
silica/acetonitrile	308 ± 2	297 ± 1
silica/aqueous (pH = 7)	310 ± 2	----
silica/aqueous (pH =4)	----	----
silica/dmso	----	----

In contrast to pNP, solvation of pNAs at the silica/alkane interface is very sensitive to solvent identity. The variation in excitation wavelengths for pNAs adsorbed to the different silica/alkane interfaces is ~20 nm with the silica/hexane interface being the least polar (λ_{exc} = 300 nm) and the silica/cyclohexane interface being the most polar (λ_{exc} = 318 nm). (Figure 4.5, right and Table 4.2). These results are consistent with data from the adsorption studies described above and again can be explained by the X-ray scattering studies performed by Doerr et al.[55] These latter experiments measured electron density at the interface formed between silicon oxide and different alkane solvents. The silicon oxide induced significant solvent depletion that extended ~1 nm across silicon-oxide/*n*-hexane interface, but at the silica/cyclohexane interface the silicon oxide imposed long range order and enhanced density in the adjacent solvent. Depletion of solvent density at the silica/*n*-hexane interface will weaken the averaged interactions that adsorbed solutes have with their

surroundings leading to a lower local interfacial polarity. In contrast, pNAs adsorbed to the silica/cyclohexane interface samples a very high dielectric environment as evidenced by an excitation wavelength of ~318 nm. A combination of strong association with the silica substrate (λ_{SHG} = 315 nm at the silica/vapor interface) *and* strong solvation interactions with the (dense) interfacial solvent will all conspire to create a more polar environment.

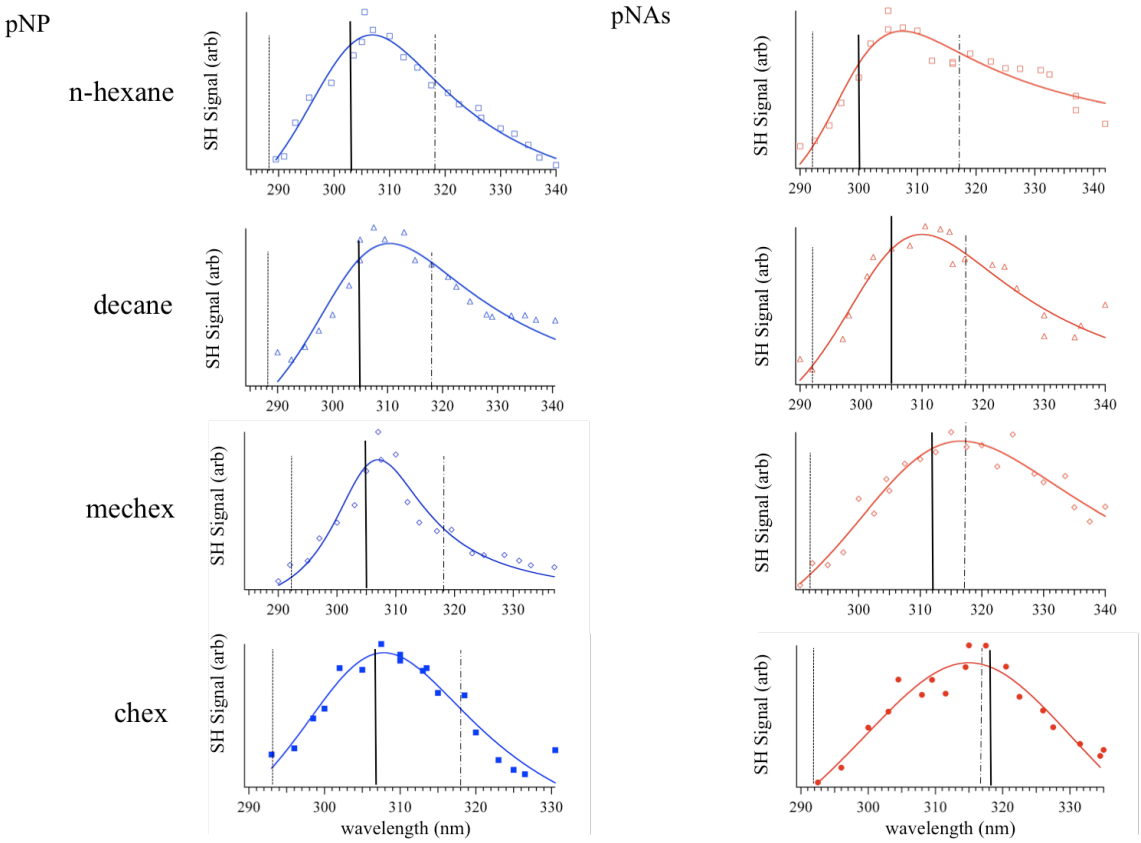

Figure 4.5: The silica/nonpolar SH-spectra of pNP (left) and pNAs (right). The SH-spectra of pNP have dashed and staggered-dashed lines representing bulk excitation maxima in alkanes (288 nm) and polar solvents (318 nm), respectively. The SH-spectra of pNAs have dashed and staggered-dashed lines representing bulk excitation maxima in alkanes (292 nm) and polar solvents (317 nm), respectively.

SHG data from pNAs adsorbed to the silica/decane interface are consistent with predictions that one would make based on surface induced changes in interfacial solvent structure and the effects these changes would have on interfacial solvation. In the aforementioned X-ray scattering studies,[55] decane is a solvent that converges abruptly to bulk solvent density without any evidence of solvent structuring or density depletion induced by the silicon oxide substrate. Consequently, if surface induced changes in solvent properties affect interfacial solvation, one would expect polarity at the silica/decane interface to be intermediate between the silica/cyclohexane and silica/*n*-hexane limits as is the case for pNAs. If interfacial solvation was dominated by substrate-solute associations, then interfacial polarity should show a weaker dependence on solvent identity as is the case for pNP adsorbed to the different silica/alkane interfaces.

The interfacial excitation maximum for pNAs at the silica/methyl-cyclohexane interface is similar to previous reports (312 ± 3 nm).[28] The difference in polarity experienced at the silica/cyclohexane and silica/methyl-cyclohexane interfaces is attributed to the ability of cyclohexane to organize at the interface. Based on the SHG data, we propose that the methyl-cyclohexane does not organize as well at the silica/liquid interface and the interfacial solvent can not provide energetic stabilization from averaged, long-range interactions in the way that cyclohexane can. This claim cannot be supported directly with X-ray scattering data, but we can draw indirect evidence from bulk solution data. Cyclohexane's T_{fus} is 7˚C, a remarkably high temperature for such a low molecular weight, saturated alkane. Methyl-cyclohexane has a melting temperature of -126˚C. The addition of a single methyl

group to cyclohexane severely disrupts the solvent's ability to pack in close registry, and this effect should play a large role in disrupting solvent structure and organization at a rigid, solid surface.

4.4.2 Solvent Polarity at Silica/Polar Solvent Interfaces

Figure 4.6 shows spectra acquired from silica/acetonitrile, silica/aqueous (pH = 7), and silica/dimethyl sulfoxide interfaces as well as the previously reported data from silica/vapor interfaces. Of these three different solid/liquid systems, pNP and pNAs both adsorb to the silica/ACN interface and pNP (but not pNAs) adsorbs to the silica/aqueous (pH = 7) interface. Neither solute shows any evidence of adsorption to the silica/DMSO interface. If one considers that both water and DMSO can hydrogen bond strongly to the interface while ACN cannot, *and* that both pNP and pNAs are both readily soluble in the polar organic solvents, then the absence of strong adsorption can be understood. Again, we note that pNP *does not* adsorb to the aqueous/silica interface if the bulk solution pH is ≤ 6. We attribute this behavior to pNP's ability to serve as an acid donating its proton to the growing number of negatively charged oxides at the solid/liquid interface at higher pH.[51] (Representative spectroscopic data are also included for the silica/aqueous (pH = 4) solid/liquid interface.) The SH-spectrum of pNP adsorbed to the silica/ACN interface has an excitation wavelength maximum of 308 nm. The similarity between this result and data from the silica/alkane interfaces implies that silica-solute interactions are largely responsible for controlling pNP's interfacial environment and that the solvent plays a limited role in interfacial solvation.

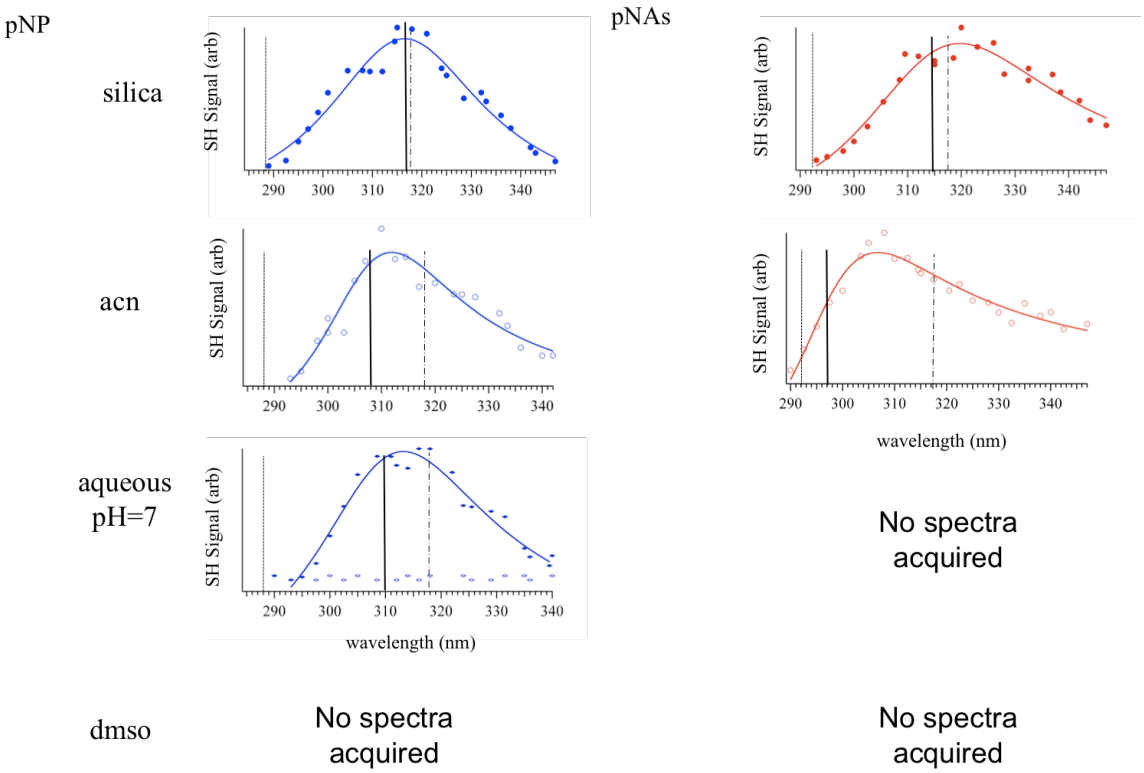

Figure 4.6: The SH spectra of pNP (left) and pNAs (right) at various silica/polar interfaces. The SH-spectra of pNP have dashed and staggered-dashed lines representing bulk excitation maxima in alkanes (288 nm) and polar solvents (318 nm), respectively. The SH-spectra of pNAs have dashed and staggered-dashed lines representing bulk excitation maxima in alkanes (292 nm) and polar solvents (317 nm), respectively. The aqueous spectrum for pNP has both spectra for pH=4 (flat line), and pH=7.

To understand these findings, we appeal to results from *ab initio* computational studies that examined solvation energies of various hydrogen bonding species adsorbed to (model) silica surfaces and solvated in bulk solution. Turov, *et al*. explored the effects that different organic solvents had on the structure of water adsorbed to silica surfaces and determined that between DMSO and ACN, DMSO had a much smaller (in magnitude) ΔG_{solv} with itself.[56] (The values, calculated using DFT (B3LYP/6-311++G(d,p)), are -0.3 kJ/mole for DMSO and -4.3 kJ/mole for ACN.) This difference is important when one considers that DMSO adsorbed to the

interface will not experience significant thermodynamic stabilization when it desorbs from a silica surface and, in fact, desorption might be thermodynamically *unfavorable* if the DMSO already associates strongly with the surface. In contrast, ACN will enjoy relatively strong association with its surroundings in bulk solution making displacement from the silica surface more favorable. These considerations can be used to rationalize why adsorption isotherms can be measured at the silica/acetonitrile interface but not at the silica/DMSO interface.

Further supporting this explanation are experimentally measured heats of immersion measured for different Brønsted acids and bases dissolved in ACN.[57] In these experiments, Arnett and Ahsan used commercial grade silica and measured the resulting exothermicity when samples were submerged in ACN solutions containing different acids, ketones, and amines. The larger the heat of immersion, the more strongly the solute associates with the surface. The authors reported that in general, Brønsted acids showed *smaller* heats of immersion, but Brønsted bases showed *larger* heats of immersion than the control experiments using neat ACN. These findings further support the notion that solvation at hydrophilic silica surfaces is dominated by the hydrogen bond donating properties of the surface silanol groups. Water's association with the silica surface was ~5% larger than that of ACN (86 J/g of silica vs. 82 J/g, respectively) and while the authors did not report results for DMSO, the tertiary amines studied all showed much stronger affinity (by as much as 25%) for the silica surface than ACN.

The computational and thermodynamic results presented above can explain the adsorption behavior observed at the strongly associating silica/liquid interfaces.

However, these arguments can not be used to rationalize the very nonpolar environment sampled by pNAs at the silica/acetonitrile interface. The SHG spectrum of pNAs adsorbed to the silica/acetonitrile solid/liquid interface has a wavelength maximum of 297 nm, 15 nm below the bulk acetonitrile limit of 312 nm and 20 nm below the silica/vapor interface. This result implies that the silica/ACN interface has an effective polarity lower than that of the different silica/alkane interfaces despite silica's obviously polar character and despite acetonitrile being a polar solvent with a dielectric constant of 37!

The solution to this dilemma can be found in studies of solvent structure and organization at the silica/liquid interface. Vibrational sum-frequency generation spectroscopy (VSFG) has measured the vibrational spectra of acetonitrile at silica/vapor, liquid/vapor and silica/liquid interfaces.[58] In these studies the authors concluded that the silica substrate creates long-range, extended structure in the adjacent acetonitrile liquid *and* that the different layers of acetonitrile adopt an anti-parallel dipole orientation. A simple consequence of this organization is that the solvent at the interface will appear less polar than bulk solution in agreement with the pNAs SHG results reported in Figure 4.6. Similar results have been observed at the silica/methanol interface,[59] although the effects are more pronounced with the acetonitrile solvent. Similar to the case of the silica/alkane systems, pNP appears to be remarkably insensitive to solvent identity with an interfacial excitation wavelength of 308 nm.

4.5 Discussion

Summarizing the data presented above, pNP and pNAs share similar electronic structure and show almost identical bulk solution solvatochromic activity. Nevertheless, these two solutes sample markedly different environments at the same solid/liquid interfaces. The similarities in solvation behavior of pNAs and pNP in bulk solvents and the differences in solvation at *the same* silica/solvent interfaces reaffirm that interfacial solvation can not be easily modeled by simple pair-wise interactions. Parametric effects of the substrate on the adjacent solvent can play a significant role in the ability of a solute to solvate. Adsorption measurements show that pNP associates more strongly to the silica/liquid interface than pNAs. This strong association renders pNP less sensitive to solvent identity. pNAs adsorbs to the different solid/liquid interfaces with adsorption energies that are on average ~10 kJ/mole smaller than those of pNP. These thermodynamic observations are also reflected in the spectroscopic studies of these two solutes. When adsorbed to the silica/vapor interface, both solutes report very polar environments based on SHG wavelength maxima very close to the polar edges of their respective solvatochromic windows. Adding a solvent affects the local environment experienced by pNP but only in a general, nonspecific way. Association with the silica surface is weakened and the excitation wavelength of pNP shifts to shorter wavelengths characteristic of a moderately polar environment.

pNAs, in contrast, is extremely sensitive to solvent identity. Despite having the same electronic excitation wavelength in different alkanes, the excitation wavelength of pNAs adsorbed to the silica/alkane interface can vary by more than 15

nm depending on the identity of the alkane. This difference in adsorbed solute sensitivity to solvent identity can be correlated with differences in solute solubility. pNP is not very soluble in alkanes and has an oil/water partitioning ratio of ~0.01. In contrast, pNAs partitioning between the same two phases is ~20.[10,27,32] The difference in SH spectra between pNAs and pNP can be understood by both the enhanced ability for the solvent to solvate pNAs, as well as the effects that the silica surface will have on the adjacent solvent molecules. Solvent structure and order at the silica substrate influence the local dielectric environment experienced by pNAs.

Differences between the various silica/liquid interfaces sampled by pNAs can be interpreted – at least in part – to reported differences in solvent density and organization at these boundaries. The x-ray studies of Doerr, *et al*. describe the silica/alkane interfaces measured in this work to all have very different densities immediately at a silica substrate. Cyclohexane has the ability to pack in a more ordered orientation giving it the greatest solvent density immediately at the substrate. Decane is next, with solvent molecules showing less order at the substrate than cyclohexane, but resulting in an environment, as sampled by pNAs, consistent with an averaged polarity of the two bulk-phases model of interfacial polarity. N-hexane, however, shows the least solvent density and results in weaker solute-substrate association, as evidenced by the apparent non-polar interface measured by pNAs.

The findings presented in this chapter illustrate that even relatively simple solvents can invoke complex and counterintuitive behavior at an interface. Adsorption and spectroscopic data imply that the predicting interfacial properties can not be accomplished simply by scaling bulk properties of the solvent and considering

a solvent invariant contribution from the surface. Solute-substrate, solute-solvent and solvent-substrate interactions all have a role to play in controlling whether or not a solute will adsorb to the interface and the local interfacial environment. Studies described in this work begin to isolate and identify how the different interactions affect solution phase surface chemistry and the results establish important benchmarks for evolving models of interfacial solvation.

4.6 References

(1) Bhatnagar, A.; Vilar, V. J. P.; Botelho, C. M. S.; Boaventura, R. A. R. *Adv. Colloid Interfac.* **2010**, *160*, 1.

(2) Kumar, A. S.; Sornambikai, S.; Deepika, L.; Zen, J. M. *J. Mat. Chem.* **2010**, *20*, 10152.

(3) Rojo, N.; Gallastegi, G.; Barona, A.; Gurtubay, L.; Ibarra-Berastegi, G.; Elias, A. *Environ. Rev.* **2010**, *18*, 321.

(4) Tirgar, A.; Golbabaei, F.; Hamedi, J.; Nourijelyani, K. *Int. J. Environ. Sci. Te.* **2011**, *8*, 237.

(5) Biswas, A.; Siegel, D. J.; Seidman, D. N. *Phys. Rev. Lett.* **2010**, *105*, 4.

(6) Simon, J. M.; Haas, O. E.; Kjelstrup, S. *J. Phys. Chem. C* **2010**, *114*, 10212.

(7) Kitayama, A.; Yamanaka, S.; Kadota, K.; Shimosaka, A.; Shirakawa, Y.; Hidaka, J. *J. Chem. Phys.* **2009**, *131*, 7.

(8) Steel, W. H.; Lau, Y. Y.; Beildeck, C. L.; Walker, R. A. *J. Phys. Chem. B* **2004**, *108*, 13370.

(9) Steel, W. H.; Walker, R. A. *Nature* **2003**, *424*, 296.

(10) Steel, W. H.; Beildeck, C. L.; Walker, R. A. *J. Phys. Chem. B* **2004**, *108*, 16107.

(11) Zhang, X. Y.; Steel, W. H.; Walker, R. A. *J. Phys. Chem. B* **2003**, *107*, 3829.

(12) Zhang, X. Y.; Cunningham, M. M.; Walker, R. A. *J. Phys. Chem. B* **2003**, *107*, 3183.

(13) Aizawa, M.; Buriak, J. M. *Chemistry of Materials* **2007**, *19*, 5090.

(14) Ashwell, G. J.; Urasinska-Wojcik, B.; Phillips, L. J. *Angew. Chem. Int. Edit.* **2010**, *49*, 3508.

(15) Galoppini, E. *Coordin. Chem. Rev.* **2004**, *248*, 1283.

(16) Hasobe, T. *Phys. Chem. Chem. Phys.* **2010**, *12*, 44.

(17) Vetterl, O.; Hulsbeck, M.; Wolff, J.; Carius, R.; Finger, E. *Thin Solid Films* **2003**, *427*, 46.

(18) Mukherjee, D.; May, M.; Vaughn, M.; Bruce, B. D.; Khomami, B. *Langmuir* **2010**, *26*, 16048.

(19) Gonzalez, M.; Mingorance, M. D.; Sanchez, L.; Pena, A. *Environ. Sci. Pollut. R.* **2008**, *15*, 8.

(20) Vincent, A.; Benoit, P.; Pot, V.; Madrigal, I.; Delgado-Moreno, L.; Labat, C. *Eur. J. Soil Sci.* **2007**, *58*, 320.

(21) Xu, Y.; Wang, W. L.; Li, S. F. Y. *Electrophoresis* **2007**, *28*, 1530.

(22) Goldreich, O.; Goldwasser, Y.; Mishael, Y. G. *J. Agr. Food Chem.* **2010**, *59*, 645.

(23) Katz, J. M.; Winter, C. K. *Food Chem. Toxicol.* **2009**, *47*, 335.

(24) Alexandridis, P.; Holzwarth, J. F.; Hatton, T. A. *J. Mol. Liq.* **1997**, *72*, 55.

(25) Higgins, D. A.; Abrams, M. B.; Byerly, S. K.; Corn, R. M. *Langmuir* **1992**, *8*, 1994.

(26) TamburelloLuca, A. A.; Hebert, P.; Brevet, P. F.; Girault, H. H. *J. Chem. Soc., Faraday Trans.* **1996**, *92*, 3079.

(27) Beildeck, C. L.; Steel, W. H.; Walker, R. A. *Langmuir* **2003**, *19*, 4933.

(28) Brindza, M. R.; Walker, R. A. *J. Am. Chem. Soc.* **2009**, *131*, 6207.

(29) Steel, W. H.; Damkaci, F.; Nolan, R.; Walker, R. A. *J. Am. Chem. Soc.* **2002**, *124*, 4824.

(30) Eisenthal, K. B. *Chem. Rev.* **2006**, *106*, 1462.

(31) Zhuang, X.; Miranda, P. B.; Kim, D.; Shen, Y. R. *Phys. Rev. B* **1999**, *59*, 12632.

(32) Steel, W. H.; Foresman, J. B.; Burden, D. K.; Lau, Y. Y.; Walker, R. A. *J. Phys. Chem. B* **2009**, *113*, 759.

(33) Castro, A.; Bhattacharyya, K.; Eisenthal, K. B. *J. Chem. Phys.* **1991**, *95*, 1310.

(34) Aljoumaa, K.; Qi, Y. H.; Ding, J. F.; Delaire, J. A. *Macromolecules* **2009**, *42*, 9275.

(35) Beildeck, C. L.; Liu, M. J.; Brindza, M. R.; Walker, R. A. *J. Phys. Chem. B* **2005**, *109*, 14604.

(36) Gielis, J. J. H.; van den Oever, P. J.; Hoex, B.; van de Sanden, M. C. M.; Kessels, W. M. M. *Phys. Rev. B* **2008**, *77*, art. no.

(37) Liu, J.; Subir, M.; Nguyen, K.; Eisenthal, K. B. *J. Phys. Chem. B* **2008**, *112*, 15263.

(38) Mao, M. Y.; Miranda, P. B.; Kim, D. S.; Shen, Y. R. *Phys. Rev. B* **2001**, *64*, art. no.

(39) Onorato, R. M.; Otten, D. E.; Saykally, R. J. *J. Phys. Chem. C* **2010**, *114*, 13746.

(40) Petersen, P. B.; Saykally, R. J. *J. Phys. Chem. B* **2006**, *110*, 14060.

(41) Salafsky, J. S.; Eisenthal, K. B. *J. Phys. Chem. B* **2000**, *104*, 7752.

(42) Wang, H. F.; Borguet, E.; Eisenthal, K. B. *J. Phys. Chem. A* **1997**, *101*, 713.

(43) Wang, H. F.; Borguet, E.; Eisenthal, K. B. *J. Phys. Chem. B* **1998**, *102*, 4927.

(44) Watanabe, H.; Yamaguchi, S.; Sen, S.; Morita, A.; Tahara, T. *J. Chem. Phys.* **2010**, *132*, art. no.

(45) Moad, A. J.; Simpson, G. J. *J. Phys. Chem. B* **2004**, *108*, 3548.

(46) Bell, A. J.; Frey, J. G.; Vandernoot, T. J. *J. Chem. Soc. Faraday T* **1992**, *88*, 2027.

(47) Gan, W.; Gonella, G.; Zhang, M.; Dai, H. L. *J. Chem. Phys.* **2010**, *134*.

(48) Song, J.; Kim, M. W. *J. Phys. Chem. B* **2011**, *115*, 1856.

(49) Hiemenz, P. C., Rajagopalan, R. *Principles of Colloid and Surface Chemistry*, 3rd ed.; Marcel Dekker, Inc.: New York, 1997.

(50) Johnson, B. B. *Environ. Sci. Technol.* **1990**, *24*, 112.

(51) Ong, S. W.; Zhao, X. L.; Eisenthal, K. B. *Chem. Phys. Lett.* **1992**, *191*, 327.

(52) Wirth, M. J.; Ludes, M. D.; Swinton, D. J. *Anal. Chem.* **1999**, *71*, 3911.

(53) Wirth, M. J.; Legg, M. A. *Annu. Rev. Phys. Chem.* **2007**, *58*, 489.

(54) Zhu, B. Y.; Gu, T. R. *Adv. Colloid Interface Sci.* **1991**, *37*, 1.

(55) Doerr, A. K.; Tolan, M.; Schlomka, J. P.; Press, W. *Europhys. Lett.* **2000**, *52*, 330.

(56) Turov, V. V.; Gun'ko, V. M.; Tsapko, M. D.; Bogatyrev, V. M.; Skubiszewska-Zieba, J.; Leboda, R.; Ryczkowski, J. *Appl. Surf. Sci.* **2004**, *229*, 197.

(57) Arnett, E. M.; Ahsan, T. *J. Am. Chem. Soc.* **1991**, *113*, 6861.

(58) Ding, F.; Hu, Z. H.; Zhong, Q.; Manfred, K.; Gattass, R. R.; Brindza, M. R.; Fourkas, J. T.; Walker, R. A.; Weeks, J. D. *J. Phys. Chem. C* **2010**, *114*, 17651.

(59) Liu, W. T.; Zhang, L. N.; Shen, Y. R. *Chem. Phys. Lett.* **2005**, *412*, 206.

(60) Onsager, L. *J. Am. Chem. Soc.* **1936**, *58*, 1486.

(61) Laurence, C.; Nicolet, P.; Dalati, M. T.; Abboud, J. L. M.; Notario, R. *J. Phys. Chem.* **1994**, *98*, 5807.

Chapter 5: Conclusion

5.1 Motivation

The goal of the measurements presented here was to gain insight into how solution phase surface chemistry depends on both solvent *and* solute identity. Of particular interest were questions about how (or even if) solvents having similar bulk solution solvating properties would create environments at interfaces that were measurably different from each other. Experiments also sought to explore differences in interfacial solute behavior from the standpoint of a solute's functional group composition. Specifically, we wanted to know if two different solutes having very similar bulk solvation behavior (and electronic structure) would sample the same long-range noncovalent forces at the same liquid surface *or* would subtle difference in solute structure lead to the same interface having effectively different properties.

Two solutes used in these studies – *p*-nitrophenol (pNP) and *p*-nitroanisole (pNAs) – were not new to the Walker Research Group.[1-3] These solutes had been used as the precursors to the first "molecular rulers," much as n-methyl-p-methoxyaniline (NMMA) was used as the parent solute for the rulers described in Chapter 2. The group has published several papers describing the difference in interfacial excitation at both weakly and strongly associating interfaces.[1,4-7] However, studies presented in this thesis – especially in Chapters 3 and 4 – are the first direct and systematic comparison of how solute *identity* of two similar solutes can sample markedly different environments at the same interface.

5.2 Summary of Experiments

Chapter 2 describes both the synthesis and characterization of new molecular ruler surfactants, as well efforts to use these surfactants to characterize hydrogen bonding across liquid/liquid interfaces. The synthetic scheme led to the creation of two types of molecular rulers. The first family was quarternized, while the second family has an alcohol group on it's amphiphilic head-group. The latter does not get used in this thesis, but the ability to synthesize these rulers enables a direct comparison to previous alcohol terminated molecular rulers that were sensitive to solvent polarity.[8] The family of surfactant rulers having quarternized headgroups were used to examine specific solvation interactions across the aqueous/methyl-cyclohexane interface. The data from these measurements were directly compared to the results of the parent solute, NMMA. In bulk solvents, NMMA shows remarkably similar absorption to both the C_5^+ and C_3^+ molecular rulers.

An interesting bi-modal excitation peak is observed for C_5^+ at the aqueous/methyl-cylcohexane interface. The smaller peak observed toward shorter wavelengths is attributed to strong association of the ruler with partially solvated water molecules at the interface. Though this finding is particularly interesting, there were instrumental restrictions that limited our ability to ascertain the origin of the long wavelength second harmonic signal observed in these experiments.

The studies reported in Chapter 3 describe the solvation of pNAs at the strongly associating silica/methanol and silica/ethanol interfaces. The spectra acquired for pNAs at the two interfaces also resulted in surprising conclusions. The silica/ethanol interface creates a region of high polarity, as probed by pNAs. The SH

excitation maxima for pNAs (~323 nm) at the silica/ethanol interface lies well outside of pNAs' solvatochromic window where the solute's excitation wavelength in polar media such as water, DMSO or methanol (~317 nm.) The region of high polarity is attributed to the association of bulk ethanol with the silica substrate. Conversely, at the silica/methanol interface, a nonpolar region is created at the interface. This nonpolar region causes a shift in the SH interfacial maxima of pNAs towards the blue in comparison to pNAs at the silica/ethanol interface.

Chapter 3 consisted of work completed while at Montana State University. New laser instrumentation and a newly rebuilt spectroscopic assembly allowed surface specific SHG spectra to be acquired over a wider wavelength range to both the blue and red. The larger range of wavelengths allowed for the second harmonic (SH) measurements of several coumarins: C151, C152, C440 and C461. SHG was used to measure the excitation spectra of these solutes to test the generality of the nonpolar region created at the silica/methanol interface. All four of these solutes also experienced blue shifts in solvation in comparison to bulk methanol excitation limits.

The adsorption measurements completed in Chapter 4 expand significantly on the results reported in Chapter 3. These experiments were performed to provide comprehensive and systematic insight into the surprisingly nonpolar region created at the silica/methanol interface. X-ray studies and calculations reported by Doerr et al. guided the choice of solvents used for the interfaces measured.[9] The findings in that paper described solvent density at a silica substrate for alkanes. For comparison, the adsorption of solutes to more strongly associating silica/liquid interfaces was attempted. Findings at the silica/dmso and silica/aqueous (pH ≤ 6) interfaces resulted

in no discernable resonance enhancement at the interface. The lack of signal was attributed to such strong association of the solvent with the substrate that the solute was unable to solvate at the interface.

Chapters 2 – 4 have either been published (Chapter 2), or submitted for publication.

5.3 Future directions

Results presented here only begin to examine specific solvation effects across liquid/liquid interfaces. Future work at the liquid/liquid interface should take advantage of improvements in instrumentation and experimental design that have occurred during the past two years. The length of the specific solvation molecular rulers should also be varied more to create an extensive "family" such as those previously synthesized for the nonspecific solvation sensitive rulers.[1] Another interesting direction would be in the use of co-solvents at the solid/liquid interface. The mixing of alcohol/aqueous solutions would provide competition for the solute at the silica interface that could provide interesting findings.

Using SHG spectroscopy to measure the adsorption of solutes to the silica/liquid interface is a particularly powerful tool. Comparing interfacial adsorption data to SHG spectra for all silica/solvent interfaces measured would provide an additional source of information to better understand what is happening at the interface. The results from the work presented here in no way encompass all that needs to be done to characterize interfaces. The hope is that this thesis provides an

interesting combination of experiments that can be used to further our understanding of interfacial solvation.

5.4 References

(1) Beildeck, C. L.; Steel, W. H.; Walker, R. A. *Langmuir* **2003**, *19*, 4933.

(2) Brindza, M. R.; Walker, R. A. *J. Am. Chem. Soc.* **2009**, *131*, 6207.

(3) Steel, W. H.; Foresman, J. B.; Burden, D. K.; Lau, Y. Y.; Walker, R. A. *J. Phys. Chem. B* **2009**, *113*, 759.

(4) Steel, W. H.; Beildeck, C. L.; Walker, R. A. *J. Phys. Chem. B* **2004**, *108*, 16107.

(5) Steel, W. H.; Damkaci, F.; Nolan, R.; Walker, R. A. *J. Am. Chem. Soc.* **2002**, *124*, 4824.

(6) Steel, W. H.; Lau, Y. Y.; Beildeck, C. L.; Walker, R. A. *J. Phys. Chem. B* **2004**, *108*, 13370.

(7) Steel, W. H.; Walker, R. A. *Nature* **2003**, *424*, 296.

(8) Zhang, X. Y.; Cunningham, M. M.; Walker, R. A. *J. Phys. Chem. B* **2003**, *107*, 3183.

(9) Doerr, A. K.; Tolan, M.; Schlomka, J. P.; Press, W. *Europhys. Lett.* **2000**, *52*, 330.

Appendix I: Experimental Schematic

Appendix I: Experimental Schematic

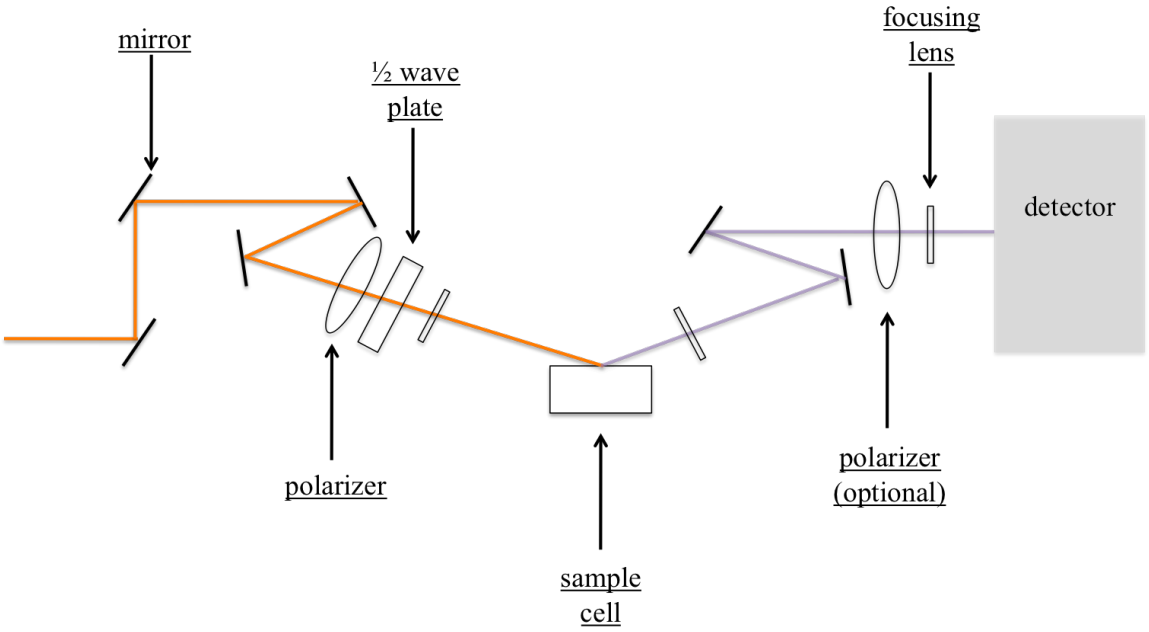

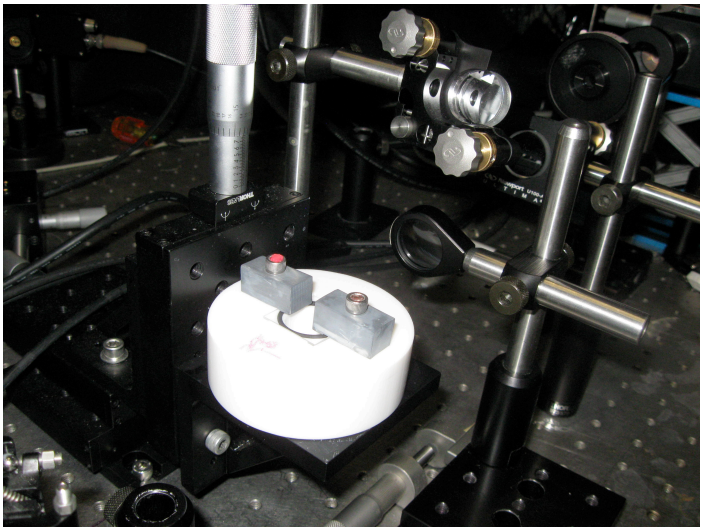

Image of sample cell

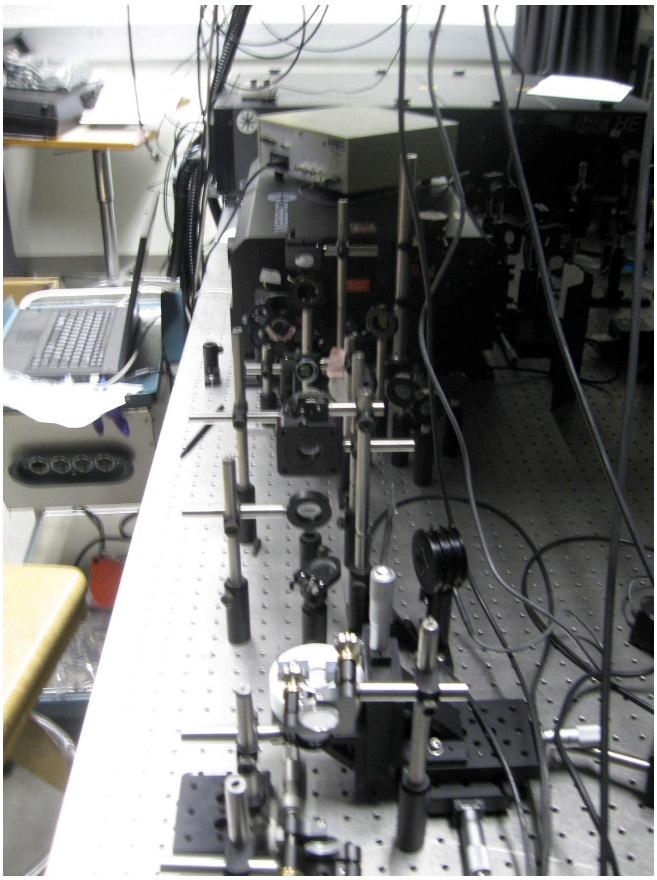

Downstream image of SHG Spectrometer

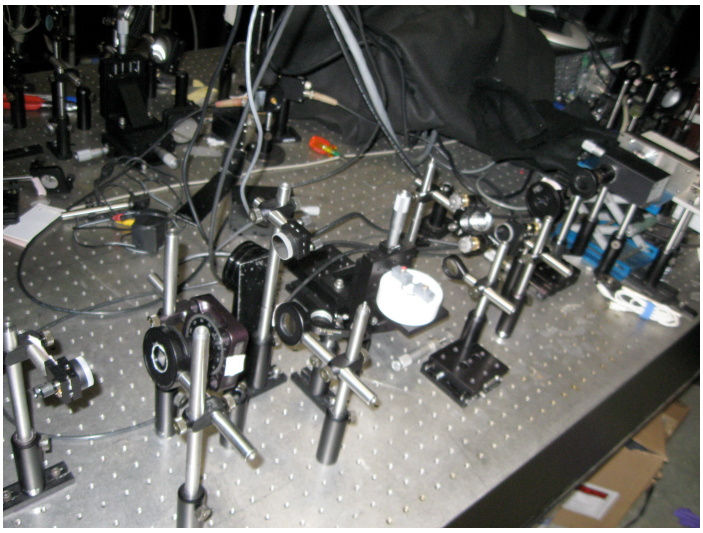

Upstream image of SHG Spectrometer

The spectrometer is designed around the visible output of an optical parametric amplifier (OPerA-Solo, Coherent, made by Light Conversion, Ltd, Lithuania). The fundamental beam is steered by a telescope upon exiting the OPA and sent through a polarizer set to pass P-polarized light. For spectra, the half wave plate is set to pass P-polarized light. The half wave plate has a filter that blocks any nonresonant SHG signal that may occur in the plate or from optics upstream of the sample, and care should be taken to place the plate with the correct orientation into the spectrometer. A focusing optic is set to focus the incident light onto the sample cell, and a second focusing optic is placed after the sample cell to focus the generated second harmonic (SH) light. Two mirrors are set to steer the SH-light into the detector. The optional polarizer set before the detector is removed, and a lens further focuses the diverging SH-light into the detector. The optics are aligned in the following order for all measurements: sample cell, half wave plate, polarizer, 1st focusing lens, 2nd focusing lens, optional polarizer, then 3rd focusing lens.

Initial measurements quantifying the quadratic response of the system are taken using either a gold mirror, or a gallium arsenide (GaAs) plate. As the SH response from these media is large, care should be taken to dampen the energy of the incident light. Several measurements should be taken at different incident energies. After a quadratic dependence is confirmed, the spectrometer should be dismantled, and the mirror or plate should be replaced by the sample cell. Typical signal strength for a gold mirror at 0.5 uJ of 630 nm incident light, and the photomultiplier tube (PMT) set to -900 V is ~ 300 counts for a 10 second acquisition.

For orientation measurements, the half wave plate is rotated 180 degrees (totaling 360 degrees) to scan all polarization combinations. The focusing optics remain in place, and the optional polarizer is placed in the beam path to pass P-polarized light. A single measurement is taken with the half wave plate set to pass M-polarized light, and the optional polarizer set to pass S-polarized light. This single point is taken to determine the remaining nonlinear susceptibility term, χ_{xzx}, defined in Chapters 3 and 4.

The adsorption measurements were taken by using a similar design as the single point measurement taken in the orientation measurements. The half wave plate is set to pass M-polarized light, and the optional polarizer is set to pass S-polarized light. This measurement isolates a single nonlinear susceptibility term that is the square of the monitored SH intensity.

Alphabetical Listing of References by First Author

(1) Aizawa, M.; Buriak, J. M. *Chemistry of Materials* **2007**, *19*, 5090.

(2) Alexandridis, P.; Holzwarth, J. F.; Hatton, T. A. *J. Mol. Liq.* **1997**, *72*, 55.

(3) Aljoumaa, K.; Qi, Y. H.; Ding, J. F.; Delaire, J. A. *Macromolecules* **2009**, *42*, 9275.

(4) Andanson, J. M.; Baiker, A. *Chem. Soc. Rev.* **2010**, *39*, 4571.

(5) Arnett, E. M.; Ahsan, T. *J. Am. Chem. Soc.* **1991**, *113*, 6861.

(6) Ashwell, G. J.; Urasinska-Wojcik, B.; Phillips, L. J. *Angew. Chem. Int. Edit.* **2010**, *49*, 3508.

(7) Barnette, A. L.; Asay, D. B.; Janik, M. J.; Kim, S. H. *J. Phys. Chem. C* **2009**, *113*, 10632.

(8) Battaglini, N.; Repain, V.; Lang, P.; Horowitz, G.; Rousset, S. *Langmuir* **2008**, *24*, 2042.

(9) Beildeck, C. L.; Liu, M. J.; Brindza, M. R.; Walker, R. A. *J. Phys. Chem. B* **2005**, *109*, 14604.

(10) Beildeck, C. L.; Steel, W. H.; Walker, R. A. *Langmuir* **2003**, *19*, 4933.

(11) Beildeck, C. L.; Steel, W. H.; Walker, R. A. *Langmuir* **2003**, *19*, 4933.

(12) Bell, A. J.; Frey, J. G.; Vandernoot, T. J. *J. Chem. Soc. Faraday T* **1992**, *88*, 2027.

(13) Benjamin, I. *Ann. Rev. Phys. Chem.* **1997**, 48, 407.

(14) Benjamin, I. *Chem. Phys. Lett* **2004**, *393*, 453.

(15) Benjamin, I. *Chem. Rev.* **2006**, *106*, 1212.

(16) Benjamin, I. *J. Phys. Chem. B* **2005**, *109*, 13711.

(17) Bhatnagar, A.; Vilar, V. J. P.; Botelho, C. M. S.; Boaventura, R. A. R. *Adv. Colloid Interfac.* **2010**, *160*, 1.

(18) Biswas, A.; Siegel, D. J.; Seidman, D. N. *Phys. Rev. Lett.* **2010**, *105*, 4.

(19) Boyd, R. W. *Nonlinear Optics*; Academic Press: New York, 2003.

(20) Boyer, R. F. *Concepts in Biochemistry*; John Wiley and Sons: New York, 2002.

(21) Brettschneider, F.; Jankowski, V.; Gunthner, T.; Salem, S.; Nierhaus, M.; Schulz, A.; Zidek, W.; Jankowski, J. *J. Chromatogr. B* **2010**, *878*, 763.

(22) Brindza, M. R.; Walker, R. A. *J. Am. Chem. Soc.* **2009**, *131*, 6207.

(23) Buchbinder, A. M.; Weitz, E.; Geiger, F. M. *J. Am. Chem. Soc.* **2010**, *132*, 14661.

(24) Buemi, G.; Millefiori, S.; Zuccarello, F.; Millefiori, A. *Can. J. Chem.* **1979**, *57*, 2167.

(25) Calvente, J. J.; Andreu, R. *Phys. Chem. Chem. Phys.* **2010**, *12*, 13519.

(26) Carnali, J. O.; Shah, P. *J. Phys. Chem. B* **2008**, *112*, 7171.

(27) Castro, A.; Bhattacharyya, K.; Eisenthal, K. B. *J. Chem. Phys.* **1991**, *95*, 1310.

(28) Catalan, J. *J. Org. Chem.* **1997**, *62*, 8231.

(29) Chen, K.; Lynen, F.; De Beer, M.; Hitzel, L.; Ferguson, P.; Hanna-Brown, M.; Sandra, P. *J. Chromatogr. A* **2010**, *1217*, 7222.

(30) Chirica, G. S.; Remcho, V. T. *Anal. Chem.* **2000**, *72*, 3605.

(31) Chowdhary, J.; Ladanyi, B. M. *J. Phys. Chem. B* **2006**, *110*, 15442.

(32) Connell, D. B.; Sander, J. G.; Riedel, G. F.; Abbe, G. R. *Environ. Sci. Technol.* **1991**, *25*, 921.

(33) Curtis, A. D.; Reynolds, S. B.; Calchera, A. R.; Patterson, J. E. *J. Phys. Chem. Lett.* **2010**, *1*, 2435.

(34) Ding, F.; Hu, Z. H.; Zhong, Q.; Manfred, K.; Gattass, R. R.; Brindza, M. R.; Fourkas, J. T.; Walker, R. A.; Weeks, J. D. *J. Phys. Chem. C* **2010**, *114*, 17651.

(35) Dion, M.; Rapp, M.; Rorrer, N.; Shin, D. H.; Martin, S. M.; Ducker, W. A. *Colloids Surf., A* **2010**, *362*, 65.

(36) Dodge, E. E.; Theis, T. L. *Environ. Sci. Technol.* **1979**, *13*, 1287.

(37) Doerr, A. K.; Tolan, M.; Schlomka, J. P.; Press, W. *Europhys. Lett.* **2000**, *52*, 330.

(38) Durbing, D. P.; El-Aasser, M. S.; Vanderhoff, J. W. *Ind. Eng. Chem. Prod. Res. Dev.* **1984**, *23*, 569.

(39) Ederth, T.; Liedberg, B. *Langmuir* **2000**, *16*, 2177.

(40) Eisenthal, K. B. *Chem. Rev.* **1996**, *96*, 1343.

(41) Eisenthal, K. B. *Chem. Rev.* **2006**, *106*, 1462.

(42) Esenturk, O.; Walker, R. A. *Phys. Chem. Chem. Phys.* **1999**, *1*, 1957.

(43) Esenturk, O.; Walker, R. A. *Phys. Chem. Chem. Phys.* **2003**, *5*, 2020.

(44) Galoppini, E. *Coordin. Chem. Rev.* **2004**, *248*, 1283.

(45) Gan, W.; Gonella, G.; Zhang, M.; Dai, H. L. *J. Chem. Phys.* **2010**, *134*.

(46) Gielis, J. J. H.; van den Oever, P. J.; Hoex, B.; van de Sanden, M. C. M.; Kessels, W. M. M. *Phys. Rev. B* **2008**, *77*, art. no.

(47) Goldreich, O.; Goldwasser, Y.; Mishael, Y. G. *J. Agr. Food Chem.* **2010**, *59*, 645.

(48) Gonzalez, M.; Mingorance, M. D.; Sanchez, L.; Pena, A. *Environ. Sci. Pollut. R.* **2008**, *15*, 8.

(49) Hasobe, T. *Phys. Chem. Chem. Phys.* **2010**, *12*, 44.

(50) Hayes, P. L.; Malin, J. N.; Korek, C. T.; Geiger, F. M. *J. Phys. Chem. A* **2008**, *112*, 660.

(51) Hiemenz, P. C., Rajagopalan, R. *Principles of Colloid and Surface Chemistry*, 3rd ed.; Marcel Dekker, Inc.: New York, 1997.

(52) Higgins, D. A.; Abrams, M. B.; Byerly, S. K.; Corn, R. M. *Langmuir* **1992**, *8*, 1994.

(53) Hills, B. A.; Barrow, R. E. *Phys. Med. Biol.* **1984**, *29*, 1399.

(54) Horng, M. L.; Gardecki, J. A.; Papazyan, A.; Maroncelli, M. *J. Phys. Chem.* **1995**, *99*, 17311.

(55) Horng, P.; Brindza, M. R.; Walker, R. A.; Fourkas, J. T. *J. Phys. Chem. C* **2010**, *114*, 394.

(56) Huang, D. M.; Cottin-Bizonne, C.; Ybert, C.; Bocquet, L. *Langmuir* **2008**, *24*, 1442.

(57) Iler, R. K. *The Chemistry of Silica: Solubility, Polymerization, Colloid and Surface Properties, and Biochemistry*; John Wiley and Sons: New York, 1979.

(58) Ishizaka, S.; Kinoshita, S.; Nishijima, Y.; Kitamura, N. *Anal. Chem.* **2003**, *75*, 6035.

(59) Ishizaka, S.; Kitamura, N. *Anal. Sciences* **2004**, *20*, 1587.

(60) Ishizaka, S.; Nishijima, Y.; Kitamura, N. *Anal. Bioanal. Chem.* **2006**, *386*, 749.

(61) Israelachvili Intermolecular and Surface Forces; 2nd ed.; Academic Press: New York, 1992.

(62) Johnson, B. B. *Environ. Sci. Technol.* **1990**, *24*, 112.

(63) Katz, J. M.; Winter, C. K. *Food Chem. Toxicol.* **2009**, *47*, 335.

(64) Kitayama, A.; Yamanaka, S.; Kadota, K.; Shimosaka, A.; Shirakawa, Y.; Hidaka, J. *J. Chem. Phys.* **2009**, *131*, 7.

(65) Kumar, A. S.; Sornambikai, S.; Deepika, L.; Zen, J. M. *J. Mat. Chem.* **2010**, *20*, 10152.

(66) Laurence, C.; Nicolet, P.; Dalati, M. T.; Abboud, J. L. M.; Notario, R. *J. Phys. Chem.* **1994**, *98*, 5807.

(67) Liddell, P. V.; Boger, D. V. *Ind. Eng. Chem. Res.* **1994**, *33*, 2437.

(68) Lin, S.; Wang, W.; Hsu, C. *Langmuir* **1997**, *13*, 6211.

(69) Liu, J.; Subir, M.; Nguyen, K.; Eisenthal, K. B. *J. Phys. Chem. B* **2008**, *112*, 15263.

(70) Liu, W. T.; Zhang, L. N.; Shen, Y. R. *Chem. Phys. Lett.* **2005**, *412*, 206.

(71) Maas, M.; Ooi, C. C.; Fuller, G. G. *Langmuir* **2010**, *26*, 17867.

(72) Mao, M. Y.; Miranda, P. B.; Kim, D. S.; Shen, Y. R. *Phys. Rev. B* **2001**, *64*, art. no.

(73) Matyushov, D. V.; Schmid, R.; Ladanyi, B. M. J. *Phys. Chem. B* **1997**, *101*, 1035.

(74) McCain, K. S.; Schluesche, P.; Harris, J. M. *Anal. Chem.* **2004**, *76*, 930.

(75) McClelland, A.; Fomenko, V.; Borguet, E. *J. Phys. Chem. B* **2006**, *110*, 19784.

(76) McFearin, C. L.; Beaman, D. K.; Moore, F. G.; Richmond, G. L. *J. Phys. Chem. C* **2009**, *113*, 1171.

(77) Mellein, B. R.; Ladewski, R. L.; Brennecke, J. F. *J. Phys. Chem. B* **2007**, *111*, 131.

(78) Mikulski, P. T.; Herman, L. A.; Harrison, J. A. *Langmuir* **2005**, *21*, 12197.

(79) Mistry, M. K.; Choudhury, N. R.; Dutta, N. K.; Knott, R. *Langmuir* **2010**, *26*, 19073.

(80) Mitrinovic, D. M.; Tikhonov, A. M.; Li, M.; Huang, Z. Q.; Schlossman, M. L. *Phys. Rev. Lett*. **2000**, *85*, 582.

(81) Moad, A. J.; Simpson, G. J. *J. Phys. Chem. B* **2004**, *108*, 3548.

(82) Mondal, S. K., Yamaguchi, S., Tahara, T. *J. Phys. Chem. C* **2011**, *115*, 3083.

(83) Montgomery, J. R.; Price, M. T. *Environ. Sci. Technol.* **1979**, *13*, 546.

(84) Mukherjee, D.; May, M.; Vaughn, M.; Bruce, B. D.; Khomami, B. *Langmuir* **2010**, *26*, 16048.

(85) Napoleon, R. L.; Moore, P. B. *J. Phys. Chem. B* **2006**, *110*, 3666.

(86) Natal-Santiago, M. A.; Dumesic, J. A. *J. Catal.* **1998**, *175*, 252.

(87) Novaki, L. P.; El Seoud, O. A. *Phys. Chem. Chem. Phys.* **1999**, *1*, 1957.

(88) Ocko, B. M.; Wu, X. Z.; Sirota, E. B.; Sinha, S. K.; Gang, O.; Deutsch, M. *Phys. Rev. E* **1997**, *55*, 3164.

(89) Ong, S. W.; Zhao, X. L.; Eisenthal, K. B. *Chem. Phys. Lett.* **1992**, *191*, 327.

(90) Onorato, R. M.; Otten, D. E.; Saykally, R. J. *J. Phys. Chem. C* **2010**, *114*, 13746.

(91) Onsager, L. *J. Am. Chem. Soc.* **1936**, *58*, 1486.

(92) Petersen, P. B.; Saykally, R. J. *J. Phys. Chem. B* **2006**, *110*, 14060.

(93) Pingali, S. V.; Takiue, T.; Luo, G.; Tikhonov, A. M.; Ikeda, N.; Aratono, M.; Schlossman, M. L. *J. Disp. Sci. Tech.* **2006**, *27*, 715.

(94) Quantitative treatments of solute/solvent interactions; Politzer, P.; Murray, J. S., Eds.; Elsevier: Amsterdam, 1994.

(95) Rechthaler, K.; Kohler, G. *Chem. Phys.* **1994**, *189*, 99.

(96) Reichardt, C. *Chem. Rev.* **1994**, *94*, 2319.

(97) Rivera, D.; Harris, J. M. *Anal. Chem.* **2001**, *73*, 411.

(98) Rojo, N.; Gallastegi, G.; Barona, A.; Gurtubay, L.; Ibarra-Berastegi, G.; Elias, A. *Environ. Rev.* **2010**, *18*, 321.

(99) Ron, H.; Rubinstein, I. *J. Am. Chem. Soc.* **1998**, *120*, 13444.

(100) Rosen, M. J. *Surfactants and Interfacial Phenomena*; Wiley-Interscience: New Jersey, 2004.

(101) Roy, D. *Interfacial Solvation and Excited State Photophysical Properties of 7-Aminocoumarins at Silica/Liquid Interfaces*. Doctoral Thesis, University of Maryland, 2010.

(102) Ruiz-Angel, M. J.; Torres-Lapasio, J. R.; Carda-Broch, S.; Garcia-Alvarez-Coque, M. C. *J. Chromatogr. A* **2010**, *1217*, 7090.

(103) Salafsky, J. S.; Eisenthal, K. B. *J. Phys. Chem. B* **2000**, *104*, 7752.

(104) Sanchez, V. M.; Sued, M.; Scherlis, D. A. *J. Chem. Phys.* **2009**, *131*, art. no.

(105) Schlossman, M. L.; Tikhonov, A. M. *Ann. Rev. Phys. Chem.* **2008**, *59*, 153.

(106) Sefler, G. A.; Du, Q.; Miranda, P. B.; Shen, Y. R. *Chem. Phys. Lett.* **1995**, *235*, 347.

(107) Sen, S.; Yamaguchi, S.; Tahara, T. *Ang. Chem.-Int. Ed.* **2009**, *48*, 6439.

(108) Shen, Y. R. *Ann. Rev. Phys. Chem.* **1989**, *40*, 327.

(109) Siler, A. R.; Brindza, M. R.; Walker, R. A. *Anal. Bioanal. Chem.* **2008**, *395*, 1063.

(110) Simon, J. M.; Haas, O. E.; Kjelstrup, S. *J. Phys. Chem. C* **2010**, *114*, 10212.

(111) Sloutskin, E.; Bain, C. D.; Ocko, B. M.; Deutsch, M. *Faraday Disc.* **2005**, *129*, 339.

(112) Smith, E. A.; Wirth, M. J. *J. Chromatogr. A* **2004**, *1060*, 127.

(113) Somasundaran, P.; Huang, L. *Adv. Colloid Interface Sci.* **2000**, *88*, 179.

(114) Somasundaran, P.; Shrotri, S.; Huang, L. *Pure Appl. Chem.* **1998**, *70*, 621.

(115) Song, J.; Kim, M. W. *J. Phys. Chem. B* **2011**, *115*, 1856.

(116) Sovago, M.; Kramer-Campen, R.; Bakker, H. J.; Bonn, M. *Chem. Phys. Lett.* **2009**, *470*, 7.

(117) Steel, W. H.; Beildeck, C. L.; Walker, R. A. *J. Phys. Chem. B* **2004**, *108*, 13370.

(118) Steel, W. H.; Beildeck, C. L.; Walker, R. A. *J. Phys. Chem. B* **2004**, *108*, 16170.

(119) Steel, W. H.; Damkaci, F.; Nolan, R.; Walker, R. A. *J. Am. Chem. Soc.* **2002**, *124*, 4824.

(120) Steel, W. H.; Foresman, J. B.; Burden, D. K.; Lau, Y. Y.; Walker, R. A. *J. Phys. Chem. B* **2009**, *113*, 759.

(121) Steel, W. H.; Lau, Y. Y.; Beildeck, C. L.; Walker, R. A. *J. Phys. Chem. B* **2004**, *108*, 13370.

(122) Steel, W. H.; Walker, R. A. *J. Am. Chem. Soc.* **2003**, *125*, 1132.

(123) Steel, W. H.; Walker, R. A. *Nature* **2003**, *424*, 296.

(124) Steinhurst, D. A.; Owrutsky, J. C. *J. Phys. Chem. B* **2001**, *105*, 3062.

(125) Suppan, P.; Ghoneim, N. *Solvatochromism*, 1st ed.; The Royal Society of Chemistry: London, 1997.

(126) TamburelloLuca, A. A.; Hebert, P.; Brevet, P. F.; Girault, H. H. *J. Chem. Soc., Faraday Trans.* **1996**, *92*, 3079.

(127) Tao, F.; Cai, Y. G.; Bernasek, S. L. *Langmuir* **2005**, *21*, 1269.

(128) Thomann, R. V. *Environ. Sci. Technol.* **1989**, *23*, 699.

(129) Tirgar, A.; Golbabaei, F.; Hamedi, J.; Nourijelyani, K. *Int. J. Environ. Sci. Te.* **2011**, *8*, 237.

(130) Tomasi, J.; Mennucci, B.; Cammi, R. *Chem. Rev.* **2005**, *105*, 2999.

(131) Tran, B. N.; Okoniewski, R.; Storm, R.; Jansing, R.; Aldous, K. M. *J. Agric. Food. Chem.* **2010**, *58*, 101.

(132) Tsukahara, S.; Watarai, H. *Chemistry Letters* **1999**, 89.

(133) Turov, V. V.; Gun'ko, V. M.; Tsapko, M. D.; Bogatyrev, V. M.; Skubiszewska-Zieba, J.; Leboda, R.; Ryczkowski, J. *Appl. Surf. Sci.* **2004**, *229*, 197.

(134) Vetterl, O.; Hulsbeck, M.; Wolff, J.; Carius, R.; Finger, E. *Thin Solid Films* **2003**, *427*, 46.

(135) Vincent, A.; Benoit, P.; Pot, V.; Madrigal, I.; Delgado-Moreno, L.; Labat, C. *Eur. J. Soil Sci.* **2007**, *58*, 320.

(136) Wang, H. F.; Borguet, E.; Eisenthal, K. B. *J. Phys. Chem. A* **1997**, *101*, 713.

(137) Wang, H. F.; Borguet, E.; Eisenthal, K. B. *J. Phys. Chem. B* **1998**, *102*, 4927.

(138) Watanabe, H.; Yamaguchi, S.; Sen, S.; Morita, A.; Tahara, T. *J. Chem. Phys.* **2010**, *132*, art. no.

(139) Williamson, R. V. *J. Phys. Chem.* **1931**, *35*, 354.

(140) Wirth, M. J.; Legg, M. A. *Annu. Rev. Phys. Chem.* **2007**, *58*, 489.

(141) Wirth, M. J.; Ludes, M. D.; Swinton, D. J. *Anal. Chem.* **1999**, *71*, 3911.

(142) Wirth, M. J.; Swinton, D. J.; Ludes, M. D. *J. Phys. Chem. B* **2003**, *107*, 6258.

(143) Wu, Y. G.; Tabata, M.; Takamuku, T. *J. Soln. Chem.* **2007**, *31*, 381.

(144) Xu, Y.; Wang, W. L.; Li, S. F. Y. *Electrophoresis* **2007**, *28*, 1530.

(145) Yam, C. M.; Tong, S. S. Y.; Kakkar, A. K. *Langmuir* **1998**, *14*, 6941.

(146) Yang, Y. J.; Pizzolatto, R. L.; Messmer, M. C. *J. Opt. Soc. B* **2000**, *17*, 638.

(147) Yaseen, M.; Lu, J. R.; Webster, J. R. P.; Penfold, J. *Langmuir* **2006**, *22*, 5825.

(148) Zapala, W.; Waksmundzka-Hajnos, M. *J. Sep. Sci.* **2005**, *28*, 566.

(149) Zdziennicka, A.; Janczuk, B. *J. Colloid Interface Sci.* **2010**, *343*, 594.

(150) Zhang, L. N.; Liu, W. T.; Shen, Y. R.; Cahill, D. G. *J. Phys. Chem. C* **2007**, *111*, 2069.

(151) Zhang, X. Y.; Cunningham, M. M.; Walker, R. A. *J. Phys. Chem. B* **2003**, *107*, 3183.

(152) Zhang, X. Y.; Steel, W. H.; Walker, R. A. *J. Phys. Chem. B* **2003**, *107*, 3829.

(153) Zhu, B. Y.; Gu, T. R. *Adv. Colloid Interface Sci.* **1991**, *37*, 1.

(154) Zhuang, X.; Miranda, P. B.; Kim, D.; Shen, Y. R. *Phys. Rev. B* **1999**, *59*, 12632.

(155) Zhuang, X.; Miranda, P. B.; Kim, D.; Shen, Y. R. *Phys. Rev. B* **1999**, *59*, 12632.